BIOMECHANICAL ANALYSES OF POSTERIOR VAGINAL PROLAPSE:

MR IMAGING AND COMPUTER MODELING STUDIES

by

Jiajia Luo

A dissertation submitted in partial fulfillment
of the requirements for the degree of
Doctor of Philosophy
(Mechanical Engineering)
in The University of Michigan
2012

Doctoral Committee:

Professor James A. Ashton-Miller, Co-Chair
Professor John O.L. DeLancey, Co-Chair
Professor Gregory M. Hulbert
Assistant Professor Mark L. Palmer

To My Family

ACKNOWLEDGEMENTS

I would like to express my earnest gratitude and deep appreciation to my two advisors, Professors James A. Ashton-Miller and John O.L. DeLancey. I thank them for bringing me into a fantastic world of interdisciplinary research that links biomechanics and pelvic floor. Their guidance, assistance, patience, and encouragement have been of enormous importance to my research and the completion of the dissertation. Their enthusiasm in research has truly inspired me along the way. I also appreciate their helpful and valuable advice on my future career development.

I would like to thank members of my dissertation committee, Professor Gregory M. Hulbert, and Professor Mark L. Palmer, for their time to discuss my work, and for their advice and comments to help to improve my dissertation. I am grateful to have their inputs into my dissertation.

I want to acknowledge NIH (grants R01 HD 038665 and P50 HD 044406), American Medical Systems, and Kimberly-Clark Corporation for their financial supports.

I would like to acknowledge all my colleagues in the Biomechanics Research Lab. I thank them for providing me a pleasant and active work environment. I thank Luyun Chen, Dejun Jing, Jinyong Kim, Hogene Kim, and Youkeun Oh, for their valuable assistance and stimulating discussion.

I also want to thank all the doctors, fellows, and staffs in the Pelvic Floor Research Group. I thank Dr. Dee Fenner, Kindra Larson, Cornelia Meier, and Tovia

Smith for all the wonderful corporations and contribution on clinical insights; Rajeev Ramanah for helping me create anatomical models; Sean Lisse for doing experiments for me when I was tied up; Julie Tumbarello and Amanda Pennington for their assistance in searching clinical data.

I would like to extend my gratitude to my friends outside the lab who have enriched my life. I want to thank other teachers and staffs who assisted, advised, and supported my research over the years.

I would like to express my deepest thanks to my parents for all the love and support they have given me. Finally, I would like to dedicate this dissertation to my wife Ling and my daughter Eileen, who have always been my source of happiness and energy, giving me endless love, and motivating me to complete my PhD study.

PREFACE

Chapters 2 - 9 of the dissertation were written as separate papers, so some repetition of material occurs, particularly in the Introduction of each chapter. Papers that have already been published include Chapters 3, 4, 5, and 7.

TABLE OF CONTENTS

LIST OF FIGURES

LIST OF TABLES

LIST OF APPENDICES

ABSTRACT

BIOMECHANICAL ANALYSES OF POSTERIOR VAGINAL PROLAPSE: MR IMAGING AND COMPUTER MODELING STUDIES

by

Jiajia Luo

Co-Chairs: James A. Ashton-Miller and John O.L. DeLancey

Pelvic organ prolapse is an abnormal downward displacement and deformation of the female pelvic organs. Because it adversely affects quality of life, over 200,000 operations are performed annually for prolapse in the U.S at a cost exceeding $1 billion. Approximately 87% of those procedures involve repair of a posterior vaginal prolapse, the etiology of which is a focus of this dissertation. But, because operative failure rates can approach 30%, new insights are needed as to how and why a posterior vaginal prolapse develops in the first place so that treatment can be improved.

We hypothesize that the occurrence, size and type of posterior vaginal prolapse is not explained by failure of any single structure; rather it involves failure of connective tissue supports at two and possibly up to as many as 20 anatomical sites, along with impairment of the levator ani muscle.

Using *in vivo* magnetic resonance imaging we first visualized the detailed 3-D pelvic floor anatomy of 84 healthy women. From these we then selected images from a pelvis of average dimensions and used them to create a detailed three-dimensional interactive model of the female pelvic floor complete with 23 structures. We then developed a method to measure and quantify the geometry of prolapse in forty 3-D magnetic resonance image-based models. Two main structures relating to the development of prolapse, fascia and apical vaginal supports, were then analyzed via two case-control studies. Finally, 2- and 3-D computer-based models were developed to identify the biomechanical interactions which lead to prolapse: levator muscle and connective tissue failure, and organ competition. These methodological approaches and computer models provide new insights into the biomechanical mechanisms underlying the development of posterior vaginal prolapse. Our hope is that they will lead to more effective surgical treatment strategies for this vexing condition.

CHAPTER 1

INTRODUCTION

1.1 Background and Significance

1.1.1 What is posterior vaginal prolapse?

Pelvic organ prolapse (POP) is a downward descent of the female pelvic organs, often including the bladder, uterus or post-hysterectomy vaginal cuff, and/or small or large bowel, resulting in protrusion of vagina, uterus or both (Hunskaar et al. 2005; Jelovsek et al. 2007). POP can prevent women from enjoying normal daily activities and can adversely affect quality of life (Jelovsek and Barber 2006). POP often occurs when the pelvic floor muscle and connective tissue supporting the female pelvic organs are damaged by vaginal childbirth, aging and increased intra-abdominal pressure, or a combination of these factors, which can vary from patient to patient (Hunskaar et al. 2005; Schaffer et al. 2005).

Posterior vaginal prolapse (PVP)**,** including the clinical problems of rectocele (rectum protrusion) and enterocele (small or large bowel protrusion), is a distressing, though rarely discussed problem. It is the second most common type of POP after cystocele (anterior compartment prolapse). Figure 1.1 illustrates the clinical problems of rectocele and enterocele. Rectocele occurs when the rectum pushes against and moves the back wall of the vagina ventrally. Enterocele (small or large bowel prolapse) occurs when the small or large bowel presses against and moves the upper wall of the vagina ventrally.

As a result of enterocele, the cervix is usually visible at the apex as shown in Figure 1.1 (right).

Figure 1.1 Rectocele (left) and enterocele (right) protruding from the vaginal opening. Note the cervix visible at the top of the enterocele. (Copyright © DeLancey)

1.1.2 Why is research to understand the mechanisms of posterior vaginal prolapse important?

Posterior vaginal prolapse including rectocele and enterocele is a remarkably common and distressing condition. It is also an important component of pelvic floor dysfunction. PVP is a socially embarrassing problem that can be disabling. Although the symptoms of POP are rarely discussed in public, women with posterior wall prolapse experience pelvic pressure and discomfort, incomplete rectal evacuation, anal incontinence, and impairment of sexual relations that often results in abstinence (Ellerkmann et al. 2001). These symptoms are strongly associated with the worsening stages of POP (Ellerkmann et al. 2001; Ghetti et al. 2005). Case series indicate that 50-75% of women with posterior wall prolapse feel that they have to strain too hard to defecate, while a third to a half need to splint the vaginal wall, or digitally disimpact the rectum, to have a bowel movement. While these symptoms demonstrate some correlation with the presence and severity of prolapse, the symptom that is most consistently acknowledged

by patients with severe prolapse is the discomfort of a bulge that can be seen or felt (Samuelsson et al. 1999; Ellerkmann et al. 2001; Burrows et al. 2004).

Eleven percent of women will undergo surgery for pelvic floor dysfunction (POP and incontinence) by the age of 80 years (Olsen et al. 1997). A majority of the approximately 300,000 female pelvic floor operations performed each year, of which over 225,000 operations are performed annually for prolapse (Boyles et al. 2003), with repair of PVP included in 87% (Silva et al. 2006). The annual estimated cost for these operations exceeds US $1 billion (Subak et al. 2001) yet PVP remains the most complex and enigmatic among the types of pelvic floor dysfunction. The surgical correction of apical and posterior wall prolapse is far more complex, for example, than the more commonly discussed and widely studied surgical management of stress urinary incontinence (SUI). There are nearly twice as many procedures required for prolapse compared to that required for correction of SUI (Boyles et al. 2003, 2004). Fortunately, surgical management of SUI is successful, with objective failures under 10% (Meschia et al. 2006), but the recurrence of prolapse is unfortunately much higher (Olsen et al. 1997; Blanchard et al. 2006). Better information about PVP is clearly needed to improve both prevention and treatment.

1.1.3 What is the normal supporting system for female pelvic floor?

The pelvic floor consists of levator ani (LA) muscle and connective tissue, with pelvic organs filling the cavity of the pelvic canal (Ashton-Miller and DeLancey 2009). The most logical anatomic structures to provide the biomechanical support of posterior compartment of the pelvic floor include the levator ani muscle, apical connective mesenteric

tissue such as cardinal and uterosacral ligaments, paravaginal connective tissue, perineal body and the posterior vaginal wall itself.

Figure 1.2 shows the structures that might be involved in the normal support of the posterior vaginal wall.

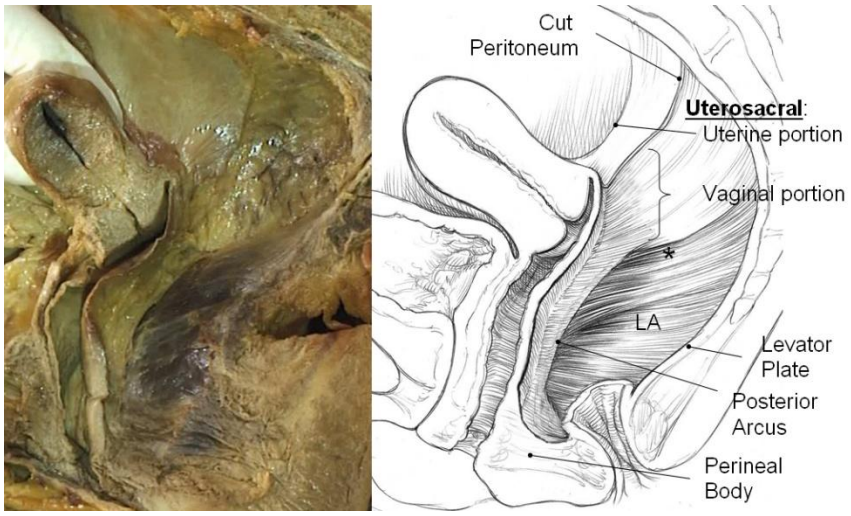

Figure 1.2 Cadaver dissection (left) and illustration (right) of posterior compartment of a 56 year old multipara showing structural relationships after the rectum has been removed. Note apical connections of the upper posterior vaginal wall to the inside of the pelvic wall in a retroperitoneal position. These lie below the peritoneum and are dorsal and caudal to what is traditionally referred to as the uterosacral ligament. These structures are continuous with the posterior arcus tendineus. At the distal end of the vagina, the wall merges into the top of the perineal body. The lateral and dorsal margins of the compartment are formed by the levator ani muscles (LA) and the levator plate. The asterisk (*) denotes the region of the sacrospinous ligament overlain by the coccygeus muscle. (Copyright © DeLancey)

The posterior vaginal wall is connected to pelvic muscle and connective tissues that are well-positioned to provide support in different regions. For example, the vaginal apex is suspended by cardinal (did not show in Figure 1.2) and uterosacral ligaments, which are referred as “apical supports” or “Level I” supports (DeLancey 1992). In the middle portion of vagina, posterior arcus tendineus fascia pelvis (Leffler et al. 2001) behind the posterior vaginal wall with other paravaginal connective tissue provide “Level II” supports (DeLancey 1992). The caudal margin is a closed structure consisting of the

perineal body and anal sphincter, which are referred as “Level III” supports (DeLancey 1992).

The levator ani muscle (Figure 1.3 and Figure 1.4) includes three components: pubovisceral complex (pubovaginal-puboperineal-puboanalis portions), puborectalis and iliococcygeus (Margulies et al. 2006). It plays an important role in maintaining closure of the urogenital hiatus while also providing support for urethral and pelvic organs (DeLancey 1994; Ashton-Miller et al. 2001).

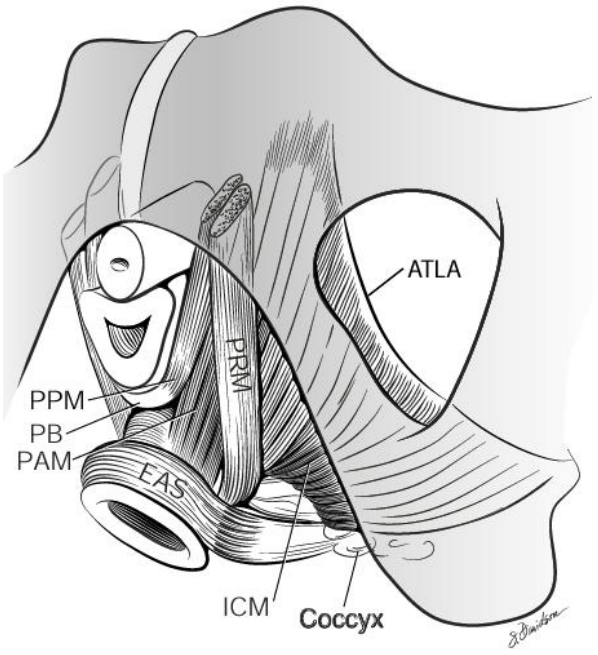

Figure 1.3 Schematic view of the levator ani muscles from below, after the vulvar structures and perineal membrane have been removed, that shows the arcus tendineus levator ani (ATLA); the external anal sphincter (EAS); the puboanal muscle (PAM); the perineal body (PB) uniting the two ends of the puboperineal muscle (PPM); the iliococcygeal muscle (ICM); and the puborectal muscle (PRM). Note that the urethra and vagina have been transected just above the hymenal ring. (Copyright © DeLancey 2003)

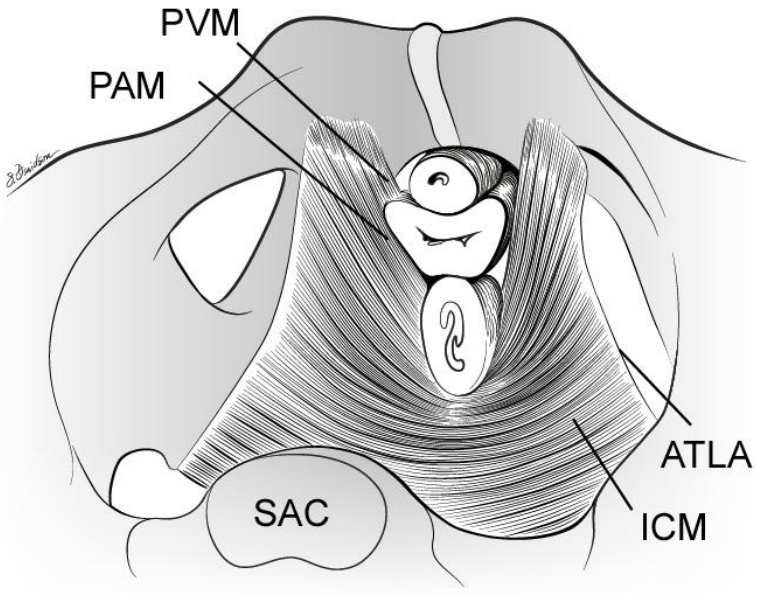

Figure 1.4 The levator ani muscle seen from above, looking over the sacral promontory (SAC), showing the pubovaginal muscle (PVM), sometimes called the pubococcygeal muscle. The urethra, the vagina, and the rectum have been transected just above the pelvic floor. PAM denotes the puboanal muscle. (The internal obturator muscles have been removed to clarify levator muscle origins.) (Copyright © DeLancey 2003)

1.2 What is the current state of PVP mechanism research?

The current concepts of structural abnormalities involved in posterior prolapse consist of observations concerning, 1) the abnormal displacement of the rectum and cul-de-sac, and 2) theories concerning structural defects presumed to explain the abnormal displacement seen in rectocele and enterocele. They can be summarized as follows:

1) Observations about abnormal displacements of rectum.

a. Abnormal protrusion of the rectum based on imaging studies (Bharucha et al. 2006).
b. Presence of intestine between vagina and rectum in enterocele (Halligan et al. 1996)
c. Abnormal cul-de-sac depth (Kuhn and Hollyock 1982; Baessler and Schuessler 2006).

Observations about displacements of posterior compartment have been helpful in correlating clinical findings with those displacements using barium defecography (Bharucha et al. 2006), ultrasound (Dietz and Steensma 2005) and MRI (Torricelli et al. 2002). Much of the debate in these areas concerns the superiority of imaging or clinical exam (Comiter et al. 1999; Cortes et al. 2004). At present, the direct study of the relationship between specific sites of tissue failure and muscle dysfunction, and posterior compartment displacement is in its infancy. Understanding the role of specific types of defect and development of specific types of prolapse requires the formulation and testing of specific hypotheses.

2) Three core hypotheses have been proposed about what leads to pelvic organ prolapse and specifically posterior wall prolapse.

a. Location of fascial failure: The rectovaginal septum, whose attachments to the suspending ligaments, vaginal wall or distal defects at the perineal body may fail (Richardson 1993, 1996).
b. Levator ani muscle: Neurological and mechanical damage (Gilpin et al. 1989; Hoyte et al. 2004).
c. Interaction between parts: There is a valve like arrangement requiring suspension of the vaginal apex over the levator plate and intact neuromuscular function. Unless the vagina overlies the levator plate, then it cannot be supported during increases in intra-abdominal pressure (Zacharin 1980). Although the role of the interaction between parts has been studied in anterior vaginal prolapse (AVP) (Chen et al. 2006; Chen et al. 2009), the posterior vaginal wall was not considered in those studies. A mechanical interaction between the anterior and posterior compartments that can diminish or increase prolapse is possible but as yet unstudied.

Each of these hypotheses concerning posterior prolapse are plausible. The next step in our scientific investigation is to test each of these hypotheses. We will seek to

develop an overall unifying disease model that can be used as the basis for experiments that will test these individual hypotheses to establish the relative contribution each makes to the presence and size of the posterior prolapse.

1.3 Hypotheses and Specific Aims

1.3.1 Working hypothesis

In this dissertation we hypothesize that the occurrence, size and type of posterior vaginal prolapse is not explained by failure of any single structure; rather it involves failure of connective tissue supports at two, and possibly up to 20, anatomical sites, along with impairment of the levator ani muscle.

1.3.2 Structure of the Dissertation

This dissertation is presented in the form of a series of manuscripts. Chapter 2, 3, 4, 5, 6, 7, 8, and 9 will be written as individual papers, including testable hypotheses, a main body and references. Then a General Discussion (Chapter 10) will link these papers together and consider the contributions of the individual chapters to a hopefully improved understanding of the biomechanics of POP, particularly PVP. It will also consider the strengths and weaknesses of the approaches, and whether the contributions have advanced the literature in any way. A brief Conclusions (Chapter 11) section will summarize the conclusions from each chapter, and from the dissertation as a whole. Finally, a chapter with suggestions for future research (Chapter 12) is included, as are Appendices.

1.3.3 Specific aims

The specific aims are as follows:

Aim 1: MR-based anatomical study of normal pelvic floor anatomy (Chapters 2 & 3)

Chapters 2 and 3 will investigate the pelvic floor anatomy of healthy women based on *in vivo* MR images. POP is associated with changes in vaginal size, shape, and position. So, Chapter 2 first develops a technique to quantify vaginal dimension and reports findings on their relationship to the demographic characteristics of 84 healthy women. Based on the finding of Chapter 2, in Chapter 3 a detailed geometric three-dimensional (3-D) interactive model of pelvic floor of an average dimensioned pelvic floor is created. This includes 23 potential structures that may be involved in pelvic organ prolapse. Those structures include the muscles, ligaments, and fascia of the pelvic floor and the organs it supports. Bones, blood vessels, and the perineum are illustrated as well. The technique used in Chapters 2 and 3 will also be used in Chapters 4, 5, 6 and 7. Results of Chapters 2 and 3 will be utilized in formulating Aim 4.

Aim 2: Investigate the pelvic organ prolapse shape and position changes at maximal Valsalva seen in 3-D MRI-based models (Chapters 4 & 5)

Chapter 4 studies the posterior vaginal prolapse shape and position changes at maximal Valsalva seen in 3-D MRI-based models. Two-dimensional magnetic resonance imaging (MRI) of PVP has been studied but the 3-D mechanism underlying it is poorly understood. With 3-D models of 10 normal controls and 10 prolapse cases, the main geometric phenomena of PVP are found and defined. The results of Chapter 4 provide the geometric basis for an accurate computer model and a check on the results in Aim 4.

Although the main purpose of the dissertation is to understand the mechanism underlying the development of PVP, in reality the main two types of prolapse such as AVP and PVP may occur at the same time, but in differing degrees. This suggests AVP and PVP may result from similar failures but different mechanisms. Chapter 5 studies the AVP in 3-D using MR imaging and will function as a complementary research to help understand more of the mechanism underlying the most common form of pelvic organ prolapse, AVP. The results of Chapter 5 will also provide insights into Aim 4 to help understand how PVP can develop without AVP.

Aim 3: Determine the contribution of fascial failures to prolapse (Chapters 6 & 7)

Chapters 6 and 7 investigate the failure of fascia and their contribution to prolapse. Chapter 6 focuses on the "Level 1" supports including cardinal and uterosacral ligaments. Based on one case and control study (10 cases and 10 controls), the apical support system is analyzed based on 3-D MRI-based prolapse and healthy models. Chapter 7 focuses on the "Level 2" supports including the arcus tendineus fascia pelvis (ATFP) and arcus tendineus levator ani (ATLA). This study analyzes the 3-D MRI-based arcus models of subjects with unilateral defects. Results of Chapters 6 and 7 will provide the basis for creating and validating the computer simulation models in Aim 4.

Aim 4: Biomechanical modeling of posterior vaginal prolapse (Chapters 8 & 9)

Chapters 8 and 9 will use data from Chapters 2 through 7 to develop and validate 2- and 3-D computer-based models, respectively, of the pelvic organ support system. The

objective is to identify the interactions between muscle and connective tissue failures, and organ competition that lead to prolapse.

References

Ashton-Miller, J. A., & DeLancey, J. O. L. (2009). On the biomechanics of vaginal birth and common sequelae. *Annual Review of Biomedical Engineering* (Vol. 11, pp. 163-176).

Ashton-Miller, J. A., Howard, D., & DeLancey, J. O. (2001). The functional anatomy of the female pelvic floor and stress continence control system. *Scand J Urol Nephrol Suppl*(207), 1-7; discussion 106-125.

Baessler, K., & Schuessler, B. (2006). Anatomy of the sigmoid colon, rectum, and the rectovaginal pouch in women with enterocele and anterior rectal wall procidentia. *Clin Anat, 19*(2), 125-129.

Bharucha, A. E., Wald, A., Enck, P., & Rao, S. (2006). Functional anorectal disorders. *Gastroenterology, 130*(5), 1510-1518.

Blanchard, K. A., Vanlangendonck, R., & Winters, J. C. (2006). Recurrent pelvic floor defects after abdominal sacral colpopexy. *J Urol, 175*(3 Pt 1), 1010-1013; discussion 1013.

Boyles, S. H., Weber, A. M., & Meyn, L. (2003). Procedures for pelvic organ prolapse in the United States, 1979-1997. *Am J Obstet Gynecol, 188*(1), 108-115.

Boyles, S. H., Weber, A. M., & Meyn, L. (2004). Ambulatory procedures for urinary incontinence in the United States, 1994-1996. *Am J Obstet Gynecol, 190*(1), 33-36.

Burrows, L. J., Meyn, L. A., Walters, M. D., & Weber, A. M. (2004). Pelvic symptoms in women with pelvic organ prolapse. *Obstet Gynecol, 104*(5 I), 982-988.

Chen, L., Ashton-Miller, J. A., & DeLancey, J. O. (2009). A 3D finite element model of anterior vaginal wall support to evaluate mechanisms underlying cystocele formation. *J Biomech, 42*(10), 1371-1377.

Chen, L., Ashton-Miller, J. A., Hsu, Y., & DeLancey, J. O. (2006). Interaction among apical support, levator ani impairment, and anterior vaginal wall prolapse. *Obstet Gynecol, 108*(2), 324-332.

Comiter, C. V., Vasavada, S. P., Barbaric, Z. L., Gousse, A. E., & Raz, S. (1999). Grading pelvic prolapse and pelvic floor relaxation using dynamic magnetic resonance imaging. *Urology, 54*(3), 454-457.

Cortes, E., Reid, W. M., Singh, K., & Berger, L. (2004). Clinical examination and dynamic magnetic resonance imaging in vaginal vault prolapse. *Obstet Gynecol, 103*(1), 41-46.

DeLancey, J. O. (1992). Anatomic aspects of vaginal eversion after hysterectomy. *Am J Obstet Gynecol, 166*(6 Pt 1), 1717-1724.

DeLancey, J. O. (1994). Structural support of the urethra as it relates to stress urinary incontinence: the hammock hypothesis. *Am J Obstet Gynecol, 170*(6), 1713-1720.

Dietz, H. P., & Steensma, A. B. (2005). Posterior compartment prolapse on two-dimensional and three-dimensional pelvic floor ultrasound: the distinction between true rectocele, perineal hypermobility and enterocele. *Ultrasound in Obstetrics & Gynecology, 26*(1), 73-77.

Ellerkmann, R. M., Cundiff, G. W., Melick, C. F., Nihira, M. A., Leffler, K., & Bent, A. E. (2001). Correlation of symptoms with location and severity of pelvic organ prolapse. *Am J Obstet Gynecol, 185*(6), 1332-1337; discussion 1337-1338.

Ghetti, C., Gregory, W. T., Edwards, S. R., Otto, L. N., & Clark, A. L. (2005). Severity of pelvic organ prolapse associated with measurements of pelvic floor function. *Int Urogynecol J, 16*(6), 432-436.

Gilpin, S. A., Gosling, J. A., Smith, A. R., & Warrell, D. W. (1989). The pathogenesis of genitourinary prolapse and stress incontinence of urine. A histological and histochemical study. *Br J Obstet Gynaecol, 96*(1), 15-23.

Halligan, S., Bartram, C., Hall, C., & Wingate, J. (1996). Enterocele revealed by simultaneous evacuation proctography and peritoneography: does "defecation block" exist? *AJR Am J Roentgenol, 167*(2), 461-466.

Hoyte, L., Jakab, M., Warfield, S. K., Shott, S., Flesh, G., & Fielding, J. R. (2004). Levator ani thickness variations in symptomatic and asymptomatic women using magnetic resonance-based 3-dimensional color mapping. *American Journal of Obstetrics and Gynecology, 191*(3), 856-861.

Hunskaar, S., Burgio, K., Clark, A., Lapitan, M., Nelson, R., Sillen, U., et al. (2005). Epidemiology of urinary (UI) and faecal (FI) incontinence and pelvic organ prolapse (POP). *Incontinence, 1*, 255-312.

Jelovsek, J. E., & Barber, M. D. (2006). Women seeking treatment for advanced pelvic organ prolapse have decreased body image and quality of life. *Am J Obstet Gynecol, 194*(5), 1455-1461.

Jelovsek, J. E., Maher, C., & Barber, M. D. (2007). Pelvic organ prolapse. *Lancet, 369*(9566), 1027-1038.

Kuhn, R. J., & Hollyock, V. E. (1982). Observations on the anatomy of the rectovaginal pouch and septum. *Obstet Gynecol, 59*(4), 445-447.

Leffler, K. S., Thompson, J. R., Cundiff, G. W., Buller, J. L., Burrows, L. J., & Schon Ybarra, M. A. (2001). Attachment of the rectovaginal septum to the pelvic sidewall. *Am J Obstet Gynecol, 185*(1), 41-43.

Margulies, R. U., Hsu, Y., Kearney, R., Stein, T., Umek, W. H., & DeLancey, J. O. (2006). Appearance of the levator ani muscle subdivisions in magnetic resonance images. *Obstet Gynecol, 107*(5), 1064-1069.

Meschia, M., Pifarotti, P., Bernasconi, F., Magatti, F., Vigano, R., Bertozzi, R., et al. (2006). Tension-free vaginal tape (TVT) and intravaginal slingplasty (IVS) for stress urinary incontinence: a multicenter randomized trial. *Am J Obstet Gynecol, 195*(5), 1338-1342.

Olsen, A. L., Smith, V. J., Bergstrom, J. O., Colling, J. C., & Clark, A. L. (1997). Epidemiology of surgically managed pelvic organ prolapse and urinary incontinence. *Obstet Gynecol, 89*(4), 501-506.

Richardson, A. C. (1993). The rectovaginal septum revisited: its relationship to rectocele and its importance in rectocele repair. *Clin Obstet Gynecol, 36*(4), 976-983.

Richardson, A. C. (1996). Female pelvic floor support defects. *Int Urogynecol J Pelvic Floor Dysfunct, 7*(5), 241.

Samuelsson, E. C., Victor, F. T., Tibblin, G., & Svardsudd, K. F. (1999). Signs of genital prolapse in a Swedish population of women 20 to 59 years of age and possible related factors. *Am J Obstet Gynecol, 180*(2 Pt 1), 299-305.

Schaffer, J. I., Wai, C. Y., & Boreham, M. K. (2005). Etiology of pelvic organ prolapse. *Clin Obstet Gynecol, 48*(3), 639-647.

Silva, W. A., Pauls, R. N., Segal, J. L., Rooney, C. M., Kleeman, S. D., & Karram, M. M. (2006). Uterosacral ligament vault suspension: five-year outcomes. *Obstet Gynecol, 108*(2), 255-263.

Subak, L. L., Waetjen, L. E., van den Eeden, S., Thom, D. H., Vittinghoff, E., & Brown, J. S. (2001). Cost of pelvic organ prolapse surgery in the United States. *Obstet Gynecol, 98*(4), 646-651.

Torricelli, P., Pecchi, A., Caruso Lombardi, A., Vetruccio, E., Vetruccio, S., & Romagnoli, R. (2002). Magnetic resonance imaging in evaluating functional disorders of female pelvic floor. *La risonanza magnetica nella valutazione dei disordini funzionali del pavimento pelvico femminile, 103*(5-6), 488-500.

Zacharin, R. F. (1980). Pulsion enterocele: review of functional anatomy of the pelvic floor. *Obstet Gynecol, 55*(2), 135-140.

CHAPTER 2

MR-BASED STUDY OF VAGINAL DIMENSIONS AND MORPHOLOGY

Abstract

Objectives: Changes in vaginal shape and size can play important roles in pelvic organ prolapse. This study presents a technique for quantifying vaginal dimensions and reports preliminary findings in healthy women.

Methods: MRI scans of 84 women (age: 46 ± 9 years) were selected from the control group of an ongoing case - control study. Each had a uterus and normal uterine support. Supine, multi-planar MR imaging was performed. ImageJ v1.44 was used to establish the vaginal and cervical locations in both axial and mid-sagittal scans. Vaginal width was assessed at 5 equally spaced locations based on axial scans. Location and dimension of cervix was also assessed. A MATLAB™ program was used for data analysis.

Results: There was more variation in vaginal width proximally than distally. The average location of cervical os is about 3 mm left of the pelvic midline (51 cases on left and 33 on right side). The mean (± SD) lengths for the following structures were: anterior vaginal wall (cervix not included): 62 ± 10 mm; the cervix: 39 ± 10 mm; and the posterior vaginal wall 97 ± 18 mm.

Conclusions: Vaginal dimensions exhibit large inter-individual variations. The average location of the cervical os was to the left of the pelvic mid-sagittal plane, and the left side

of the vagina extends further from the midline than the right side, on average, and there was more in variation in vaginal dimension and shape in the upper vagina than distally.

Key words: vagina, pelvic floor, dimension, shape, 3D model, magnetic resonance imaging, anatomy

2.1 Introduction

Changes in vaginal shape and size can play important roles in pelvic organ prolapse (Chen et al. 2009). Knowing what is abnormal can only be determined after the full extent of variation within a normal population is known.

MR imaging has provided high quality images to help analyzing female pelvic floor system in a non-invasive way (Tan et al. 1998; Margulies et al. 2006; Hsu et al. 2008; Luo et al. 2011). Recent studies (Hsu et al. 2005; Barnhart et al. 2006) have shown the ability to use MR images to measure the vaginal dimensions in 2- or 3- dimensional images (2-D or 3-D), which also provide useful information on vaginal length, thickness, fornix length, etc. However, the sample size and age range of those studies were small. Other studies used casting to obtain and analyze variation in vaginal shape (Pendergrass et al. 1991; Pendergrass et al. 1996, 2000). However a methodological limitation is the possibility that the casting compound artificially distorted the vagina. So, we are unaware that the variation in the normal range of vaginal size and shape has been systematically documented with a non-contact measurement method. In addition, there is no method for comparing vaginal morphology from women of different sizes and body types.

This study was therefore undertaken to address these knowledge gaps. We used a secondary analysis of data gathered from a larger on-going case-control study of pelvic

organ prolapse (IRB # 1999-0395), but using a new technique for quantifying the vaginal dimensions and shape that we described in this paper. We tested the hypotheses that vaginal dimension and shape cannot be explained by any single demographic characteristic and the degree of variation will not be uniform along the vaginal length. The results of this study could help designing products related to pelvic organ prolapse, such as pessary, surgical tools, etc.

2.2 Materials and Methods

MRI scans of 84 women with normal support (controls) were selected from an ongoing University of Michigan institutional review board-approved (IRB # 1999-0395) case-control study of pelvic organ prolapse. Women in the control group were recruited by newspaper and radio advertisement for healthy volunteers and had to be asymptomatic and have normal vaginal support with all pelvic organ prolapse quantification (POP-Q) points < -1 cm. None of the subjects had previously undergone hysterectomy or prior pelvic floor surgery.

As described in our previous work (Larson et al. 2010; Luo et al. 2011; Larson et al. 2012; Luo et al. 2012), each subject underwent supine multi-planar, two-dimensional, fast spin, proton density MR imaging both at rest and during maximal Valsalva using a 3 T superconducting magnet (Philips Medical Systems Inc, Bothell, WA) with version 2.5.1.0 software. At rest, 30 images were serially obtained in the axial, sagittal, and coronal planes using a 20x20 cm field of view, 4 mm slice thickness, and a 1 mm gap between slices.

ImageJ v1.44 was used to establish the vaginal and cervical location and contour in both axial and mid-sagittal scans.

Figure 2.1 shows the method for the vaginal width measurement. On the axial scan, and moving in a distal to proximal direction, we began to trace the vaginal wall in the scan where we identified the transition from the labia being in the sagittal plane to the vagina lying in the frontal plane, and we ended the tracing when we could no longer see either the anterior vaginal wall (AVW) or posterior vaginal wall (PVW). The AVW and PVW were first traced together by considering that they were in contact with one another, and then once they were at least 1 cm separate (on the axial scan), they were traced separately. This process was made easier by some of the women having had ultrasound gel inserted into the vagina.

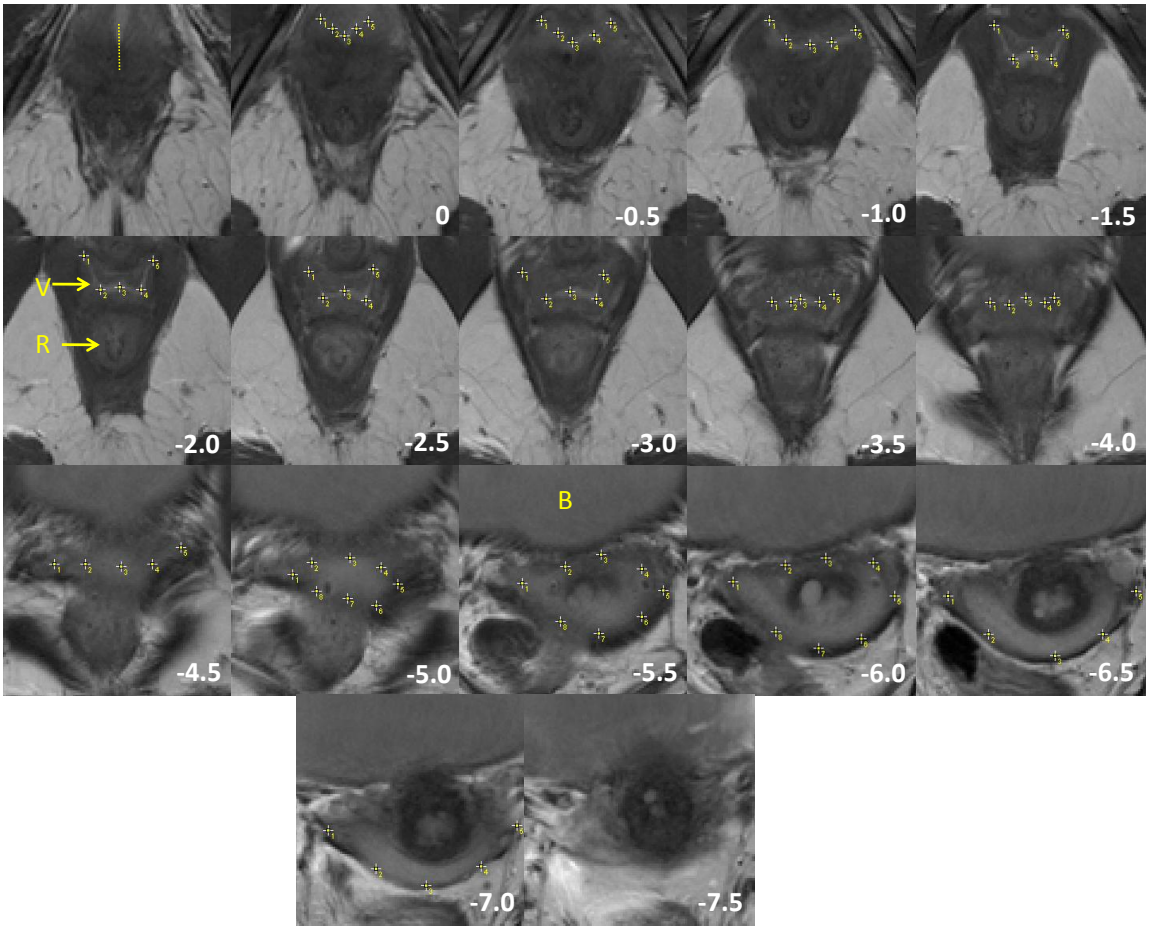

Figure 2.1 Vaginal width measurement. Axial slices with 5 mm intervals are arranged from caudal to cephalad from the image in the upper left. The first vaginal wall tracing (image 0) was

made when there was transition from ‘vertical’ to ‘horizontal’. Last vaginal wall tracing (image -7.0) was made on the last slice where vaginal wall can be seen. Points 1 to 5 are used to identify contacted AVW and PVW (images 0 to -4.0). Points 1 to 8 are used to identify AVW (1 to 5) and PVW (1, 8, 7, 6 and 5) from images -4.5 to -6.0, where the biggest gap between AVW and PVW is at least 1 cm. When only PVW is visible, points 1 to 5 are used to only identify PVW (images -6.5 to -7.0). Point 1 is always at the most anatomical lateral right and point 5 is always at the most anatomical lateral left. V: vagina; R: rectum; B: bladder.

The cervix tracing based on axial slice was shown in Figure 2.2. The axial tracing of cervix is used to identify the cervical width and the location cervical os.

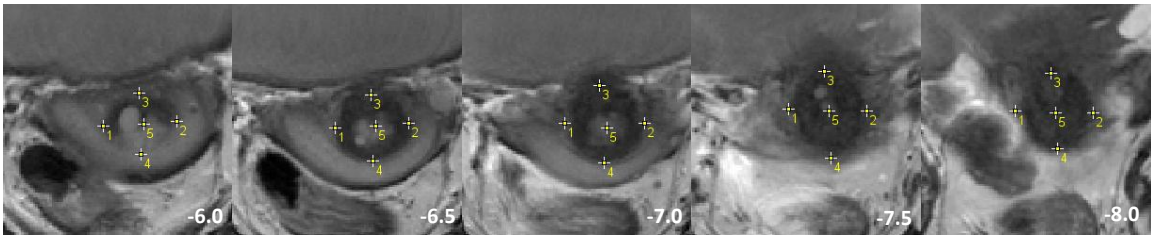

Figure 2.2 Cervix measurement. Five points on axial slices were used to identify the cervix location. Point 1 and point 2 are on the most anatomical lateral right and left. Point 3 and point 4 are on the most anterior and posterior. Point 5 is at the center of the cervix. Especially, the first point 5 (slice -6.0 cm) identified the location of the cervical os.

In order to identify the symmetry of the vaginal wall and cervix, a reference bony pelvis mid plane was created using three points (Figure 2.3): one point at the middle of pubic symphysis and two points at the lower center and middle center of the sacrum.

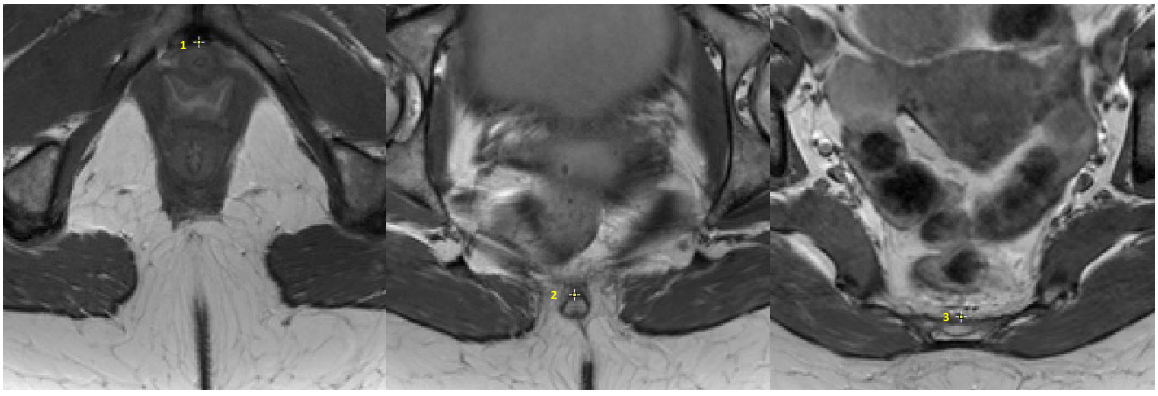

Figure 2.3 Bony pelvis mid plane. The mid plane was identified using three points with specific landmarks on different axial slices: Point 1 is at the center of pubic symphysis, Point 2 is at the center of lower sacrum, and Point 3 is at the center of middle sacrum.

To compare the regional differences in vaginal width among different women, the vaginal width measurement result was resampled at five locations from the hymen (0%) to the top of vagina (100%) (Figure 2.4).

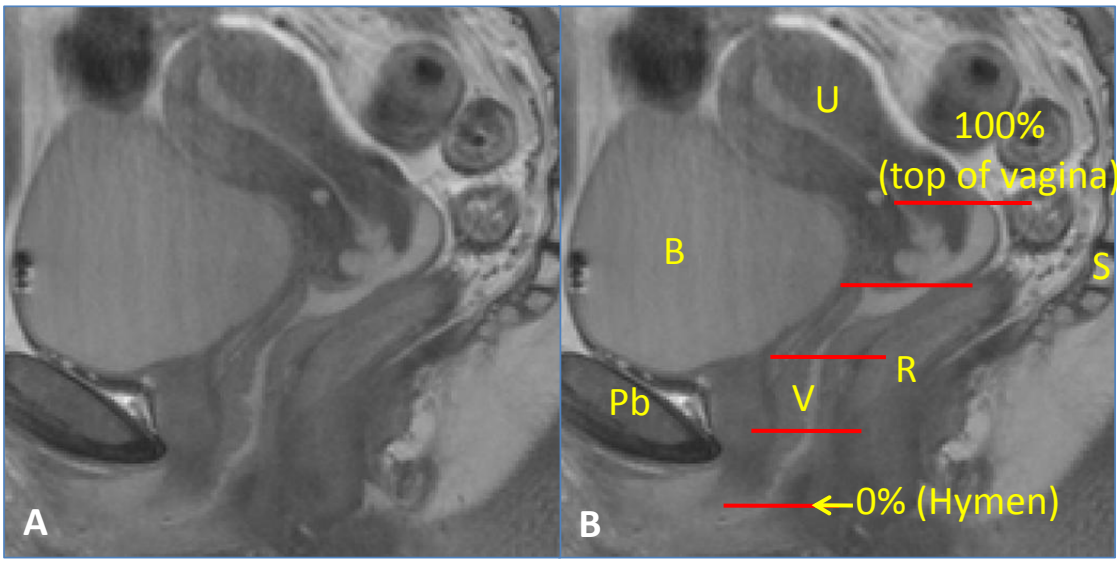

Figure 2.4 Vaginal width. (A) and (B) middle sagittal MR image seen from left without and with labels, respectively. To compare transverse vaginal width at different locations along vaginal canal among different subjects, the width was resampled at five locations: 0% (level of hymen), 25%, 50%, 75%, and 100% (top of vagina). Pb: pubic bone; U: uterus; V: vagina; R: rectum; B: bladder; S: sacrum.

Vaginal wall length and configuration was measured in the mid sagittal plane for the vagina (Figure 2.5). In the mid sagittal plane of the vagina, the AVW, PVW and cervix were identified separately. The AVW was traced from the introitus to the anterior fornix. The PVW was traced from the introitus to the posterior fornix. Five points was used to identify the cervix location, with first point at the anterior fornix, third point at the cervical os, and the fifth point at the posterior fornix. To analyze the variation in vaginal wall shape among different women, a local coordinate system was created using bony landmarks: no significant differences were found between women with and without pelvic organ prolapse (Berger et al. 2012). A reference axis OX was created using the

sacrococcygeal-inferior pubic point (SCIPP) line, the axis OY is then perpendicular to the SCIPP line.

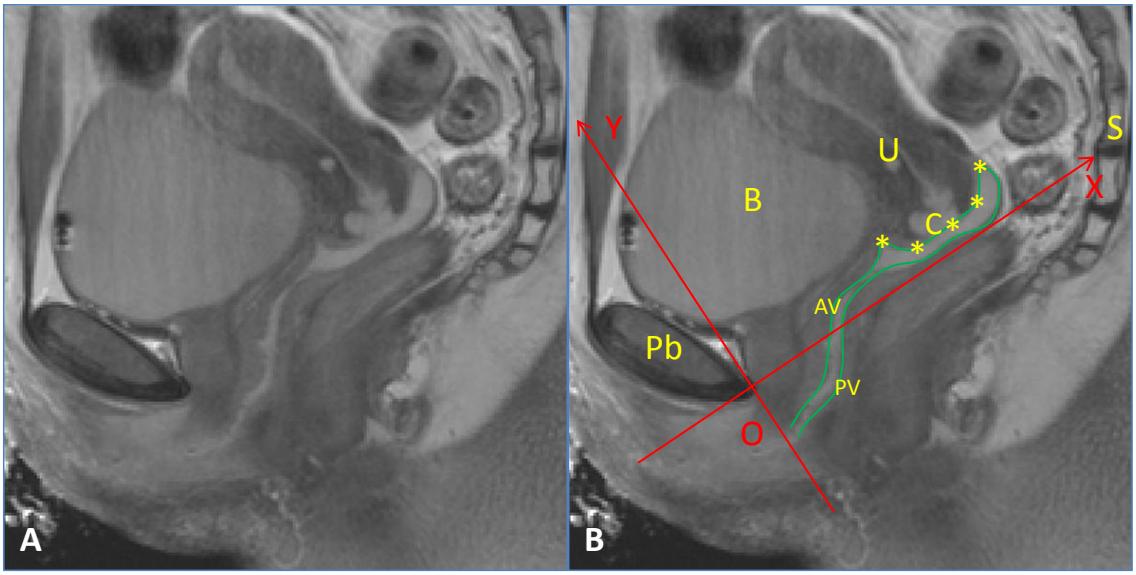

Figure 2.5 Vaginal wall length and shape analyses system. (A) and (B), middle sagittal MR image seen from left without and with labels, respectively. In panel (B), anterior vaginal wall and posterior vaginal wall are identified with green lines (in reality, sampling points were put along the lines in Image J to get the coordinates); cervix is identified from anterior fornix to the posterior fornix using five points, with the third point at cervical os. To compare vaginal wall size and shape among different subjects, a local coordinate system (XOY in red) was created to quantify the morphology. Axis OX is the sacrococcygeal-inferior pubic point (SCIPP) line. Pb: pubic bone; B: bladder; U: uterus; C: cervix; AV: anterior vaginal wall; PV: posterior vaginal wall; and S: sacrum.

A MATLAB™ program was used for data analysis, including analyzing the vaginal dimension, transforming MRI coordinates into local coordinates, and analyzing the vaginal shape. Vaginal width was measured as a frontal plane diameter, and also along the curve of the AVW and also the PVW in certain transverse plane sections. In this dissertation, these are defined as the 'vaginal diameter', and the AVW or PVW 'curved width', respectively.

The Pearson correlation analysis was applied to analyze the correlation between the vaginal dimension and the main demographics such height, age, weight, BMI and parity. Two-sided independent t tests were used with significance levels at $p < 0.05$, $p < 0.01$ and $p < 0.001$.

2.3 Results

Subjects' characteristics and POP-Q values are shown in Table 2.1. No subjects in this group had undergone a hysterectomy. Among the 84 subjects, only two of them were above 60 years, one was 67 years and another was 70 years. There were 6 nulliparous subjects among the 84 women.

Table 2.1 Demographics

Characteristics	n=84	Minimum	Maximum
Age (yrs)[a]	45.5(8.9)	28	70
Height (in)[a]	64.3(3.1)	50.3	72
Weight (lbs)[a]	161.4(33.7)	100	265
BMI (kg/m^2)[a]	27.5(5.5)	18.7	44.1
Parity[a]	2.1(1.2)	0	5
Race[b]			
Caucasian	77(92%)		
POP-Q (cm)[a]			
Aa	-1.4(1.0)	-3	1
Ba	-1.4(1.0)	-3	1
C	-6.6(1.3)	-10	-3
D	-9.0(1.3)	-13	8.5
Ap	-1.6(0.9)	-3	0
Bp	-1.5(1.0)	-3	0
GHrest	3.3(1.0)	1	5.5
LHrest	6.3(1.1)	4	11
TVL	10.8(1.4)	7	14

GHrest denotes genital hiatus at rest; *LHrest*, levator hiatus at rest; and *TVL*, total vaginal length

[a] Data are mean (SD)

[b] Data are n (%)

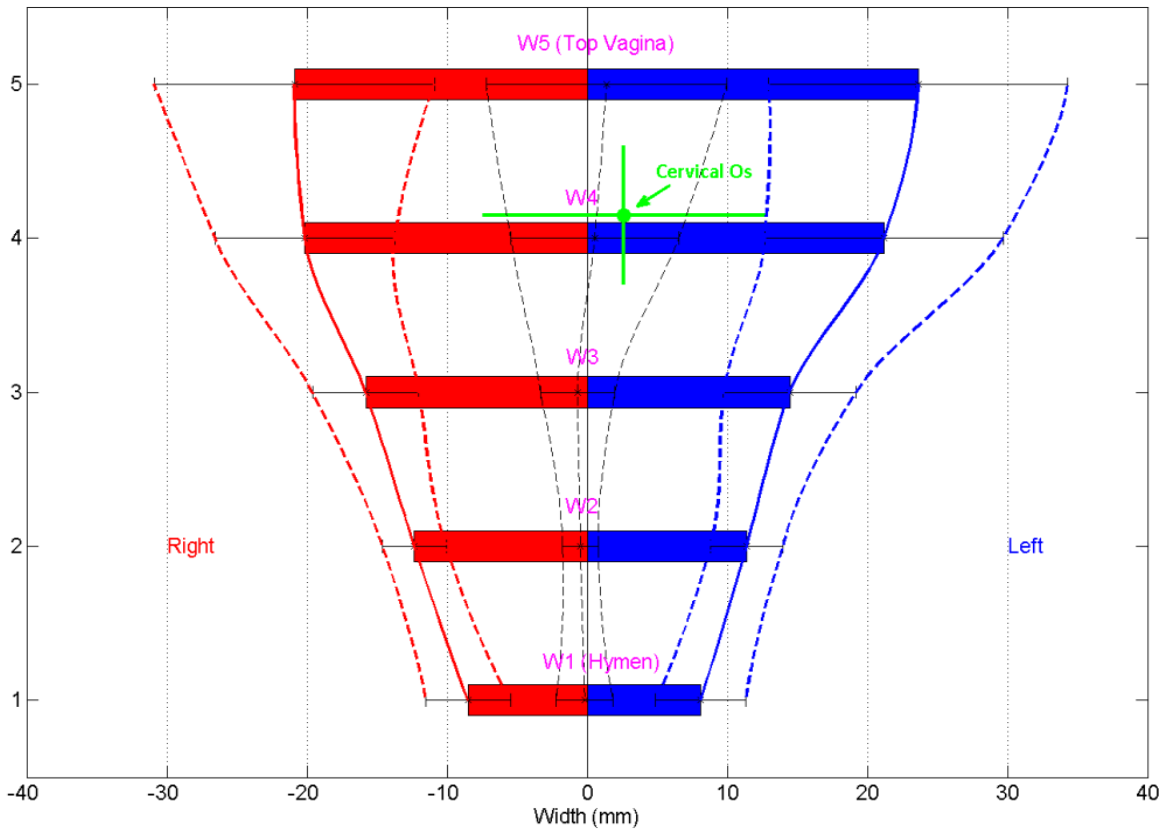

Figure 2.6 Vaginal dimension and symmetry analysis. Vaginal width and symmetry information are shown in a bar plot at five equal locations as W1 to W5. W1 denotes vaginal width just above the hymen, W5 at vagina top, and other three (W2, W3, and W4) are equally located between W1 and W5. Vaginal width mean (solid) and standard deviation (dash) on both left and right sides of bony middle plane are also shown. Zero on axis x denotes the pelvic mid line. Thin black lines show the average location (solid) and standard deviation (dash) of mid vagina point. Average location and standard deviation of cervical Os are shown in green.

Descriptive statistics for vaginal width and symmetry analysis are shown in Figure 2.6. There was more variation in vaginal width at the top of the vagina than distally. On average, the vagina is essentially symmetric relative to the pelvic mid-sagittal plane, but again there was more variation proximally. W1 (17 $\pm$5 mm) was a little more towards to the right, W2 (24 $\pm$4 mm) and W3 (30 $\pm$7) mm were located more towards to the right too, but W4 (41 $\pm$9 mm) and W5 (45 $\pm$12 mm) were more towards to the left. The left side of the vagina was wider than the right side, on average. The average location

of cervical os was 83% of vaginal length and about 3 mm left from the pelvic mid-sagittal plane (51 cases on left and 33 on right side).

The vaginal wall shape analysis is shown in Figure 2.7. Again, there was more in variation in vaginal length and shape proximally than distally. The average location of introitus is (12, -12) mm in the local coordinate system, which is 17 mm away from the local origin (pubic symphysis). All the locations of the cervix lay above the SCIPP line although a large variation exists. The coordinates for the average location of cervix was (53, 28) (anterior fornix), (59, 21), (66, 24) (cervical os), (74, 22) and (81, 31) (posterior fornix) in mm. The length of the SCIPP line was 115 ± 9 mm, and the angle between SCIPP line and horizontal line was 35 ± 6 degree.

Figure 2.8 shows only cervix location as in Figure 2.7. Figure 2.9 shows the vaginal shape aligned with the average location with introitus.

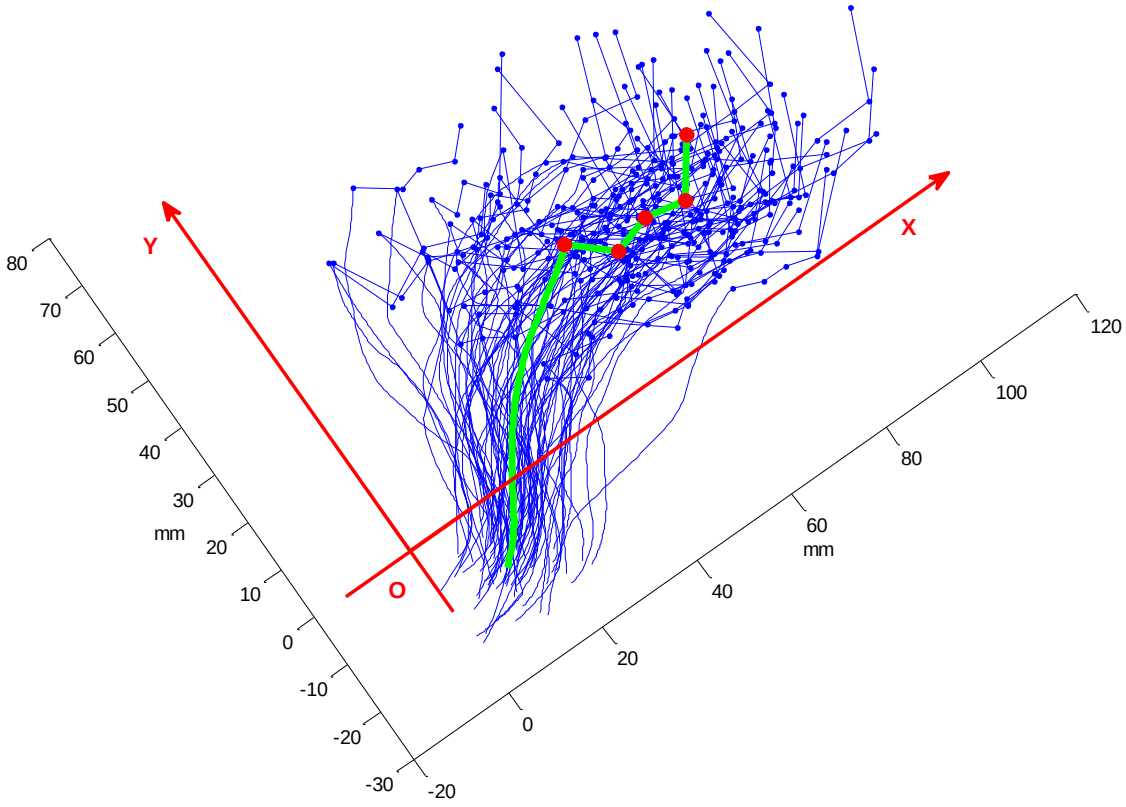

Figure 2.7 Vaginal shape analysis. Middle sagittal shape and mean shape for anterior vaginal wall and cervix are shown in the local coordinate system with OX as SCIPP line (average angle of SCIPP line from horizontal line is 35.02° and the average length is 115 mm for the 84 subjects). Blue lines are profiles for 84 subjects with little blue dots showing the cervix location. Green line is the average shape with big red dots showing the cervix location.

The main vaginal dimension and correlation with height, age, weight, BMI and parity were shown in Table 2.2. The AVW length was 62 ± 10 mm (28 ~ 84 mm) and the PVW length was 97 ± 18 mm (51 ~ 144 mm) which is about 3 cm longer than the AVW length.

From this table, the vaginal dimension cannot be explained by any single demographic parameter, such as height, or weight. Height was only positively correlated with PVW length, anterior fornix length, SCIPP line length and VW 'straight line' width W5, with p value < 0.05. Age was related with posterior fornix length (negatively) and VW driving width W2 and W5 (positively), with a p value < 0.05. Age was more related

with PVW length (negatively), anterior fornix length (negatively) and PVW curved width W4 (positively), with a *p* value < 0.01. Age was highly related with SCIPP line angle (negatively), VW frontal plane diameter width W3 and W4 (positively), AVW curved width W3 and W4 (positively), and PVW curved width W3 (positively), *p* value < 0.001. Weight was only positively correlated with SCIPP line length, AVW width W3 along the vaginal margin and PVW width W2 along the vaginal margin, *p* value < 0.05. BMI was not correlated with vaginal dimensions. Surprisingly, parity was only correlated positively with AVW width W3 along the vaginal margin with *p* value < 0.05.

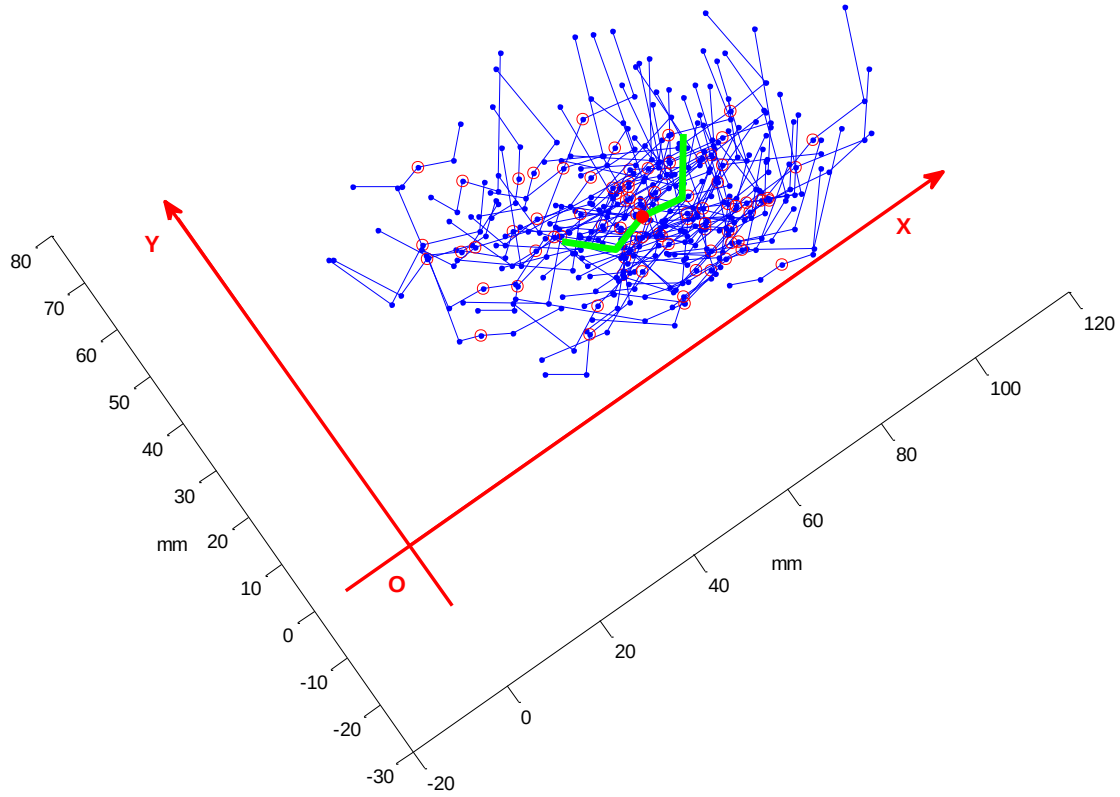

Figure 2.8 Cervix location. Middle sagittal shape and mean shape for cervix only, are shown in the local coordinates system with OX as SCIPP line. Blue lines are for 84 subjects and Green line is the average shape, with big red dots showing the cervix os location.

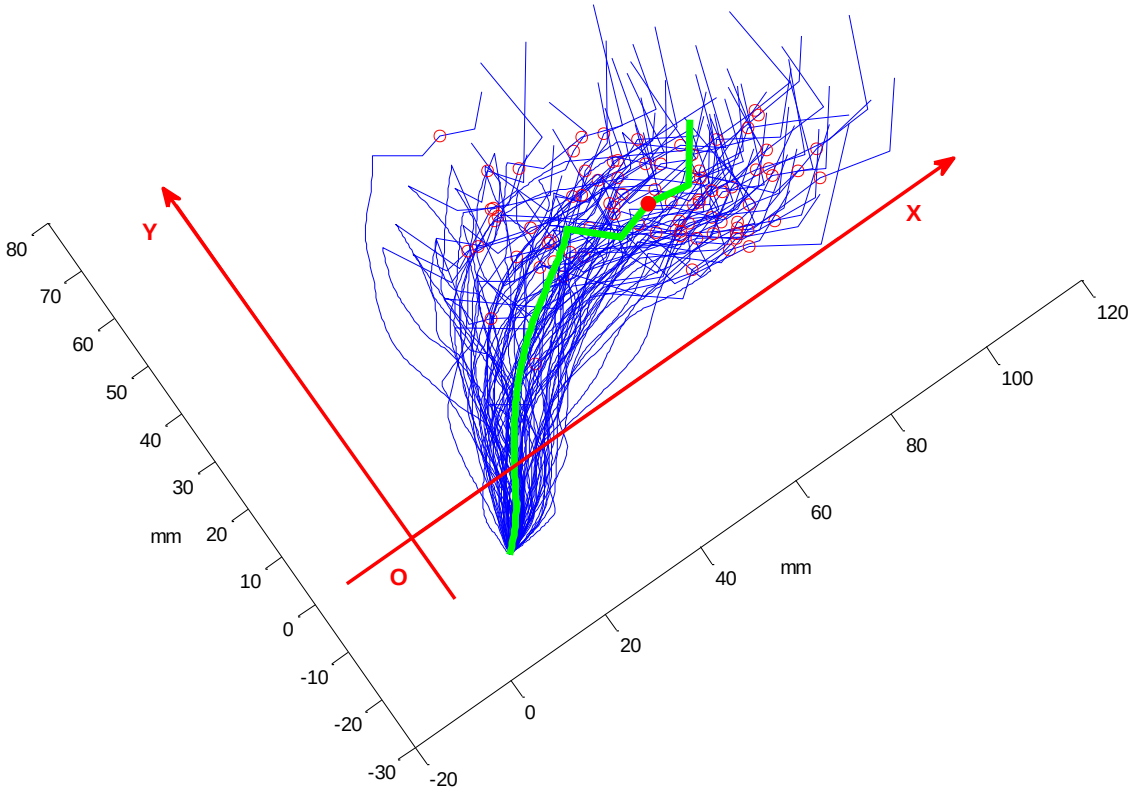

Figure 2.9 Vaginal shape aligned with introitus. Middle sagittal shape and mean shape for anterior vaginal wall and cervix are shown in the local coordinates system with OX as SCIPP line, aligned at the average location of introitus, with Blue lines are for 84 subjects and Green line is the average shape, with red dots showing the cervix os location.

Table 2.2 Correlation between vaginal dimension and demographics

Parameters	(n=84)	Height		Age		Weight		BMI		Parity	
	Value[a]	Correlation	*p* value[b]	Correlation	*p* value[b]	Correlation	*p* value[b]	Correlation	*p* value[b]	Correlation	*p* value[b]
AVW Length	62(10)	.132	.232	-.168	.128	-.141	.202	-.196	.074	-.026	.812
PVW Length	97(18)	.216*	.048	-.290**	.007	.056	.614	-.048	.666	.100	.364
Anterior Fornix Length	18(7)	.236*	.031	-.322**	.003	.187	.089	.075	.498	-.017	.878
Posterior Fornix Length	21(5)	.105	.340	-.267*	.014	.196	.075	.150	.174	.059	.592
Cervix Width	25(5)	.127	.252	-.030	.784	.167	.128	.123	.264	.081	.462
SCIPP Line Length	115(9)	.272*	.012	-.188	.087	.275*	.011	.148	.180	-.063	.569
SCIPP Line Angle	$35^{o}(6^{o})$	-.054	.623	-.398***	.000	-.060	.591	-.035	.752	.103	.351
Vaginal Diameter W1	17(5)	.141	.201	.125	.258	.076	.491	.022	.841	.026	.814
Vaginal Diameter W2	24(4)	-.094	.394	.226*	.039	.013	.907	.041	.712	.139	.207
Vaginal Diameter W3	30(7)	.148	.180	.376***	.000	-.089	.420	-.194	.077	.190	.084
Vaginal Diameter W4	41(9)	.115	.299	.374***	.000	-.072	.517	-.158	.150	.137	.213
Vaginal Diameter W5	45(12)	.221*	.043	.232*	.033	-.084	.447	-.201	.067	.053	.633
AVW Curved Width W1	19(6)	.129	.242	.202	.066	.171	.119	.118	.287	-.044	.693
AVW Curved Width W2	32(5)	.025	.824	.086	.439	.225*	.039	.199	.070	.041	.714
AVW Curved Width W3	35(7)	.060	.586	.376***	.000	-.064	.561	-.118	.286	.236*	.030
AVW Curved Width W4	47(13)	.139	.209	.387***	.000	.050	.649	-.050	.652	.122	.267
AVW Curved Width W5	50(14)	.172	.118	.145	.188	-.096	.386	-.201	.067	.060	.590
PVW Curved Width W1	19(6)	.129	.242	.202	.066	.171	.119	.118	.287	-.044	.693
PVW Curved Width W2	32(5)	.016	.884	.077	.486	.227*	.038	.206	.060	.050	.649
PVW Curved Width W3	36(8)	.064	.566	.382***	.000	.000	.998	-.059	.591	.184	.094
PVW Curved Width W4	46(12)	.137	.215	.339**	.002	.029	.795	-.070	.525	.151	.171
PVW Curved Width W5	50(14)	.149	.176	.212	.053	-.073	.512	-.163	.139	.036	.746

[a] Data are mean (SD), unit is mm except unit for SCIPP Line Angle is degree

[b] *p* value is for pearson correlation

***. Correlation is significant at the 0.001 level (2-tailed).

**. Correlation is significant at the 0.01 level (2-tailed).

*. Correlation is significant at the 0.05 level (2-tailed).

2.4 Discussion

The hypotheses were supported. Although there was large variation in vaginal dimension and shape found in these 84 healthy women, no single demographic characteristic could explain the variation in vaginal dimensions, and there was more variation in vaginal dimension and shape proximally than distally.

The vagina is narrower caudally and becomes wider proximally based on the analysis of axial images. In the mid sagittal plane, although the curves of AVW have large variation at the top, the bottom of curves are quite near each other. Those characteristics can be explained by the presence of the levator ani muscle reducing the distal variability through the imposition of a spatial constraint in the 'high pressure' zone. In this region the vagina is surrounded by the U-shaped levator ani at the back and sides of the vagina, which contract to close the hiatus and support the pelvic floor organs (Ashton-Miller and DeLancey 2009).

Our findings are consistent with other studies (Barnhart et al. 2006) but quantitatively provide more information than they provide. Barnhart found that vaginal width was largest in the proximal vagina, decreased as it passed through the pelvic diaphragm and smallest at the introitus. We have quantified that the absolute variation at the top of vagina (W4: 41 $\pm$9 mm; W5: 45 $\pm$12 mm) is about twice the variation at the bottom (W1: 17 $\pm$5 mm; W2: 24 $\pm$4 mm). There are also similar findings on the location of the introitus and cervical os. The location for the introitus was 12 $\pm$5 and -12 $\pm$5 mm on the left and right sides, but for the cervical os the corresponding measures were 66 $\pm$ 15 and 24 $\pm$10 mm indicating considerably more absolute variation. We also find that the cervical os has 50% more variation along the SCIPP line than perpendicular to the SCIPP

line. Those findings may be also explained by the functional anatomy of the levator ani muscle and the apical supports (DeLancey 1992), which includes the cardinal ligament holding the uterocervical portion vertically and the uterosacral ligament holding the cervix portion horizontally (Ramanah et al. 2012; Chen et al. 2012), but less traction force on the ligaments compared to the levator ani muscle (Bartscht and DeLancey 1988; Ashton-Miller and DeLancey 2009). Thus this helps explain why there is much flexibility in the proximal versus the distal vagina.

Height was positively correlated with PVW length, anterior fornix length, SCIPP line length and VW diameter width W5, with p value < 0.05. The correlation between height and VW diameter W5 is consistent with another study (Barnhart et al. 2006). However, the correlation between height and PVW length was different than the other study (Barnhart et al. 2006). One reason might be that the other study had a smaller sample size and so the correlation result may have arisen by chance, which might be similar here, since the correlation is not very strong here also.

The positive correlation between age and vaginal width is consistent with another study (Barnhart et al. 2006), but in our study we found negative correlation between age and fornix length and PVW length. This might show that with aging and more vaginal activity, the vaginal wall becomes more compliant in the transverse direction. But the lateral margin of the vaginal wall fuses with the levator ani muscle, as arcus tendineus facial pelvis (ATFP) (DeLancey 1992) in the front and posterior arcus tendineus fascia pelvis (Leffler et al. 2001; Hsu et al. 2008) in the back. In the conjoined region the levator fiber direction is longitudinal, while the fiber direction is transverse away from that region. With the effect of fiber direction, the conjoined region was rendered stiffer in

the longitudinal direction while the laterally-located levator ani should be stiffer in the transverse direction. Under low intra-abdominal pressure (IAP), the vaginal wall length was probably constrained in the longitudinal direction, whereas the vaginal width may be constrained by levator ani under higher IAP. Meanwhile, considering the vaginal wall as a non-compressible continuum solid, with larger vaginal width, the length of vaginal wall then becomes smaller.

Surprisingly, parity was only weakly positively correlated with AVW curved width W3 ($p < 0.05$). We did not find a significant correlation between parity and fornix length which has been shown in one study (Barnhart et al. 2006), but not another (Pendergrass et al. 2000). However, because we only had recruited six nulliparous women, our data may not be reliable.

We have showed that the vagina is not symmetric in quantitative terms (top towards left) and cervical os is also more towards to the left (51 in the left versus 33 in the right). In addition, although we have shown there were large variation in vaginal dimensions and shape, we still found several significant correlations between the vaginal dimension and demographic characteristics. That information may be useful for the design of vaginal products.

Several factors must be kept in mind when interpreting the result of these studies. This study has a moderate sample size with selected women having normal support. The MR images were obtained in the supine position, which might systematically affect vaginal shape with respect to the standing posture. As we stated in Methods, the MR images have 4 mm slice thickness, and a 1 mm gap between slices, and this might generate partial volume errors. To avoid large measurement errors, we chose to measure

the vaginal width on axial scans, and to measure the vaginal length on the sagittal scans. It is a limitation that we used gel in the vagina of some women (23 of 84) to help with visualization; in some instances it filled the upper vagina thereby changing the contour and the internal surface of vagina (Barnhart et al. 2001). However, by using gel, it helps us to identify the AVW and PVW separately, and also help to identify the anterior and posterior fornix.

This study is a first step towards analyzing the vaginal dimension and shape of the healthy women. It quantifies vaginal dimensions based on axial and sagittal 2-D images with 3-D coordinates. The results were normalized in order to compare different subjects. In the future, one might study the vaginal shape in 3-D space and divide them statistically into characteristic shapes in order to better understand the role of the vaginal morphology in pelvic organ prolapse.

References

Ashton-Miller, J. A., & DeLancey, J. O. L. (2009). On the biomechanics of vaginal birth and common sequelae. *Annual Review of Biomedical Engineering* (Vol. 11, pp. 163-176).

Barnhart, K., Izquierdo, A., Pretorius, E. S., Shera, D. M., Shabbout, M., & Shaunik, A. (2006). Baseline dimensions of the human vagina. *Hum Reprod, 21*(6), 1618-1622.

Barnhart, K., Pretorius, E. S., Stolpen, A., & Malamud, D. (2001). Distribution of topical medication in the human vagina as imaged by magnetic resonance imaging. *Fertil Steril, 76*(1), 189-195.

Bartscht, K. D., & DeLancey, J. O. (1988). A technique to study the passive supports of the uterus. *Obstet Gynecol, 72*(6), 940-943.

Berger, M. B., Doumouchtsis, S. K., & Delancey, J. O. (2012). Bony pelvis dimensions in women with and without stress urinary incontinence. *Neurourol Urodyn*.

Chen, L., Ashton-Miller, J. A., & DeLancey, J. O. (2009). A 3D finite element model of anterior vaginal wall support to evaluate mechanisms underlying cystocele formation. *J Biomech, 42*(10), 1371-1377.

Chen, L., Ramanah, R., Hsu, Y., Ashton-Miller, J. A., & Delancey, J. O. (2012). Cardinal and deep uterosacral ligament lines of action: MRI based 3D technique development and preliminary findings in normal women. *Int Urogynecol J*.

DeLancey, J. O. (1992). Anatomic aspects of vaginal eversion after hysterectomy. *Am J Obstet Gynecol, 166*(6 Pt 1), 1717-1724.

Hsu, Y., Chen, L., Delancey, J. O., & Ashton-Miller, J. A. (2005). Vaginal thickness, cross-sectional area, and perimeter in women with and those without prolapse. *Obstet Gynecol, 105*(5 Pt 1), 1012-1017.

Hsu, Y., Lewicky-Gaupp, C., & DeLancey, J. O. (2008). Posterior compartment anatomy as seen in magnetic resonance imaging and 3-dimensional reconstruction from asymptomatic nulliparas. *Am J Obstet Gynecol, 198*(6), 651 e651-657.

Larson, K. A., Hsu, Y., Chen, L., Ashton-Miller, J. A., & DeLancey, J. O. (2010). Magnetic resonance imaging-based three-dimensional model of anterior vaginal wall position at rest and maximal strain in women with and without prolapse. *Int Urogynecol J, 21*(9), 1103-1109.

Larson, K. A., Luo, J., Yousuf, A., Ashton-Miller, J. A., & Delancey, J. O. (2012). Measurement of the 3D geometry of the fascial arches in women with a unilateral levator defect and "architectural distortion". *Int Urogynecol J, 23*(1), 57-63.

Leffler, K. S., Thompson, J. R., Cundiff, G. W., Buller, J. L., Burrows, L. J., & Schon Ybarra, M. A. (2001). Attachment of the rectovaginal septum to the pelvic sidewall. *Am J Obstet Gynecol, 185*(1), 41-43.

Luo, J., Ashton-Miller, J. A., & DeLancey, J. O. L. (2011). A model patient: Female pelvic anatomy can be viewed in diverse 3-dimensional images with a new interactive tool. *Am J Obstet Gynecol, 205*(4), 391.e391-391.e392.

Luo, J., Larson, K. A., Fenner, D. E., Ashton-Miller, J. A., & Delancey, J. O. (2012). Posterior vaginal prolapse shape and position changes at maximal Valsalva seen in 3-D MRI-based models. *Int Urogynecol J, 23*(9), 1301-1306.

Margulies, R. U., Hsu, Y., Kearney, R., Stein, T., Umek, W. H., & DeLancey, J. O. (2006). Appearance of the levator ani muscle subdivisions in magnetic resonance images. *Obstet Gynecol, 107*(5), 1064-1069.

Pendergrass, P. B., Reeves, C. A., & Belovicz, M. W. (1991). A technique for vaginal casting utilizing vinyl polysiloxane dental impression material. *Gynecol Obstet Invest, 32*(2), 121-122.

Pendergrass, P. B., Reeves, C. A., Belovicz, M. W., Molter, D. J., & White, J. H. (1996). The shape and dimensions of the human vagina as seen in three-dimensional vinyl polysiloxane casts. *Gynecol Obstet Invest, 42*(3), 178-182.

Pendergrass, P. B., Reeves, C. A., Belovicz, M. W., Molter, D. J., & White, J. H. (2000). Comparison of vaginal shapes in Afro-American, caucasian and hispanic women as seen with vinyl polysiloxane casting. *Gynecol Obstet Invest, 50*(1), 54-59.

Ramanah, R., Berger, M. B., Parratte, B. M., & Delancey, J. O. (2012). Anatomy and histology of apical support: a literature review concerning cardinal and uterosacral ligaments. *Int Urogynecol J*.

Tan, I. L., Stoker, J., Zwamborn, A. W., Entius, K. A. C., Calame, J. J., & Lamérris, J. S. (1998). Female pelvic floor: Endovaginal MR imaging of normal anatomy. *Radiology, 206*(3), 777-783.

CHAPTER 3

A MODEL PATIENT: FEMALE PELVIC ANATOMY CAN BE VIEWED IN DIVERSE 3-DIMENSIONAL IMAGES WITH A NEW INTERACTIVE TOOL

3.1 Case Notes

We developed, in portable document format (PDF), a detailed 3-dimensional (3D) interactive anatomic model of 23 pelvic structures that include the muscles, ligaments, and fascia of the pelvic floor and the organs it supports. Bones, blood vessels, and the perineum are illustrated as well. To produce this tool, 3D volumetric models were created from serial 5-mm–thick images that were obtained with a 3-Tesla magnetic resonance scanner. The subject was a healthy, 45-year-old, multiparous woman who was at the 50th percentile for height. Magnetic resonance images were then imported into 3D Slicer software (version 3.4.1; Brigham and Women's Hospital, Boston, MA). Each structure was traced with the use of the most clearly visible axial and/or coronal plane images and lofted into a 3D virtual model that was based on our previous anatomic work(Hsu et al. 2005; Margulies et al. 2006; Hsu et al. 2008; Brandon et al. 2009; Larson et al. 2010). Models were validated against the original scans and tracings.

Next, the 3D models that had been generated by 3D Slicer were imported into Adobe 3D Reviewer (version 9.0; Adobe Systems Inc, San Jose, CA), exported as a universal 3D file, and, with the aid of the program's 3D tool, inserted into Adobe Acrobat 9 Pro (Adobe Systems Inc) and saved as a PDF file.

3.2 Conclusion

The 3D PDF file allows the user to view and manipulate detailed 3D models of pelvic anatomy without any specialized visualization software. For example, the model can be rotated and magnified; and structures can be hidden or rendered transparent, which makes it easier to understand complex anatomic relationships (Figure 3.1 and Figure 3.2; an interactive model is available online at www.AJOG.org and in Appendix B). All that is needed is the readily available (and free) Adobe Reader; cross-section capability is available with Adobe Acrobat. Availability of this anatomically accurate model is critical to avoiding errors in comprehension that can arise from conceptually based anatomic representations.

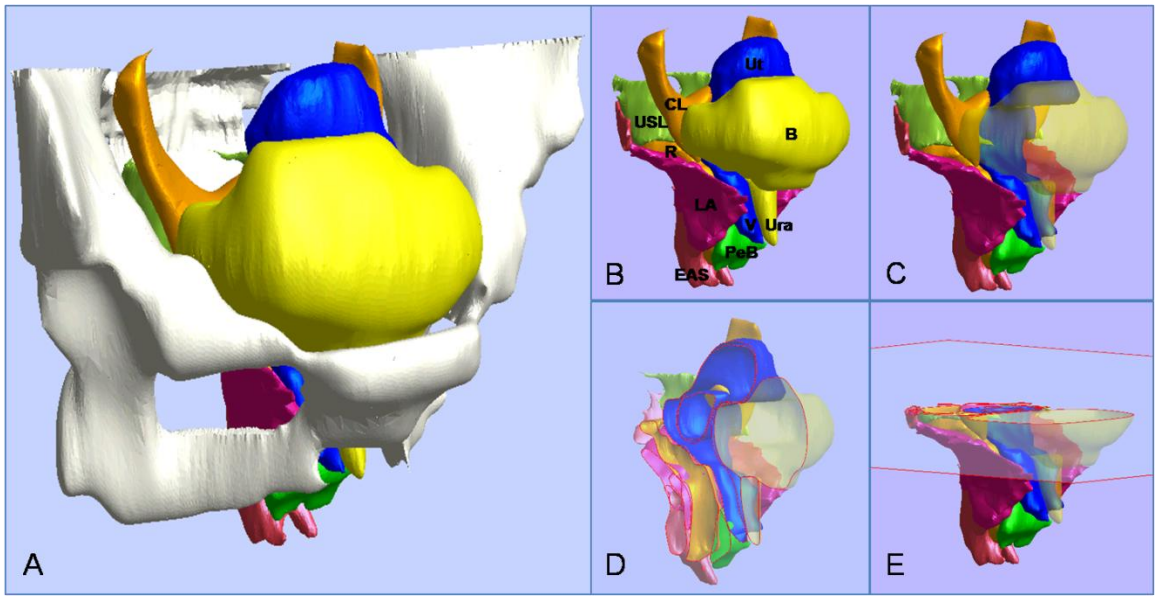

Figure 3.1 The user can manipulate the 3-dimensional model of pelvic structures. **A**, A three-quarter right anterolateral view. **B**, Hiding the bones reveals selected features. **C**, Making the bladder and urethra transparent reveals the underlying structures. **D**, Sample sagittal cross-section of the remaining structures. **E**, Sample axial cross-section. B, bladder; CL, cardinal ligament; EAS, external anal sphincter; LA, levator ani; PeB, perineal body; R, rectum; Ura, urethra; USL, uterosacral ligament; Ut, uterus; V, vagina. © University of Michigan Pelvic Floor Research Group (2011).

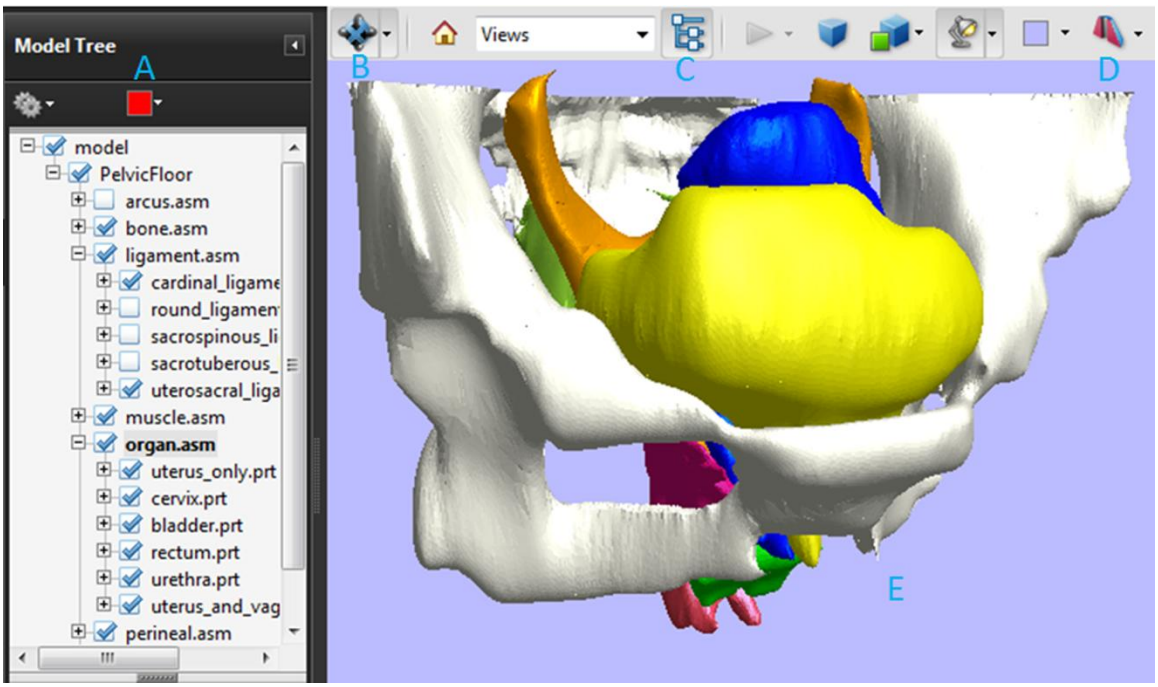

Figure 3.2 The manipulation interface includes a model tree and toolbar. **A**, The model tree allows users to hide, isolate, or render transparent individual anatomic structures by right clicking on the label. **B**, Using this button in the 3-dimensional toolbar at the top, it is possible to zoom in or out, rotate the model, spin it, and pan over it. **C**, The model tree can be toggled on and off with this button. **D**, Cross-sections can be cut at a given location and orientation. E, The 3-dimensional model is activated by clicking on the portable document format file. © University of Michigan Pelvic Floor Research Group (2011).

References

Brandon, C. J., Lewicky-Gaupp, C., Larson, K. A., & Delancey, J. O. (2009). Anatomy of the perineal membrane as seen in magnetic resonance images of nulliparous women. *Am J Obstet Gynecol, 200*(5), 583 e581-586.

Hsu, Y., Fenner, D. E., Weadock, W. J., & DeLancey, J. O. (2005). Magnetic resonance imaging and 3-dimensional analysis of external anal sphincter anatomy. *Obstet Gynecol, 106*(6), 1259-1265.

Hsu, Y., Lewicky-Gaupp, C., & DeLancey, J. O. (2008). Posterior compartment anatomy as seen in magnetic resonance imaging and 3-dimensional reconstruction from asymptomatic nulliparas. *Am J Obstet Gynecol, 198*(6), 651 e651-657.

Larson, K. A., Yousuf, A., Lewicky-Gaupp, C., Fenner, D. E., & DeLancey, J. O. (2010). Perineal body anatomy in living women: 3-dimensional analysis using thin-slice magnetic resonance imaging. *Am J Obstet Gynecol, 203*(5), 494 e415-421.

Margulies, R. U., Hsu, Y., Kearney, R., Stein, T., Umek, W. H., & DeLancey, J. O. (2006). Appearance of the levator ani muscle subdivisions in magnetic resonance images. *Obstet Gynecol, 107*(5), 1064-1069.

CHAPTER 4

POSTERIOR VAGINAL PROLAPSE SHAPE AND POSITION CHANGES AT MAXIMAL VALSALVA SEEN IN 3-D MRI-BASED MODELS

Abstract

Introduction and Hypothesis: Two-dimensional magnetic resonance imaging (MRI) of posterior vaginal prolapse has been studied. However, the three-dimensional (3-D) mechanisms causing such prolapse remain poorly understood. This discovery project was undertaken to identify the different 3-D characteristics of models of rectocele-type posterior vaginal prolapse (PVP^R) in women.

Methods: Ten women with (cases) and 10 without (controls) PVP^R were selected from an ongoing case-control study. Supine, multi-planar MR imaging was performed at rest and maximal Valsalva. 3-D reconstructions of the posterior vaginal wall and pelvic bones were created using 3D Slicer v. 3.4.1. In each slice the posterior vaginal wall and perineal skin were outlined to the anterior margin of the external anal sphincter to include the area of the perineal body. Women with predominant enteroceles or anterior vaginal prolapse were excluded.

Results: The case and control groups had similar demographics. In women with PVP^R two characteristics were consistently visible (10 of 10): 1) the posterior vaginal wall displayed a folding phenomenon similar to a person beginning to kneel ("Kneeling"

shape); and 2) a downward displacement in the upper 2/3 of the vagina. Also seen in some, but not all of the scans were: 3) forward protrusion of the distal vagina (6 of 10); 4) perineal descent (5 of 10); and 5) distal widening in lower third of the vagina (3 of 10). **Conclusions:** Increased folding ("Kneeling") of the vagina and an overall downward displacement are consistently present in rectocele. Forward protrusion, perineal descent and distal widening are sometimes seen as well.

Key words: posterior vaginal wall prolapse, pelvic organ prolapse, rectocele, 3D model, magnetic resonance imaging, anatomy

4.1 Introduction

Pelvic floor dysfunction results in 11% of women undergoing surgery (Olsen et al. 1997) in the USA during their lifespan. Over 200,000 operations are performed for prolapse (Boyles et al. 2003) with repair of posterior vaginal prolapse (PVP) included in 87% (Silva et al. 2006). The annual estimated cost for these operations exceeds US $1 billion (Subak et al. 2001).

The structural deformations seen in women with anterior vaginal prolapse (cystocele) have received considerable attention and study (Hsu et al. 2008a; Chen et al. 2009; Larson et al. 2010). The pathomechanics of PVP has received less attention and so is not yet well understood. Current imaging studies concerning rectocele have focused on the contour of the rectum seen in midline sagittal projection (Kelvin et al. 2000; Ganeshan et al. 2008). Changes in the overall contour of the posterior vaginal wall are less well documented and there is no consensus on what to measure. Although there is obvious deformation of the posterior vaginal wall in PVP, the exact nature of this 3-D

deformation has not been clarified. The potential changes present in posterior vaginal wall width and the relationships involving the lateral margins of the posterior vaginal wall are also not clear (Pannu et al. 2009; Lewicky-Gaupp et al. 2010).

This study was therefore undertaken by conducting a secondary analysis of data from a larger on-going case-control study of pelvic organ prolapse. We tested the hypothesis that it is possible to identify characteristic shapes of PVP visible on MR scans at rest and maximum Valsalva.

4.2 Materials and Methods

MRI scans of 10 women with rectocele type posterior vaginal prolapse (PVP^R) and 10 with normal support (controls) were selected from an ongoing University of Michigan institutional review board-approved (IRB # 1999-0395) case-control study of pelvic organ prolapse. Women in the control group were recruited by newspaper and radio advertisement for healthy volunteers and had to be asymptomatic and had normal vaginal support with all pelvic organ prolapse quantification (POP-Q) points < -1 cm. All PVP^R cases had posterior vaginal prolapse with posterior vaginal wall (PVW) extending at least 1 cm below the hymen based on POP-Q and had symptoms of bulging or protrusion. In order to be included the rectocele had to be the predominant aspect of the prolapse and extend at least one centimeter lower than the most dependent part of anterior wall or the uterus/apex. Women with predominant enteroceles or anterior vaginal prolapse were excluded. None of the subjects had previously undergone hysterectomy or prior pelvic floor surgery. The 26 scans of women with rectocele were further evaluated for inclusion according to the following criteria: prolapse size consistent with clinical examination (POP-Q), ability to hold Valsalva for the entire 17 seconds of scan

acquisition, freedom from significant motion artifact, inclusion of all necessary structures, evenly distributed intravaginal ultrasound gel and sufficient definition of vaginal walls to allow models to be made. Ten of the 26 scans were selected based on above criteria. Similarly, the matched controls (who had an age difference within ±2 years, number of vaginal deliveries within ±1, and were of similar race) had to meet the above criteria with the exception of not having prolapse.

As described in our previous work (Larson et al. 2010; Larson et al. 2012b), each subject underwent supine multi-planar, two-dimensional, fast spin, proton density MR imaging both at rest and during maximal Valsalva using a 3 T superconducting magnet (Philips Medical Systems Inc, Bothell, WA) with version 2.5.1.0 software. At rest, each 30 images were serially obtained at the axial, sagittal, and coronal, with 20x20 cm fields of view, 4 mm slice thickness, and a 1 mm gap between slices. During maximal Valsalva, each 14 images were serially obtained at the same three serial planes, with 36x36 cm fields of view, 6 mm slice thickness, and 1 mm gap. In order for the images to be considered adequate, they had to allow visualization of vaginal margins.

The MR images from axial, sagittal and coronal planes were imported into 3D Slicer 3.4.2009-10-15 (Brigham and Women's Hospital, Boston, MA). The resting axial and sagittal images were aligned first, with manual registration and fixed landmarks such as pubic bone and sacrum. 3-D models were made of the following resting structures: bony pelvis and ischial spines using axial images, and posterior vaginal wall using sagittal images based on our previous anatomic work (DeLancey 1999; Hsu et al. 2008b; Lewicky-Gaupp et al. 2010). Figure 4.1 illustrates the 3-D model generation process and subsequent reference line as described below. The vaginal wall was modeled using

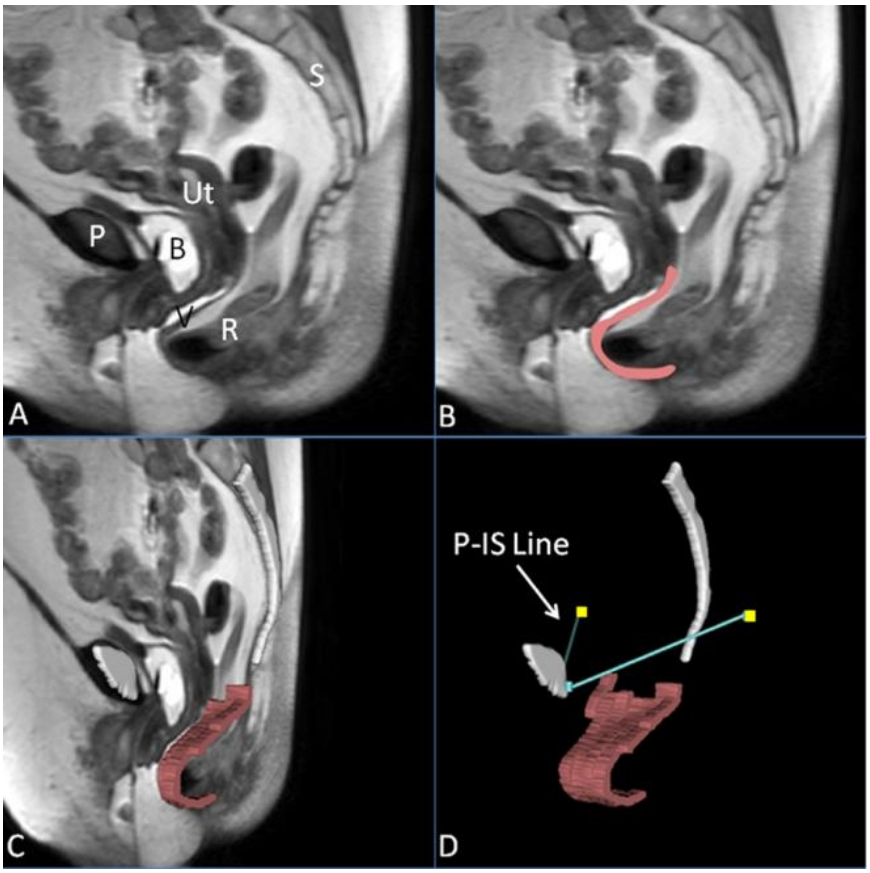

Figure 4.1 Making a 3D prolapse model including the P-IS line. (**A**) Mid-sagittal MR image of subject with posterior prolapse; (**B**) Outline of posterior vaginal wall in *pink*; (**C**) Addition of midsagittal pelvic bones (*white*) and 3D model of posterior vaginal wall shown in slightly skewed sagittal image; (**D**) Straining posterior vaginal wall model and its relationship to the normalized ATFP, shown here as the *turquoise* lines extending from the public symphysis to the ischial spines (*yellow squares*), or the P-IS line. P, pubic symphysis; S, sacrum; B, bladder; R, rectum; V, vagina; Ut, uterus; IS, ischial spine. (© DeLancey 2011)

sagittal strips to avoid artifacts from smoothing. The models were compared to the original MR images to confirm their fidelity.

To analyze deformation of posterior vaginal wall under load, 3-D models of mid-sagittal pubic symphysis and sacrum were reconstructed using the MR images from maximal Valsalva and aligned with the pelvic bones of the resting images. This registration information was then applied to the soft tissue images making it possible to align the subsequently constructed 3-D posterior vaginal wall with the previously created resting models using the pubic symphysis and sacrum. A reference line was constructed on each side of the pelvis representing the normal location of the arcus tendineus fascia pelvis (ATFP) from its pubic attachments to the ipsilateral ischial spine ("P-IS" line) for visual reference and consideration for future measurement purposes (Larson et al. 2010; Larson et al. 2012b).

To compare the 3-D reconstruction models among case and control groups, the resting and maximal Valsalva 3-D models were imported into Microsoft PowerPoint ®. All models were aligned by the position of the pubis and with a dotted line indicating the usual location of perineal body. Then the above models were compared visually among the case and control groups, with morphological changes identified using descriptive terminology. Two physician co-authors scored the frequency for the characteristic in both case and control groups. A descriptive statistical analysis was performed of case and control demographics. Fisher's exact tests were used to determine the statistical significance ($p<.01$) of the proportions of women in each group who manifest each phenomenon.

4.3 Results

Subjects' characteristics and POP-Q values are shown in Table 4.1. The case and control groups were matched by race, age, and vaginal parity. No subjects in either group had undergone a hysterectomy and all cases were rectocele type prolapse predominantly. Statistically significance differences were found at points C, Ap, and Bp during clinical POP-Q examination for the two groups.

The lateral views of rest and strain models in all 20 subjects are shown in Figure 4.2. With Valsalva, two characteristics were consistently visible in women with PVPR (10/10): 1) the posterior vaginal wall displayed a folding phenomenon similar to a person beginning to kneel ("Kneeling") (Figure 4.3C); and 2) downward displacement in the upper 2/3 part of the vagina (Figure 4.3C). In addition to the "Kneeling" and downward displacement characteristics, in women with PVPR the posterior vaginal wall underwent other morphologic changes. For example, forward protrusion of the distal vagina (6/10) can be seen in some subjects (Figure 4.3C). About half subjects (5/10) had perineal descent. To be considered as forward protrusion and perineal descent phenomena, the amount of forward or downward movement have to be significant enough (e.g., lower 1/3 of vaginal wall lose contact compared to control group). In addition, distal widening in lower third of the vagina was seen in a few (3/10) subjects. The complete comparison of the frequency of the above morphologic findings is shown in Table 4.2 for the case and control groups.

Table 4.1 Demographics

Characteristics	Cases (n=10)	Controls (n=10)	*p* value
Age (yrs)[a]	54.9(8.7)	54.2(8.9)	.860
BMI (kg/m^2)[a]	28.9(5.5)	28.4(8.6)	.825
Parity[a]	2.6(0.7)	2.8(1.0)	.678
Race[b]			
Caucasian	9 (90%)	10 (100%)	1.00[c]
POP-Q (cm)[a]			
Aa	-1.2(0.9)	-1.9(1.0)	.111
Ba	-1.0(0.9)	-1.9(1.0)	.081
C	-5.2(1.4)	-6.8(1.2)	<.001
D	-7.5(1.6)	-8.9(1.4)	.003
Ap	1.7(0.8)	-1.7(0.7)	<.001
Bp	1.7(0.8)	-1.7(0.7)	<.001
GHrest	3.9(1.3)	3.3(1.0)	.240
LHrest	7.5(1.7)	6.4(0.8)	.066
TVL	10.3(1.3)	10.2(1.2)	.790

GHrest, genital hiatus at rest; *LHrest*, levator hiatus at rest; *TVL*, total vaginal length
[a] Data are mean (SD)
[b] Data are n (%)
[c] *p* is from Fisher's exact test

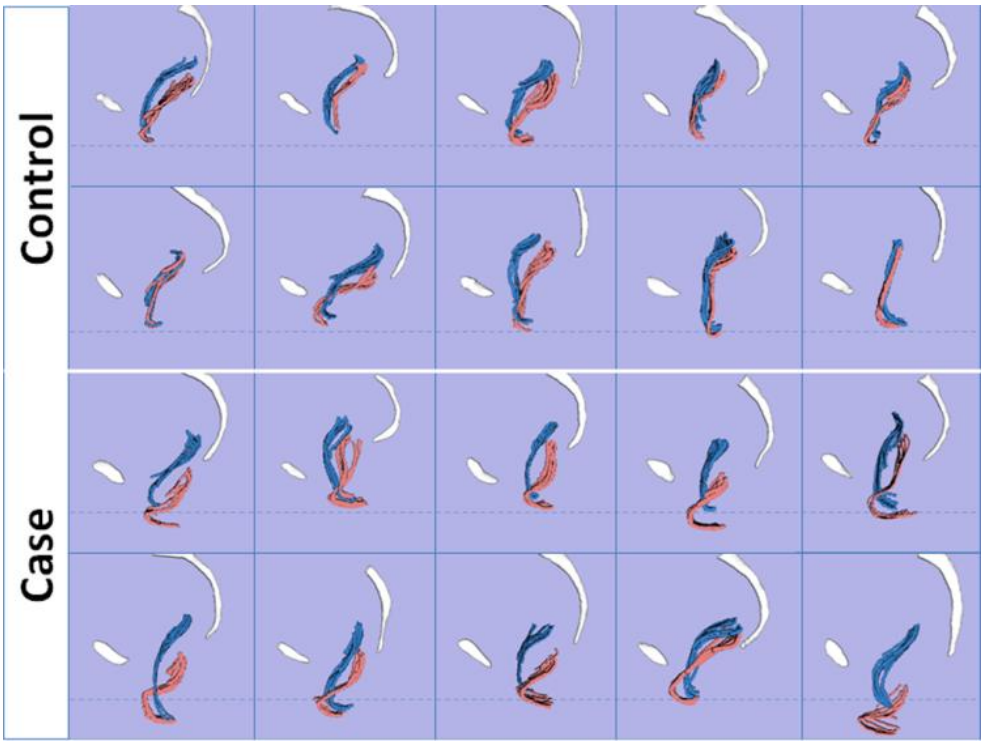

Figure 4.2 3D case and control models comparison. Lateral view of posterior vaginal walls of 10 controls and 10 cases during rest (*blue*) and Valsalva (*pink*). The vaginal wall was modeled using sagittal strips to avoid artifacts from smoothing. Pubis and sacrum are shown in *white*. *Dotted lines* indicate the average level of the perineal body for visual reference. (© DeLancey 2011)

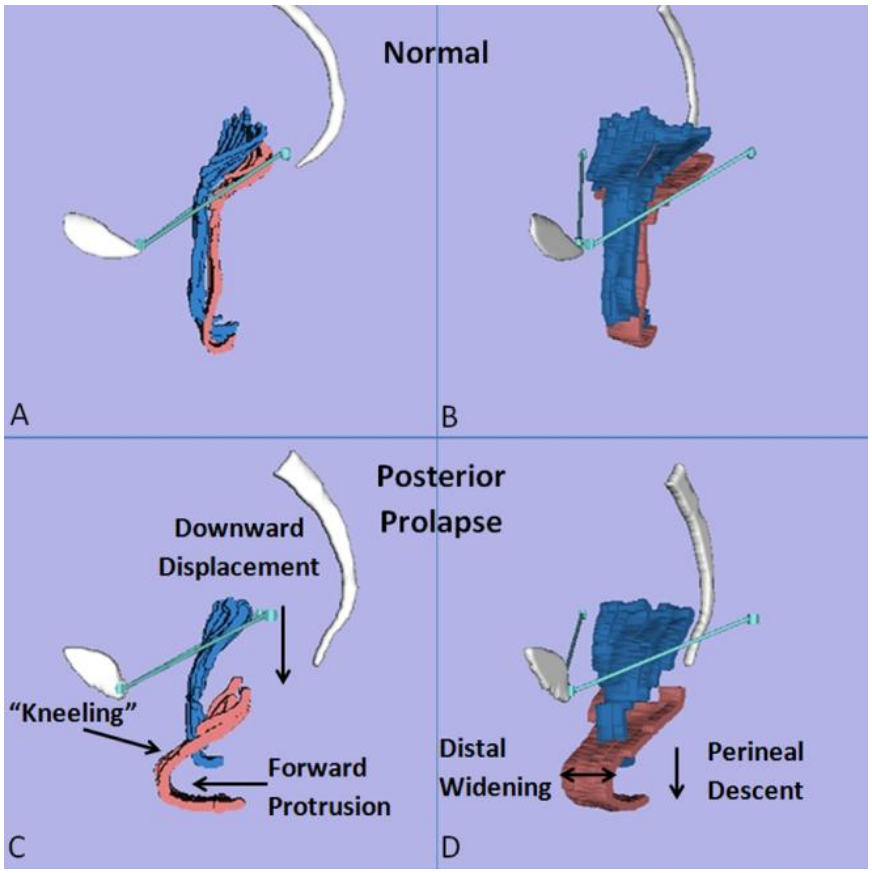

Figure 4.3 Characteristics of posterior prolapse. Comparison of control (**A**,**B**) and case (**C**,**D**) in lateral view (**A**,**C**) and oblique view (**B**,**D**) showing five characteristic features (**C**,**D**) during rest (*blue*) and Valsalva (*pink*): 1) Increased folding ("Kneeling"); 2) Downward displacement in the upper 2/3 part of the vagina; 3) Forward protrusion; 4) Perineal descent; 5) Distal widening in the lower third part of the vagina. Pubis and sacrum are shown in *white*. The P-IS line is shown in *turquoise*. (© DeLancey 2011)

Table 4.2 Frequency of morphologic characteristics within case and controls

Characteristics	Cases (n=10)	Controls (n=10)	*p* value (Fisher's exact)
Kneeling[a]	10(100%)	2(20%)	<0.001
Downward Displacement[a]	10(100%)	3(30%)	<0.01
Forward Protrusion[a]	6(60%)	2(20%)	0.170
Perineal Descent[a]	5(50%)	3(30%)	0.650
Distal Widening[a]	3(30%)	0(0%)	0.211

[a] Data are n(%); Downward displacement is mainly for upper 2/3 of vagina; Distal widening is mainly for the lower third of vagina.

4.4 Discussion

We examined the appearance of the posterior vaginal wall at maximal Valsalva in normal women and women with rectocele as a secondary analysis of an on-going case-control study of pelvic organ prolapse. The hypothesis was supported in that we found consistent changes in the shape and position of the vagina in women with posterior vaginal prolapse. Increased folding ("Kneeling") of the vagina and an overall downward displacement were consistently present in rectocele. Other less consistent phenomena included forward protrusion, perineal descent, and distal widening.

The "Kneeling" is not just a forward protrusion of the distal vaginal wall, but a more complex phenomenon as it can occur in the absence of forward protrusion. The addition of descent of the upper vagina in those with "Kneeling" seemed to 'pinch off' the bowel as the upper vagina moved toward the levator plate; this suggests that it may play a role in obstructive defecatory dysfunction. Further measurements will be needed to confirm or refute this hypothesis.

These findings are consistent with findings in 2-D sagittal imaging (Lewicky-Gaupp et al. 2010) but qualitatively are much richer in the information they provide. In addition, with this 3-D MR imaging-based modeling technique, we can better visualize the relationship between the lateral wall and reference lines such as the P-IS line so that a quantitative unified 3-D biomechanical model can be created to test different hypotheses related to mechanism of the PVP^R. Furthermore, it allows us to evaluate the degree of vaginal widening that is seen in some subjects.

We were surprised that distal widening of the vagina was not seen universally in the population with PVP^R. Certainly it is an expected finding, but on reflection this fits

with clinical experience that not all rectoceles are the same. Now that it is possible to image vaginal width, researchers can pursue explanations for why one woman has this phenomenon and others do not, and determine if it is related to defecatory dysfunction seen in some women with PVP.

One prominent aspect of rectoceles was the downward displacement of the upper vagina. This is accompanied by a change in the relationship between the vagina and the P-IS line that identifies the normal location of the fascial arch. This raises the issue of whether or not there is a "posterior paravaginal defect". In work on the anterior vaginal wall (Summers et al. 2006; Larson et al. 2012a) we have seen that paravaginal defect and apical descent are essentially two aspects of the same phenomenon. Further work will be needed to clarify this issue.

There are significant differences of opinion among experts in the field regarding the anatomical factors responsible for rectoceles and the relationship between surgical approaches and outcome (Paraiso et al. 2006; Kleeman and Karram 2008). The differences of opinion start simply with how to define or quantify the rectocele. Urogynecologists often struggle with an adequate way of describing the rectocele (Kenton et al. 1997; Altman et al. 2005). Most imaging studies to date have focused on measurements of the rectal contour with contrast during defecation which is a different phenomenon than the movement of the posterior vaginal wall elicited during pelvic examination (Kenton et al. 1999; Kelvin et al. 2000). Both have their separate roles in understanding problems with posterior vaginal wall support. Obtaining accurate 3-D information about the structural changes present in individual women shows great promise as an investigative technique and may lead to specific surgical therapies.

A lack of objective reproducible preoperative tests that can identify the specific nature of each patient's defect has prevented clinical trials that test the hypothesis that a specific approach may have better results in patients who have a specific type of rectocele. The current project is a start towards developing an assessment strategy that can identify different anatomical defects responsible for a woman's anatomical problem. Next steps might include quantitative measures of posterior vaginal wall morphology to test specific hypotheses and then evaluation of these abnormalities to the status of surrounding structures such as the levator ani muscle and the pelvic fascia. We are not implying by this research that we believe MR imaging is, at present, necessary for the clinical management of a rectocele, but if this line of investigation is successful in capturing clinically important differences between different types of rectoceles that affect surgical outcome then it may become helpful. Of course symptoms are not always tied to anatomy and this line of investigation does not diminish the importance of assessing other causes of defecation difficulty (Cundiff and Fenner 2004).

Several factors must be kept in mind when interpreting the result of these studies. This is a small sample of specifically selected women with distal posterior vaginal wall prolapse. We specifically selected women with predominant rectoceles in order to have a more homogeneous sample to analyze. It will be necessary to study women who also have significant cystocele or uterine prolapse in association with rectocele to gain an understanding of more complex prolapses. In addition, the changes seen in women with enteroceles will also need to be studied. The MR images are obtained in the supine position and not during defecation. However, these studies are similar to supine pelvic examination with Valsalva that clinicians use to examine the prolapse and perform a

POP-Q examination (except for somewhat less thigh abduction). It is a limitation that we used gel in the vagina to help with visualization and in some instances in normal women it fills the upper vagina thereby slightly changing the contour. The characteristic features were identified by consensus between two of the clinical authors (JOLD, KAL) based on morphological patterns in preparation for developing a quantitative system.

This study is a first step to analyze the structural 3-D deformations involved in rectocele. It includes qualitatively studying the characteristic changes of posterior vaginal wall both at rest and maximal Valsalva from MR images for case and control groups. Future quantification of the differences between women with and without prolapse should give insights into the mechanism of the posterior vaginal wall prolapse and potentially lead to better surgical treatment strategies.

References

Altman, D., Lopez, A., Kierkegaard, J., Zetterstrom, J., Falconer, C., Pollack, J., et al. (2005). Assessment of posterior vaginal wall prolapse: comparison of physical findings to cystodefecoperitoneography. *Int Urogynecol J, 16*(2), 96-103; discussion 103.

Boyles, S. H., Weber, A. M., & Meyn, L. (2003). Procedures for pelvic organ prolapse in the United States, 1979-1997. *Am J Obstet Gynecol, 188*(1), 108-115.

Chen, L., Ashton-Miller, J. A., & DeLancey, J. O. (2009). A 3D finite element model of anterior vaginal wall support to evaluate mechanisms underlying cystocele formation. *J Biomech, 42*(10), 1371-1377.

Cundiff, G. W., & Fenner, D. (2004). Evaluation and treatment of women with rectocele: focus on associated defecatory and sexual dysfunction. *Obstetrics & Gynecology, 104*(6), 1403-1421.

DeLancey, J. O. (1999). Structural anatomy of the posterior pelvic compartment as it relates to rectocele. *Am J Obstet Gynecol, 180*(4), 815-823.

Ganeshan, A., Anderson, E. M., Upponi, S., Planner, A. C., Slater, A., Moore, N., et al. (2008). Imaging of obstructed defecation. *Clin Radiol, 63*(1), 18-26.

Hsu, Y., Chen, L. Y., Summers, A., Ashton-Miller, J. A., & DeLancey, J. O. L. (2008a). Anterior vaginal wall length and degree of anterior compartment prolapse seen on dynamic MRI. *Int Urogynecol J, 19*(1), 137-142.

Hsu, Y., Lewicky-Gaupp, C., & DeLancey, J. O. (2008b). Posterior compartment anatomy as seen in magnetic resonance imaging and 3-dimensional reconstruction from asymptomatic nulliparas. *Am J Obstet Gynecol, 198*(6), 651 e651-657.

Kelvin, F. M., Maglinte, D. D., Hale, D. S., & Benson, J. T. (2000). Female pelvic organ prolapse: a comparison of triphasic dynamic MR imaging and triphasic fluoroscopic cystocolpoproctography. *AJR Am J Roentgenol, 174*(1), 81-88.

Kenton, K., Shott, S., & Brubaker, L. (1997). Vaginal topography does not correlate well with visceral position in women with pelvic organ prolapse. *Int Urogynecol J, 8*(6), 336-339.

Kenton, K., Shott, S., & Brubaker, L. (1999). The anatomic and functional variability of rectoceles in women. *Int Urogynecol J, 10*(2), 96-99.

Kleeman, S. D., & Karram, M. (2008). Posterior pelvic floor prolapse and a review of the anatomy, preoperative testing and surgical management. *Minerva Ginecol, 60*(2), 165-182.

Larson, K. A., Hsu, Y., Chen, L., Ashton-Miller, J. A., & DeLancey, J. O. (2010). Magnetic resonance imaging-based three-dimensional model of anterior vaginal wall position at rest and maximal strain in women with and without prolapse. *Int Urogynecol J, 21*(9), 1103-1109.

Larson, K. A., Luo, J., Guire, K. E., Chen, L., Ashton-Miller, J. A., & DeLancey, J. O. (2012a). 3D analysis of cystoceles using magnetic resonance imaging assessing midline, paravaginal, and apical defects. *Int Urogynecol J, 23*(3), 285-293.

Larson, K. A., Luo, J., Yousuf, A., Ashton-Miller, J. A., & Delancey, J. O. (2012b). Measurement of the 3D geometry of the fascial arches in women with a unilateral levator defect and "architectural distortion". *Int Urogynecol J, 23*(1), 57-63.

Lewicky-Gaupp, C., Yousuf, A., Larson, K. A., Fenner, D. E., & Delancey, J. O. (2010). Structural position of the posterior vagina and pelvic floor in women with and without posterior vaginal prolapse. *Am J Obstet Gynecol, 202*(5), 497 e491-496.

Olsen, A. L., Smith, V. J., Bergstrom, J. O., Colling, J. C., & Clark, A. L. (1997). Epidemiology of surgically managed pelvic organ prolapse and urinary incontinence. *Obstet Gynecol, 89*(4), 501-506.

Pannu, H. K., Scatarige, J. C., & Eng, J. (2009). Comparison of Supine Magnetic Resonance Imaging With and Without Rectal Contrast to Fluoroscopic Cystocolpoproctography for the Diagnosis of Pelvic Organ Prolapse. *J Comput Assist Tomo, 33*(1), 125-130.

Paraiso, M. F., Barber, M. D., Muir, T. W., & Walters, M. D. (2006). Rectocele repair: a randomized trial of three surgical techniques including graft augmentation. *Am J Obstet Gynecol, 195*(6), 1762-1771.

Silva, W. A., Pauls, R. N., Segal, J. L., Rooney, C. M., Kleeman, S. D., & Karram, M. M. (2006). Uterosacral ligament vault suspension: five-year outcomes. *Obstet Gynecol, 108*(2), 255-263.

Subak, L. L., Waetjen, L. E., van den Eeden, S., Thom, D. H., Vittinghoff, E., & Brown, J. S. (2001). Cost of pelvic organ prolapse surgery in the United States. *Obstet Gynecol, 98*(4), 646-651.

Summers, A., Winkel, L. A., Hussain, H. K., & DeLancey, J. O. (2006). The relationship between anterior and apical compartment support. *Am J Obstet Gynecol, 194*(5), 1438-1443.

CHAPTER 5

3D ANALYSIS OF CYSTOCELES USING MAGNETIC RESONANCE IMAGING ASSESSING MIDLINE, PARAVAGINAL, AND APICAL DEFECTS

Abstract

Introduction and hypothesis: This study assesses relative contributions of "midline defects" (widening of the vagina) and "paravaginal defects" (separation of the lateral vagina from the pelvic sidewall).

Methods: Ten women with anterior predominant prolapse and ten with normal support underwent pelvic MR imaging. 3-D models of the anterior vaginal wall (AVW) were generated to determine locations of the lateral AVW margin, vaginal width, and apical position.

Results: The lateral AVW margin was farther from its normal position in cases than controls throughout most of the vaginal length, most pronounced midvagina (effect sizes, 2.2–2.8). Vaginal widths differed in the midvagina with an effect size of 1.0. Strong correlations between apical and paravaginal support were evident in mid- and upper vagina ($r = 0.77–0.93$).

Conclusions: Changes in lateral AVW location were considerably greater than changes in vaginal width in cases vs controls, both in number of sites affected and effect sizes. These "paravaginal defects" are highly correlated with apical descent.

Key words: Cystocele, Paravaginal defect, Midline defect, Anterior wall prolapse, Pelvic organ prolapse, MR imaging

5.1 Introduction

The anterior vaginal wall is the most common site of pelvic organ prolapse and the most frequent site of operative failure (Benson et al. 1996; C. Maher and Baessler 2006; C. F. Maher et al. 2001; J. K. Nguyen 2001; J. N. Nguyen and Burchette 2008; Olsen et al. 1997; Shull et al. 2000). The traditional discussion of causal factors involved in anterior compartment prolapse has centered on debate between midline and paravaginal defects. Apical descent has recently been strongly associated with cystocele size (Hsu et al. 2008; Rooney et al. 2006; Summers et al. 2006). Although surgical decisions are often based on which defect is presumed present, data are lacking regarding the relative importance of these defects. Furthermore, a technique which quantifies the magnitude of these clinically important factors is not currently available.

Recently, 3-D magnetic resonance (MR) studies have allowed us to visualize not just the midline deformation of the anterior vaginal wall with Valsalva, but also the entire vaginal wall including its lateral margin (Larson et al. 2010). The present study quantifies changes in vaginal width in order to evaluate the effect of "midline defects" and changes in the position of the lateral vagina in order to evaluate the "paravaginal defect." In addition, we determine the correlation between these "paravaginal defects" and vaginal apex location.

5.2 Materials and methods

Magnetic resonance imaging (MRI) scans from 20 women (ten cases and ten controls) were selected from an ongoing University of Michigan institutional review board-approved (IRB no. 1999–0395), case–control study of pelvic organ prolapse. All women in the control group were asymptomatic based on Pelvic Floor Distress Inventory and Pelvic Floor Impact Questionnaires, had negative full bladder stress tests, and did not have prolapse beyond the hymen. All cases were symptomatic and had a Ba pelvic organ prolapse–quantification (POP-Q) value at least 1 cm beyond the hymenal ring on clinical examination. Selected subjects had cystocele-predominant prolapse; women in whom the cervix or posterior wall was the leading point of prolapse were excluded. None of the subjects had previously undergone hysterectomy or prior pelvic floor surgery. For our cases, we screened 21 of the most recent MR images to find ten with adequate visualization of the vaginal margins. The images of the ten selected cases also adequately demonstrated the full extent of their prolapse on dynamic MRI, allowing visualization of the changes in the anterior vaginal wall at Valsalva.

As described in our previous studies (Larson et al. 2010), each woman underwent supine MR imaging both at rest and during maximal Valsalva using a 3 Telsa Philips Achieva scanner (Philips Medical Systems, Best, The Netherlands) with a six-channel, phased array coil. Ultrasound gel was placed in the vagina to outline its contour. For standard anatomical scans made at rest, turbo spin echo techniques were used to image the sagittal, coronal, and axial planes. At rest, 30 images were obtained in each plane (repetition time (TR) range, 2,300–3,000 ms; echo time (TE), 30 ms; 4-mm slice thickness; 1-mm gap; number of signal averages (NSA), 2; 256 × 255 voxels). Subjects

then performed a Valsalva maneuver which they held for approximately 20 s to obtain images of the pelvis with the prolapse protruding maximally. With the prolapse protruding, 14 images were serially obtained from one ischial spine to the other in sagittal plane (TR range, 1,249–1,253 ms; TE, 80 ms; 6-mm slice thickness; 1-mm gap; SENSE factor, 4; NSA, 2; 320 × 178 voxels). A research associate with the POP-Q data from each subject's clinical examination was present during MR imaging to assure that the prolapse reached the same size that had been previously identified in the clinic. If the prolapse did not reach the same magnitude as had been observed on clinical examination, the MR study was repeated with additional coaching to obtain images with the prolapse at its fullest extent.

The original axial, sagittal, and coronal Digital Imaging and Communications in Medicine static images were aligned with one another using rigid registration in the 3-D Slicer® software program (version 2.1b1, Brigham and Women's Hospital, Boston, MA), ensuring that structures co-localized in all three axes by simultaneous review of 3-D scan planes in the viewer. Satisfactory alignment was possible in all 20 scans. Three-dimensional models were made of the following resting structures: bony pelvis and ischial spines using the axial images. Figure 5.1a–f illustrates the modeling process and subsequent generation of a reference line as described below.

To analyze the deformation of the anterior vaginal wall under load, 3-D models of the midsagittal pelvic bones (the pubic symphysis and sacrum) were constructed from the sagittal maximal Valsalva images and then aligned with the pelvic bones of the resting model. This identified the transformation (both rotation and translation) for the sagittal maximal Valsalva images such that subsequently constructed 3-D anterior vaginal wall

models could be aligned with previously created resting models of the ischial spines. This step was necessary to allow creation a reference line established on each side of the pelvis representing the normal location of the arcus tendineus fascia pelvis (ATFP) from its pubic attachments to the ipsilateral ischial spine (P-IS line).

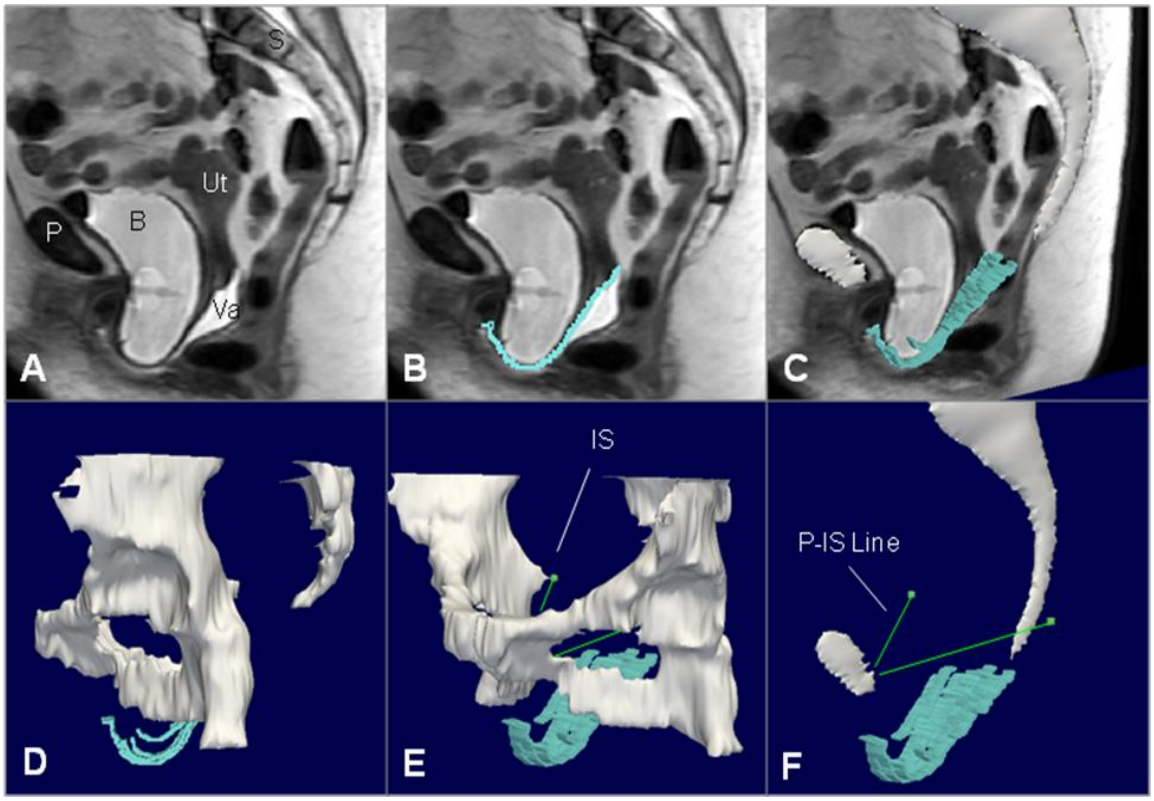

Figure 5.1 Making a 3-D model with P-IS line. **a** Mid-sagittal MR image of subject with prolapse. **b** Outline of anterior vaginal wall in *blue* with cervicovaginal junction marked with a *purple square*. **c** 3D model of anterior vaginal wall shown in slightly skewed sagittal image. Mid-sagittal pelvic bones also in this image. **d** Illustrates more complete view of pelvic bones and rotating this slightly in **e** we can see the IS. A line from the insertion of the arcus tendineus fascia pelvis on the pubic bone to the ipsilateral ischial spine is then constructed (P-IS line in **f**). This serves as the reference line to generate the sidewall measurements. *P* pubic symphysis, *S* sacrum, *B* bladder, *Va* vagina, *Ut* uterus, *IS* ischial spine. ©DeLancey 2010

The maximal Valsalva models were imported into Imageware® (version 12, UGS Corporation, 2005) for measurement of vaginal width and determination of the distance of the lateral margin of the vagina from normal. Figure 5.2 illustrates how anterior vaginal wall width at maximal Valsalva was measured at five equidistant locations between the cervicovaginal and urethrovaginal junctions for both cases and controls. This measurement did take into account the nonlinear configuration of the anterior vaginal wall. This measurement, therefore, was not a straight-line distance between the lateral margins but followed the curve of the vagina so that the distance, in some cases, might be larger than the transverse diameter of the pelvis. In addition, we measured vaginal length between the cervicovaginal and urethrovaginal junctions. Secondly, we developed a technique to quantify the "paravaginal defect." Using the P-IS line as our reference x-axis, the normal location of the lateral margin of the vagina was determined by calculating the mean three-dimensional coordinates (x, y, z) of women in the control group at each of these five equidistant points (see five points as illustrated on Figure 5.2, with their relationship to the P-IS line). Subsequently, for each subject at these five points, we calculated how far the lateral margin of the vagina was from the normal mean determine, if there was a difference in paravaginal distance in women with prolapse compared to those with normal support (Figure 5.3). A similar process was done to assess the distance of the apex from the normal mean position at the cervicovaginal junction. From this point onward, these two measurements will be referred to as the paravaginal distance and apical distance.

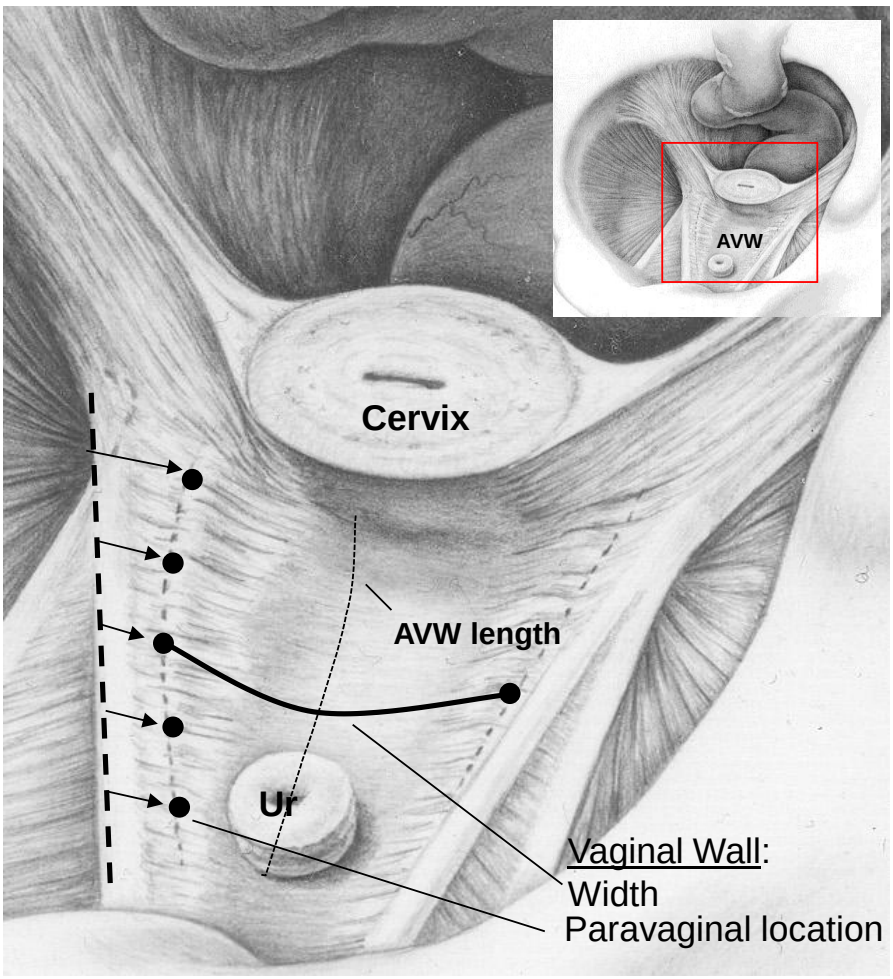

Figure 5.2 Measurement concept. Inset orients one to the view into the pelvis looking over the pubic symphysis towards the rectum. Five *black dots* are shown along the lateral portion of the anterior vaginal wall (*AVW*) on the patient's right side illustrating the division of the vagina in five equidistant locations between the cervicovaginal junction and the urethrovaginal junction. Vaginal wall length between these two is indicated by the *dotted line*. The *solid line* represents an example of the vaginal width measurement. The arrows indicate paravaginal location relative to a reference line along the ATFP on the sidewall. ©DeLancey 2010

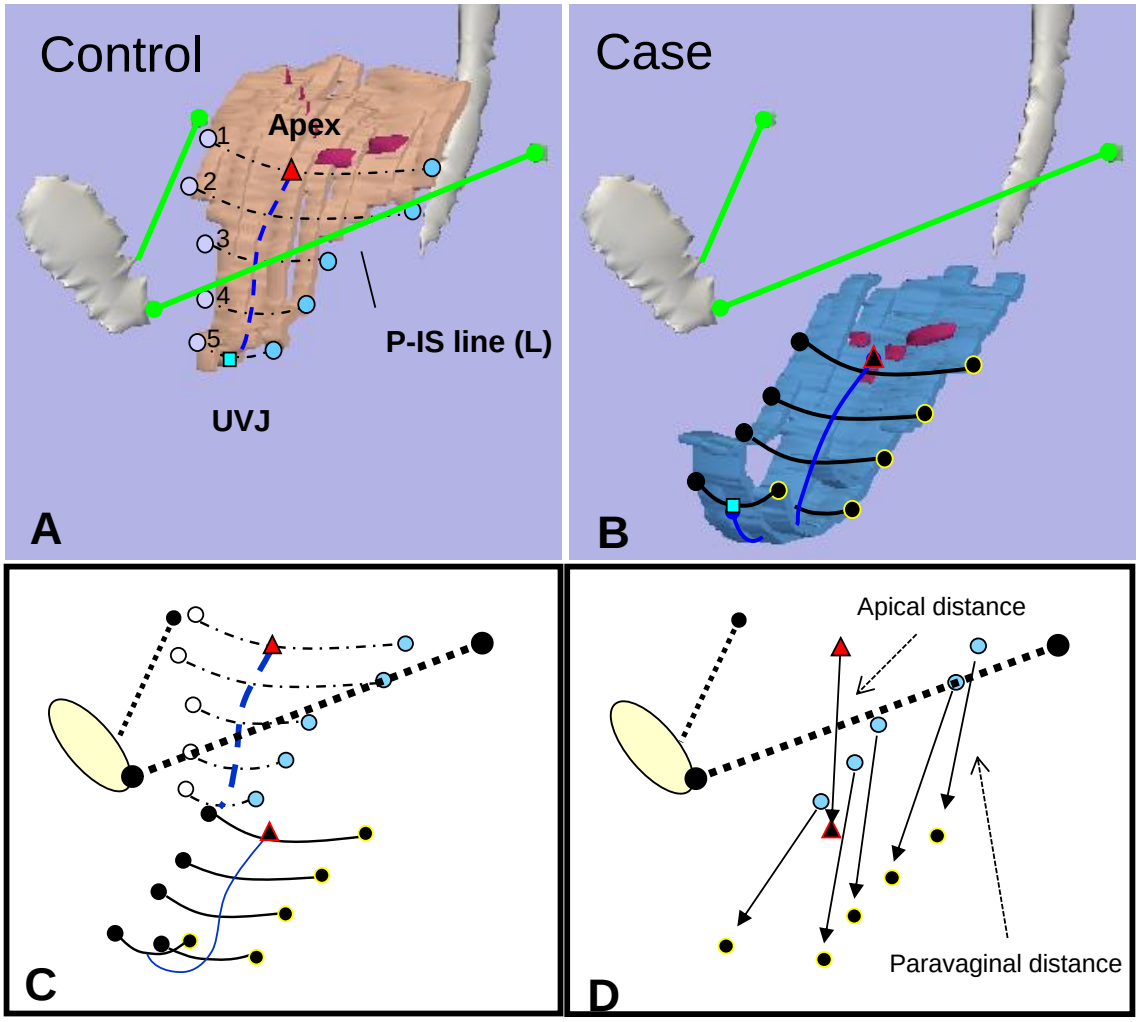

Figure 5.3 Determining distance from normal. **a** Vaginal width and lateral wall locations at five equidistant points from apex at cervicovaginal junction to urethrovaginal junction (*UVJ*) in normal support. Pubis-ischial spine (*P-IS line*) in *green* from insertion of ATFP on pubic symphysis to ipsilateral ischial spine. **b** Similar markings in anterior compartment prolapse. Note, cervicovaginal junction modeled as *purple dots*along the vaginal wall. **c** Alignment of control and prolapse data using P-IS reference line. **d** The distance that lateral locations and apex lie from normal is shown with *arrows* extending from normal location to location in prolapse. Apex (*triangle*), UVJ (*square*), lateral vaginal wall (*circles*), vaginal length (*blue lines*). ©DeLancey 2010

Standard statistical analysis was applied using t tests to compare means of vaginal length and distance of apex from normal. PROC MIXED in SAS® (SAS statistical software version 9.1, SAS Institute, Inc., Cary, NC) was used to carry out a repeated measures analysis of variance for vaginal width and paravaginal distances. Spearman's correlation coefficients were determined to assess the relationships between apical and paravaginal distances. Lastly, Cohen's d effect sizes were determined for statistically significant relationships to determine the strength of their relationship with their case/control status. There was no previous work in this area to provide data for an a priori power analysis; post hoc analysis were performed to determine if the study was adequately powered to conclude that there truly is no difference in non-statistically, but clinically, significant findings.

5.3 Results

Subject characteristics and mean POP-Q values are shown in Table 5.1. The case and control groups were matched for age, parity, and BMI. No statistically significant differences existed between the two groups with the exception of the POP-Q, as was the study design.

Group comparisons for paravaginal distances, vaginal width, and apical distance are shown graphically in Figure 5.4. Table 5.2 details the magnitude of these differences. At maximal Valsalva, the lateral margin of the vagina lies significantly farther from its normal position in women with prolapse than in women with normal support. As can be seen in Figure 5.4a, these phenomenon occurred along the length of the vagina, locations "1 to 4," with the largest difference at location "3" in the mid-vagina, the area corresponding to the exposed area that slides beyond the support of the levator muscles

and perineal body. At this point, the prolapse group mean (combining right and left sides) was 1.8 cm farther from the normal position than the control group mean (3.2 ± 0.8 cm vs. 1.4 ± 0.6 cm; $p = 0.0001$).

Table 5.1 Demographics

Characteristics	Cases ($n = 10$)	Controls ($n = 10$)	p value
Age (years)[a]	56.3 (6.7)	62.9 (13.1)	0.17
BMI (kg/m^2)[a]	27.2 (4.4)	25.19 (4.5)	0.32
Median parity (range)	2 (1–5)	2.5 (2–6)	
Race[b]			
Caucasian	8 (80%)	10 (100%)	0.47
African American	2 (20%)	0 (0%)	
POP-Q[a]			
Aa	1.5 (1.0)	−1.7 (0.9)	0.0001
Ba	2.2 (1.6)	−1.6 (1.0)	0.0001
C	−3.2 (1.6)	−6.0 (1.1)	0.0002
D	−6.5 (1.1)	−8.9 (1.1)	0.0001

BMI body mass index
[a] Data are mean (SD) unless otherwise specified
[b] Fisher's exact used to calculate *P*

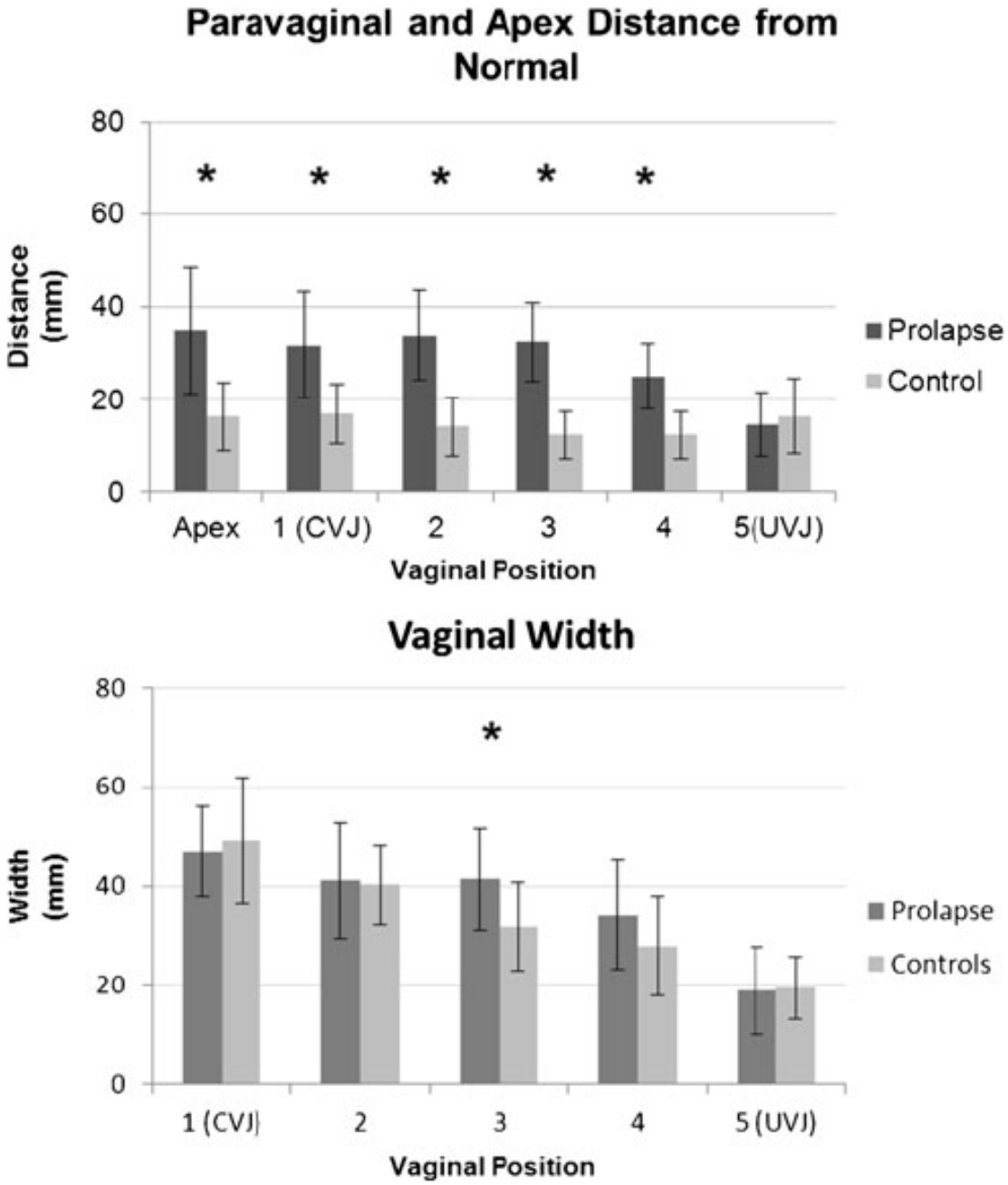

Figure 5.4 Comparing apical and paravaginal distances from normal (**a**) and vaginal width (**b**). Note that "1" represents the apex at the cervicovaginal junction (CVJ) and position "*5*," the urethrovaginal junction (UVJ) at the distal end. *Asterisks* mark statistically significant differences. Note that right and left paravaginal distance means have been combined to one overall mean. Standard deviation shown. ©DeLancey 2010

Table 5.2 Effect sizes and correlations

Measurement	Case mean[a]	Control mean[a]	Difference	*P*[b]	Effect size	Spearman correlation with apex	*P*[c]
Paravaginal right[d]							
1	31.9 (12.5)	15.5 (8.2)	16.4	<0.001	1.6	0.92	<0.001
2	36.0 (9.3)	16.5 (6.5)	19.5	<0.001	2.5	0.93	<0.001
3	34.4 (8.9)	14.0 (5.9)	20.4	<0.001	2.8	0.85	<0.001
4	25.1 (6.7)	12.1 (5.0)	13	0.001	2.2	0.69	<0.001
5	15.3 (8.4)	12.2 (4.7)	3.1	0.419	0.5	0.42	0.06
Paravaginal left[d]							
1	31.8 (11.1)	17.3 (7.0)	14.5	<0.001	1.6	0.85	<0.001
2	32.0 (9.9)	17.3 (7.0)	14.7	<0.001	1.7	0.9	<0.001
3	30.7 (7.9)	14.1 (7.0)	16.6	<0.001	2.2	0.77	<0.001
4	25.0 (8.1)	12.4 (7.0)	12.6	0.0004	1.8	0.55	<0.001
5	13.7 (5.6)	12.4 (5.8)	1.3	0.689	0.2	0.32	0.17
Vaginal width[d]							
1	46.9 (9.0)	49.2 (12.7)	−2.2	0.616			
2	41.1 (11.5)	40.3 (7.9)	0.8	0.851			
3	41.3 (10.2)	31.9 (8.9)	9.5	0.035	1		
4	34.2 (11.0)	27.9 (10.1)	6.4	0.154			
5	18.9 (8.9)	19.5 (6.4)	−0.6	0.89			
Apex[e]	35.0 (13.6)	16.4 (8.0)	18.6	0.0016	1.7		
Vaginal length[f]	72.4 (15.3)	58.3 (7.4)	14.1	0.0216	1.2		

[a] Data presented as mean (SD)
[b] *P* value for test of equal means
[c] *P* value for test of correlations
[d] PROC MIXED
[e] Equal variance *t* test
[f] Unequal variance *t* test

In addition, the apex was significantly farther from the normal mean location in women with prolapse (3.5 ± 1.4 vs. 1.6 ± 0.8 cm in controls; $p = 0.002$). The apical distance strongly correlated with paravaginal distances for locations 1 to 3 with Spearman correlation coefficients ranging from 0.77 to 0.93. This relationship was slightly weaker for position "4" and did not hold at position "5" near the urethrovaginal junction. Figure 5.4 contains scatter plots of these relationships at positions "1–5." Please note that while Figure 5.4a combines right and left sides when comparing cases and controls to simplify the comparison, these scatter plots keep right and left sides separate to better visualize the raw data. Statistical analysis using PROC MIXED did not show any statistically significant difference between sides.

The mid-vagina was wider in women with prolapse compared to their normal counterparts. At location "3," the mean vaginal width was 4.1 ± 1.0 cm in women with prolapse as opposed to 3.2 ± 0.9 cm in those with normal support ($p = 0.04$). There was a similar trend in position "4"; however, at the study sample size, this finding was not statistically significant (Figure 5.4b). We considered 20% a clinically significant difference in vaginal width, and at both positions "3" and "4," the difference exceeded this. Post hoc power analysis for the non-statistically significant position "4" revealed that the current study was not powered adequately to detect this difference at position "4" and would require approximately 55 individuals in each group to reach 80% power with an alpha of 0.05. In addition, the mean anterior vaginal length was different in cases and controls (7.2 ± 1.5 and 5.8 ± 0.7 cm, respectively; $p = 0.02$).

Effect sizes for statistically significant findings show that case–control paravaginal distances are more than twice as large as vaginal width changes (Table 5.2).

5.4 Discussion

It has been possible to quantify apical descent, cystocele size, and vaginal length in the midline sagittal straining images. However, it has not previously been possible to quantify the size of paravaginal defects and the degree of vaginal widening, both of which are relevant to the two major hypotheses of cystocele causation. This study uses a recently developed 3-D MR imaging strategy (Larson et al. 2010) to visualize and quantify anterior vaginal wall displacement and deformation at maximal Valsalva so that women with prolapse can be compared to women with normal support. It objectively measures the deformation, determining whether the vaginal wall is wider, suggesting a midline defect, or separates from the sidewall, suggesting a paravaginal defect. The outcomes of our study include the following findings: (1) the largest differences are in paravaginal distance in women with prolapse; (2) this distance is strongly correlated with apical distance; (3) in women with prolapse, the vaginal wall widens somewhat in the area at mid-vagina, that region that extends below, the support of the levator muscles and perineal body; and (4) this effect size of vagina width between cases and controls was smaller than that associated with paravaginal changes.

In essence, what this study shows is that the lateral vagina is displaced from its normal position in women with anterior wall prolapse proving the hypothesis that paravaginal defects exist. It also confirms anterior vaginal wall widening, albeit at a much lesser extent than the paravaginal changes. It is of special interest that paravaginal distance is highly correlated with apical distance. This confirms the mechanistic observation that these two phenomenon are related (DeLancey 2002) and the recent predictions of biomechanical models (Chen et al. 2009). While the 3D models appear

consistent with paravaginal defects, whether this fits with the classical description of the defect is another issue. We are not suggesting, at present, that MRI is required before selecting surgical management in treating anterior vaginal wall prolapse. However, it is possible to see the day when the ability to quantify paravaginal defect, apical descent, and vaginal widening could have great clinical utility and help in selecting which woman might need an apical suspension and which may need steps to reduce vaginal widening.

This study both corroborates and extends existing literature and our current understanding of anterior vaginal wall support. As in other studies, our subjects with prolapse had increased apical distance and increased vaginal length when compared to women with normal support (Chen et al. 2006; Hsu et al. 2008; Rooney et al. 2006; Summers et al. 2006). Our findings expand upon our earlier published study (Larson et al. 2010) establishing the appearance of the anterior vaginal wall at maximal Valsalva in which we describe the morphological changes seen in 3-D models to include downward translation (or downward movement along the length of the vagina) and vaginal cupping. This study quantifies these changes by defining the extent of lateral movement from normal and vaginal widening in response to Valsalva.

The concept of a paravaginal defect has been described since the early 1900s. The first description of separation of the lateral vagina from the arcus tendineus fascia pelvis along the pelvic sidewall is attributed to White (White 1909). This observation went largely unnoticed until the landmark contributions of Richardson in the late 1970s/early 1980s. Richardson et al. described the paravaginal defect and reported on the results of a novel repair in a large series of surgical patients (Richardson et al. 1981; Richardson et al. 1976). Despite the fact that this separation had been described a century ago and actively

discussed for almost 30 years, there remains significant controversy on the subject, ranging from its prevalence in population studies of women with anterior wall prolapse (ranging from 37% to 88%) to the ability to diagnose these defects both preoperatively and intraoperatively (Barber et al. 1999; DeLancey 2002; Dietz et al. 2005; J. K. Nguyen 2001; Richardson et al. 1981; Richardson et al. 1976; Segal et al. 2004). Barber et al. reported good sensitivity and negative predictive values, but poor specificity and positive predictive values for preoperative identification of these defects on physical examination (Barber et al. 1999). Segal et al. found lower sensitivities and higher specificities for clinical evaluation of these defects and found that the classic teaching of presence or absence of rugae did not correlate with defect status (Segal et al. 2004). Intraoperative identification of these defects is plagued with concerns of missing defects with vaginal assessment or creating iatrogenic defects when trying to assess the integrity of these tissues. In his comparison of clinical exam with ultrasound imaging of paravaginal defects, Dietz et al. found poor correlations between the two and suggested the paravaginal defect "be regarded as an unproven concept." (Dietz et al. 2005). To date, we are not aware of other studies that have measured the degree of a paravaginal defect and widening of the vagina so that they could be compared between symptomatic and asymptomatic women.

Our observations concern the distance that the lateral margin of the prolapsed vagina lies from its position in women with normal support. Technology currently limits our ability to see and model the thin ATFP accurately in women at maximal Valsalva, even though we can model it at rest. Therefore, although we know there is the significant difference in the paravaginal distance compared to women with normal support, we do

not know the relationship of the ATFP with the lateral vagina in these women. Even without knowing the position of the ATFP, the displacement described in our study clearly is what is clinically recognized in women as a paravaginal defect. One of the classic tests for diagnosing a paravaginal defect is to correct the presumed defect with support during Valsalva (using either a ring forceps, vaginal analyzer, or tongue depressor along the lateral vagina at the ischial spine to see if it reduces the prolapse, and if so, this is deemed a paravaginal defect). This "test" would also be minimizing the apical movement and may be reducing the cystocele for this reason. We propose that it is at least plausible that these are manifestations of the same phenomenon.

The observation that apical and paravaginal distances are part of the same phenomena is in agreement with surgical results. For example, abdominal sacrocolpopexy eliminates cystocele in the vast majority of cases. Shippey et al. recently reported anatomic outcomes of sacrocolpopexy in women with and without paravaginal repair. Sixty-two patients had concomitant paravaginal repair while 108 subjects did not. Although the data trended towards higher anterior wall failure rates in the group without a paravaginal repair, the study was not powered to detect this difference. In addition, once they controlled for concomitant Burch, the presence/absence of a paravaginal repair did not seem as influential (Shippey et al. 2010). Although this may solely have been an inadequate power issue, it does raise the thought that perhaps restoration of the apical position in these women was adequate to restore normal anterior vaginal wall support.

Although this "jibes" with why addressing apical support at the time of cystocele repair is crucial, it then begs the question as to why surgical approaches such as an anterior repair alone are successful for cystocele repair. In his discussion on the clinical

relevance of a paravaginal defect, Karram raises a similar question concerning anterior compartment recurrence rates of 5–15% which are independent of whether or not a paravaginal repair is performed (Karram 2004). Our study did reveal widening at one position in this area of exposed vagina, but it seems that this minor difference is not sufficient to explain why narrowing the vagina would correct the entire cystocele. A second area within this region (position 4) also appeared to trend towards having a significant (22%) widening, although was not statistically significant at this smaller sample size. Perhaps anterior colporrhaphy, by reducing the surface area of the exposed vagina, brings the anterior wall back into contact with the posterior vaginal wall, reducing the tension on the support ligaments. In a sample size of ten women with anterior wall predominant prolapse we cannot capture the full spectrum of defects: clinically we see women with good apical support and isolated anterior wall defects. Perhaps this latter population is the one that has a successful outcome with an isolated anterior repair. It is not possible to conclude this from our study; however, the present measurement technique allows quantification of the degree of defects present so that future outcome studies could determine which factors are correlated with treatment success or failure.

So is there a midline defect? The widening visible in the mid to distal region of the vagina indicates a change from normal. It does not indicate whether this is the cause or effect of cystocele, nor whether it is a change in the material properties of the vaginal wall or the result of a break in the "anteroposterior separation of the fascia [that] occurs between the vagina and overlying bladder and/or urethra" as described by Richardson et al. (White 1909). The observed stretching may also be the result of the increased pressure

differential across the exposed portion of the vagina that no longer has the posterior vaginal wall to counteract increases in intra-abdominal pressure. This study cannot differentiate between stretching of the anterior vaginal wall and a break in the fascia (if these exist) because we are unable to visualize the presence of a break or separation of the fascia with the current MRI technology. Our results do indicate, however, that regardless of the underlying mechanism, this widening has a much smaller effect size than the paravaginal distances.

Several factors must be considered when interpreting the results of this study. While we are able to identify large and significant changes in the location of the lateral vagina in women with prolapse and assess the relative size of the differences in paravaginal distance and vaginal width, our study sample size did not have the power to detect more subtle changes in vaginal width. These changes are of lesser magnitude as reflected in their small effect sizes and are not as great as the paravaginal distance changes. In addition, we recognize that a larger sample size and further studies are indicated to capture the full spectrum of different cystoceles. While mentioning this, it is important to recognize that we had to screen 21 cases to find ten adequate image sets in women with prolapse. Certainly, as imaging techniques improve, this ratio will also improve. As in our previous studies, supine MR images were obtained which may limit the descent of the pelvic floor, although earlier studies do not document differences when compared with images obtained in the seated position in open scanners (Bertschinger et al. 2002; Fielding et al. 1998). Clinicians do make the majority of their clinical decisions based on examinations performed in women who are supine, and we feel that with adequate Valsalva, the maximal extent of the prolapse can be achieved. The ability to

sustain Valsalva is difficult in some women and is a likely contributor to the large number excluded in the initial subject selection process. Because the sulci are difficult to differentiate on MR images, vaginal gel was used to illuminate the lateral extent of the vagina. Although it significantly improved visualization, this gel does result in some degree distortion of the vaginal shape by filling the vagina. We suspect this effect is minimal as the gel's viscosity was such that Valsalva efforts seemed to result in expulsion of gel, rather than a redistribution which could distort the vaginal wall.

So is it a midline or paravaginal defect? Our results indicate that there are changes in both regions of the vagina but show that the changes at the lateral vagina and the altered relationship with the pelvic sidewall are much larger than the widening of the mid-distal region of the vaginal wall. In addition, the strong correlation between the "paravaginal defect" and apical distance causes us to theorize that these may be manifestations of the same phenomenon. Which came first—the apical displacement or the pulling away from the pelvic sidewall? Although an answer is not possible with this study, the present method not only provides the means to explore this in the future, but also provides the ability to quantify paravaginal defects, apical descent and vaginal widening to aid in analyzing the outcomes of specific interventions and, ultimately, clinically impact treatment selection.

References

Barber, M. D., Cundiff, G. W., Weidner, A. C., Coates, K. W., Bump, R. C., & Addison, W. A. (1999). Accuracy of clinical assessment of paravaginal defects in women with anterior vaginal wall prolapse. *American Journal of Obstetrics and Gynecology, 181*(1), 87-90.

Benson, J. T., Lucente, V., & McClellan, E. (1996). Vaginal versus abdominal reconstructive surgery for the treatment of pelvic support defects: a prospective randomized study with long-term outcome evaluation. *Am J Obstet Gynecol, 175*(6), 1418-1421; discussion 1421-1412.

Bertschinger, K. M., Hetzer, F. H., Roos, J. E., Treiber, K., Marincek, B., & Hilfiker, P. R. (2002). Dynamic MR imaging of the pelvic floor performed with patient sitting in an open-magnet unit versus with patient supine in a closed-magnet unit. *Radiology, 223*(2), 501-508.

Chen, L., Ashton-Miller, J. A., & DeLancey, J. O. L. (2009). A 3D finite element model of anterior vaginal wall support to evaluate mechanisms underlying cystocele formation. *Journal of Biomechanics, 42*(10), 1371-1377.

Chen, L., Ashton-Miller, J. A., Hsu, Y., & DeLancey, J. O. L. (2006). Interaction among apical support, levator ani impairment, and anterior vaginal wall prolapse. *Obstetrics and Gynecology, 108*(2), 324-332.

DeLancey, J. O. L. (2002). Fascial and muscular abnormalities in women with urethral hypermobility and anterior vaginal wall prolapse. *American Journal of Obstetrics and Gynecology, 187*(1), 93-98.

Dietz, H. P., Pang, S., Korda, A., & Benness, C. (2005). Paravaginal defects: a comparison of clinical examination and 2D/3D ultrasound imaging. *Australian & New Zealand Journal of Obstetrics & Gynaecology, 45*(3), 187-190.

Fielding, J. R., Griffiths, D. J., Versi, E., Mulkern, R. V., Lee, M. L. T., & Jolesz, F. A. (1998). MR imaging of pelvic floor continence mechanisms in the supine and sitting positions. *American Journal of Roentgenology, 171*(6), 1607-1610.

Hsu, Y., Chen, L., Summers, A., Ashton-Miller, J. A., & DeLancey, J. O. L. (2008). Anterior vaginal wall length and degree of anterior compartment prolapse seen on dynamic MRI. *International Urogynecology Journal, 19*(1), 137-142.

Karram, M. M. (2004). What is the clinical relevance of a paravaginal defect? *International Urogynecology Journal, 15*(1), 1-2.

Larson, K. A., Hsu, Y., Chen, L., Ashton-Miller, J. A., & DeLancey, J. O. L. (2010). Magnetic resonance imaging-based three-dimensional model of anterior vaginal wall position at rest and maximal strain in women with and without prolapse. *International Urogynecology Journal, 21*(9), 1103-1109.

Maher, C., & Baessler, K. (2006). Surgical management of anterior vaginal wall prolapse: an evidencebased literature review. *International Urogynecology Journal, 17*(2), 195-201.

Maher, C. F., Murray, C. J., Carey, M. P., Dwyer, P. L., & Ugoni, A. M. (2001). Iliococcygeus or sacrospinous fixation for vaginal vault prolapse. *Obstetrics and Gynecology, 98*(1), 40-44.

Nguyen, J. K. (2001). Current concepts in the diagnosis and surgical repair of anterior vaginal prolapse due to paravaginal defects. *Obstetrical & Gynecological Survey, 56*(4), 239-246.

Nguyen, J. N., & Burchette, R. J. (2008). Outcome after anterior vaginal prolapse repair - A randomized controlled trial. *Obstetrics and Gynecology, 111*(4), 891-898.

Olsen, A. L., Smith, V. J., Bergstrom, J. O., Colling, J. C., & Clark, A. L. (1997). Epidemiology of surgically managed pelvic organ prolapse and urinary incontinence. *Obstetrics and Gynecology, 89*(4), 501-506.

Richardson, A. C., Edmonds, P. B., & Williams, N. L. (1981). TREATMENT OF STRESS URINARY-INCONTINENCE DUE TO PARAVAGINAL FASCIAL DEFECT. *Obstetrics and Gynecology, 57*(3), 357-362.

Richardson, A. C., Lyon, J. B., & Williams, N. L. (1976). NEW LOOK AT PELVIC RELAXATION. *American Journal of Obstetrics and Gynecology, 126*(5), 568-573.

Rooney, K., Kenton, K., FitzGerald, M. P., & Brubaker, L. (2006). Advanced anterior vaginal wall prolapse is highly corretated with apical prolapse. *American Journal of Obstetrics and Gynecology, 195*(6), 1837-1840.

Segal, J. L., Vassallo, B. J., Kleeman, S. D., Silva, W. A., & Karram, M. M. (2004). Paravaginal defects: prevalence and accuracy of preoperative detection. *International Urogynecology Journal, 15*(6), 378-383.

Shippey, S. H., Quiroz, L. H., Sanses, T. V. D., Knoepp, L. R., Cundiff, G. W., & Handa, V. L. (2010). Anatomic outcomes of abdominal sacrocolpopexy with or without paravaginal repair. *International Urogynecology Journal, 21*(3), 279-283.

Shull, B. L., Bachofen, C., Coates, K. W., & Kuehl, T. J. (2000). A transvaginal approach to repair of apical and other associated sites of pelvic organ prolapse with uterosacral ligaments. *Am J Obstet Gynecol, 183*(6), 1365-1373; discussion 1373-1364.

Summers, A., Winkel, L. A., Hussain, H. K., & DeLancey, J. O. L. (2006). The relationship between anterior and apical compartment support. *American Journal of Obstetrics and Gynecology, 194*(5), 1438-1443.

White, G. R. (1909). Cystocele--a radical cure by suturing lateral sulci of the vagina to the white line of pelvic fascia. 1909. *Int Urogynecol J Pelvic Floor Dysfunct, 8*(5), 288-292.

CHAPTER 6

CHANGES IN LENGTH AND AXIS OF THE CARDINAL AND UTEROSACRAL LIGAMENTS IN WOMEN WITH AND WITHOUT PELVIC ORGAN PROLAPSE

Abstract

Introduction and Hypothesis: We needed to develop a technique and strategy to test hypotheses concerning changes in the apical ligaments at rest and under maximal Valsalva. In this study we aimed to use subject-specific 3-D models based on MRI scans to test the hypotheses under physiological loading (maximal Valsalva) that a) the length of the ligaments at rest is no different between prolapse and normal women, and b) ligament elongation (length change from rest to Valsalva) for each ligament is greater in prolapse than normal women, and c) the change of length and angle of each ligament is not the same between women with and without prolapse.

Methods: Ten women with (cases) and ten without (controls) pelvic organ prolapse were selected from an ongoing case-control study. Supine, multi-planar stress MR imaging was performed at rest and maximal Valsalva. Axial, sagittal, and coronal scans under both conditions were imported into an imaging software 3D Slicer v. 3.4.1 (Brigham and Women's Hospital, Boston, MA) and aligned with bony anatomic landmarks. 3-D

reconstructions of the uterus and vagina, cardinal ligament, deep uterosacral ligament and pelvic bones were then created in 3D Slicer.

Results: The mean age was 53.7 ± 4.5 (SD) for control group and 55.3 ± 8.1 years for prolapse group, and mean parity was 2.7 and 2.4, respectively. The length change of cardinal ligament was 15 ± 9 mm and 30 ± 16 mm ($p = 0.033$) for healthy and prolapse group, respectively. The length change of uterosacral ligament was 7 ± 4 mm and 15 ± 12 mm ($p = 0.094$) for healthy and prolapse group. During straining, the cardinal ligament was lengthened more in the prolapse group (101 ± 21 mm) than in the healthy group (73 ± 11 mm) with $p = 0.003$, while uteosacral ligament was lengthened to 50 ± 13 mm in prolapse group and 39 ± 6 mm in healthy group ($p = 0.037$). The angle with body axis of the cardinal ligament was 21 ± 6 deg in prolapse group and 30 ± 7 deg in the healthy group, while the angle with body axis of the uterosacral ligament was significantly smaller in the prolapse group (57 ± 16 deg) than in the healthy group (74 ± 18 deg), with $p < 0.001$ comparing the angle changing for CL vs USL.

Conclusions: The length of both pairs of apical support ligaments at rest are no different between prolapse and normal women at rest; CL ligament elongation (length change from rest to Valsalva) was greater in prolapse than normal women, while USL was not (at this same sample size); CL exhibits greater differences in the ligament length, while USL exhibits larger differences in ligament inclination angle when comparing women with normal support and prolapse.

Key words: pelvic organ prolapse, apical support, cardinal ligament, uterosacral ligament, 3D model

6.1 Introduction

Pelvic floor dysfunction has resulted in 11% of women undergoing surgery (Olsen et al. 1997) during their lifespan in the USA. Over 200,000 operations are performed for prolapse (Boyles et al. 2003) each year and the annual estimated cost for these operations exceeds US $1 billion (Subak et al. 2001).

The apical support provided by cardinal (CL) and uterosacral ligament (USL) is one of the main factors related to pelvic organ prolapse (Summers et al. 2006). However, the behaviour of CL and USL in living women with prolapse has not been studied.

This study was therefore undertaken by conducting a secondary analysis of data from an on-going case-control study of pelvic organ prolapse. We built subject-specific 3-D models of the CL and deep USL for each subject using MRI scans at rest and during Valsalva to establish ligament length in these conditions. We then tested the hypotheses that a) the length of the ligaments at rest is no different between prolapse and normal women at rest; b) ligament elongation (length change from rest to Valsalva) for each ligament is greater in prolapse than normal women; and c) the changes of length and angle of the ligaments are not the same. By quantifying how much each ligament lengthens, we can gain information about the degree of ligament shortening required to restore normal apical location and ligament prolapse dynamics.

6.2 Materials and methods

MRI scans of 10 women with pelvic organ prolapse (cases) and 10 with normal support (controls) were selected from an ongoing University of Michigan institutional review board-approved (IRB # 1999-0395) case-control study of pelvic organ prolapse.

Women in the control group were recruited by newspaper and radio advertisement for healthy volunteers and had to be asymptomatic and have normal vaginal support with all pelvic organ prolapse quantification (POP-Q) points < -1 cm. The prolapse group included five cystocele type anterior vaginal prolapse (AVP) subjects and five rectocele type posterior vaginal prolapse (PVP) predominant subjects. All cystocele cases had anterior vaginal wall (AVW) extending at least 1 cm below the hymen based on POP-Q. In order to be included, the cystocele had to be the predominant aspect of the prolapse and extend at least 1 cm lower than the most dependent part of posterior vaginal wall or the uterus/apex. Similarly, all rectocele cases had posterior vaginal prolapse with posterior vaginal wall (PVW) extending at least 1 cm below the hymen based on POP-Q and had symptoms of bulging or protrusion. In order to be included, the rectocele had to be the predominant aspect of the prolapse and extend at least 1 cm lower than the most dependent part of anterior wall or the uterus/apex. Women with predominant enteroceles were excluded. None of the subjects had previously undergone hysterectomy or prior pelvic floor surgery. Twenty scans of women with cystocele or rectocele were further evaluated for inclusion according to the following criteria: prolapse size consistent with clinical examination (POP-Q), ability to hold Valsalva for the entire 17 seconds of scan acquisition, freedom from significant motion artifact, inclusion of all necessary structures, evenly distributed intravaginal ultrasound gel and sufficient definition of vaginal walls to allow models to be made. Ten of 20 scans were selected based on above criteria. Similarly, the matched controls (who had an age difference within ± 3 years, number of vaginal deliveries within ± 1, and were of similar race) had to meet the above criteria with the exception of not having prolapse.

As described in our previous work (Larson et al. 2010; Larson et al. 2012; Luo et al. 2012), each subject underwent pelvic floor stress MRI. This involved obtaining supine multi-planar, two-dimensional, fast spin, proton density MR imaging both at rest and during maximal Valsalva using a 3 T superconducting magnet (Philips Medical Systems Inc, Bothell, WA) with version 2.5.1.0 software. At rest, each 30 images were serially obtained at the axial, sagittal, and coronal, with 20x20 cm fields of view, 4 mm slice thickness, and a 1 mm gap between slices. During maximal Valsalva, 14 images were obtained at the same three serial planes, with 36x36 cm fields of view, 6 mm slice thickness, and 1 mm gap. In order for the images to be considered adequate, they had to allow visualization of vaginal margins.

The axial, sagittal and coronal MR images were imported into imaging software 3D Slicer 3.4.2009-10-15 (Brigham and Women's Hospital, Boston, MA). The resting

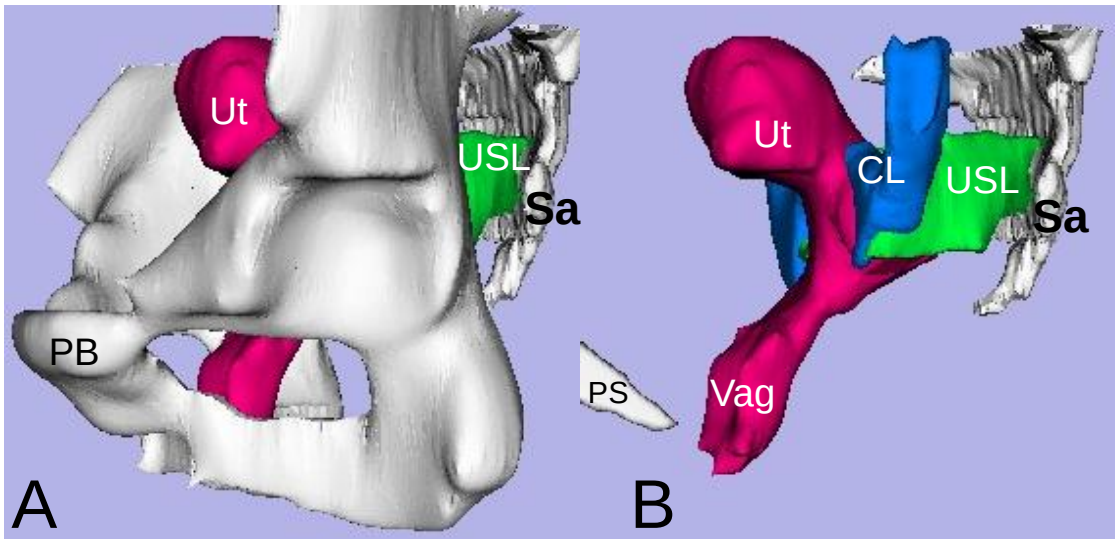

Figure 6.1 3D Model. (A) and (B), 3D models of pubic bone (**PB**), Sacrum (**Sa**), Uterus (**Ut**), Vagina (**Vag**), Cardinal ligaments(**CL**), and Uterosacral ligament (**USL**) in three quarters view. **PS**: Pubic symphysis.

axial, sagittal and coronal MR images were manually aligned first with fixed landmarks such as pubic bone, hip joint, and sacrum. 3-D reconstructions of the uterus and vagina, CL, deep uterosacral ligament and pelvic bones were then created in 3D Slicer. The deep USL was identified (Umek et al. 2004) and traced on axial MR images with its origins from genital track and insertions to sacrospinous ligament-coccygeus muscle. The CL was identified (Tunn et al. 2001) and traced on coronal MR images with its origins from the pelvic side wall at the top of the greater sciatic foramen to its insertion on the genital tract centered on the cervix and upper vagina. Figure 6.1 illustrates the 3D models generated in three quarters view at rest with and without pelvic bone. The models were compared to the original MR images to check model fidelity.

To analyze the deformation of CL and USL under load, 3-D models of mid-sagittal pubic symphysis and sacrum were reconstructed using the MR images from

maximal Valsalva (straining) and aligned with the pelvic bones of the resting images. This registration information was then applied to the soft tissue images making it possible to align the mid-sagittal straining images with resting images. The strain axial and coronal MR images were then manually aligned with the straining mid-sagittal images using bony landmarks as above. As described in our previous study (Chen et al. 2012), the models and anatomical landmarks were imported into Imageware v.13 (Siemens Product Lifecycle Management Software Inc, Plano, TX). The model and measurement strategy are shown in Figure 6.2 based on the model from MR scans under rest. The 3-D lines-of-action of the four ligaments were determined by connecting center of the origin and insertion points (Figure 6.2A, B). To accurately measure the length and curvature of these ligaments, a cross-section was constructed for each ligament by cutting the model with a plane defined by its line-of-action and genital origin point of opposite side. The best fit curve of the ligament was constructed by connecting the center line of the cross-section. The curve length of the ligaments was measured and distance between origins and insertions was assessed (Figure 6.2). The measurement for ligaments under maximal Valsalva was then executed following the same strategy.

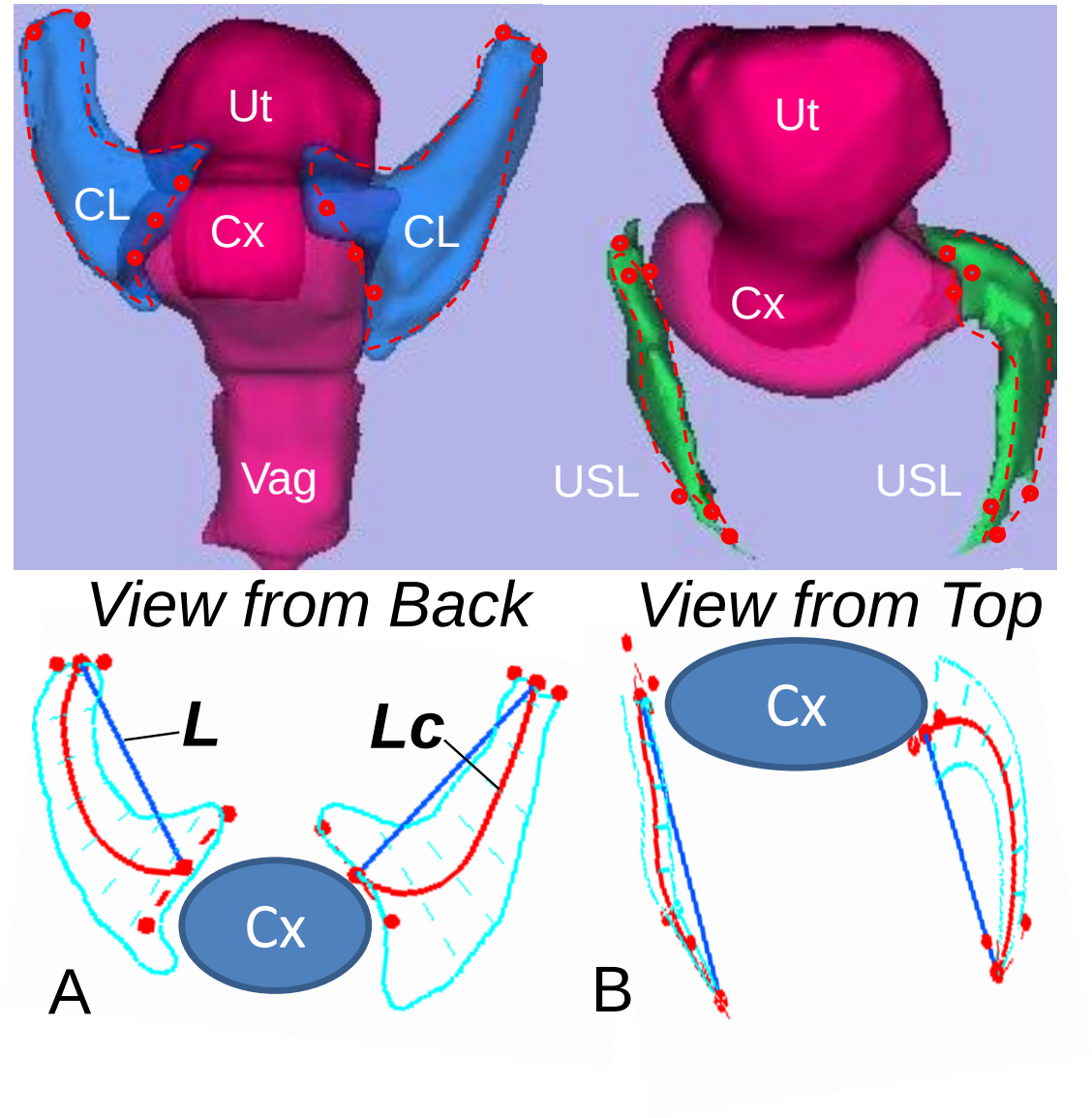

Figure 6.2 Method of measurement. (A) Identification of origin-insertion line and best fit curve for the cardinal ligament in back view. Red dots are the landmarks identified for origins and insertions. Dark blue line connects the center of landmarks to establish the line-of-action. Red curve present the best fit curve of the ligaments on the cross-section showed as red dash on the top model and cyan line in the bottom. Length of the line-of-action is ***L***. Length of the curve is ***Lc.*** (B) Identify uterosacral ligament line-of-action and best fit curve in axial plane. **Ut**: uterus; **Cx**: cervix; **Vag**: vagina; **CL**: cardinal ligament; **USL**: uterosacral ligament. (Modified from (Chen et al. 2012))

Descriptive statistical analysis and independent-samples T-test analysis were applied with a *p* value at significant levels of 0.05, 0.01 and 0.001.

6.3 Results

The demographics and POP-Q data of the 20 subjects are shown in Table 6.1. None of the patients in case or control group has undergone hysterectomy.

Table 6.1 Demographics

Characteristics	Cases (n=10)		Controls (n=10)	*p* value
	AVP (n=5)	PVP (n=5)		
Age (yrs)[a]	53.2 (7.8)	57.4 (8.8)	53.7(4.5)	0.538
BMI (kg/m2)[a]	24.7 (2.0)	29.7 (3.3)	26.5 (5.1)	0.181
Parity[a]	2.6 (0.9)	2.2 (1.3)	2.7 (1.3)	0.745
Race[b]				
Caucasian	4 (80%)	5 (100%)	9 (90%)	
POP-Q (cm)[a]				
Aa	1.4 (1.1)	-1.0 (1.4)	-1.9 (0.9)	< 0.001
Ba	2.6 (1.5)	-1.4 (0.9)	-1.9 (0.9)	< 0.001
C	-0.8 (3.4)	-5.5 (1.6)	-7.0 (1.3)	< 0.001
D	-5.8 (2.6)	-7.3 (1.3)	-9.3 (1.2)	0.004
Ap	-0.6 (1.7)	1.6 (0.5)	-2.2 (0.4)	< 0.001
Bp	-0.6 (1.7)	1.8 (0.8)	-2.2 (0.4)	< 0.001
GHrest	5.3 (2.2)	4.4 (1.9)	3.0 (0.9)	0.031
LHrest	8.5 (2.1)	7.5 (1.7)	6.7 (1.3)	0.139
TVL	10.6 (1.1)	9.6 (1.1)	10.5 (1.1)	0.319

GHrest, genital hiatus at rest; *LHrest*, levator hiatus at rest; *TVL*, total vaginal length

[a] Data are mean (SD)

[b] Data are n (%)

The lateral view of rest and strain models of one normal and one prolapse subjects were shown in Figure 6.3. The public symphysis (PS) to the ischial spines (yellow squares), or the P-IS line (Luo et al. 2012; Larson et al. 2012), was also shown for spatial reference.

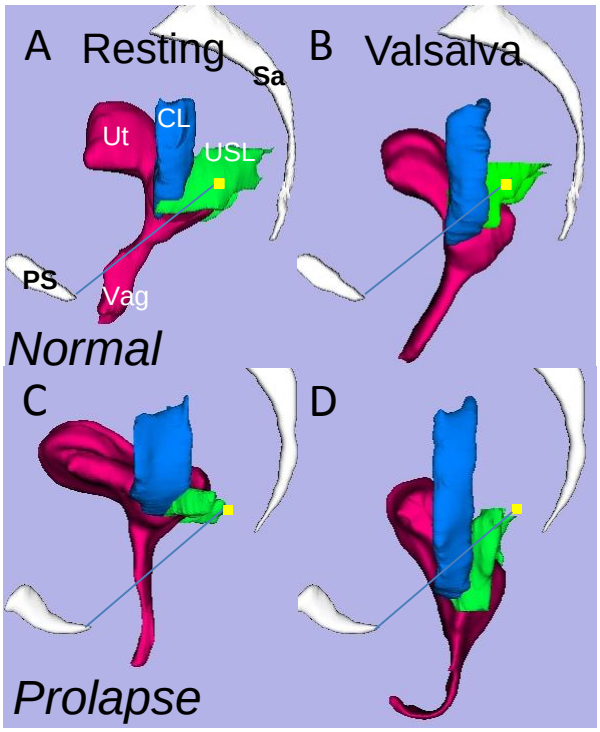

Figure 6.3 Normal and prolapse ligaments comparison under resting and maximal Valsalva. (A) and (B) are left side view of 3D models of one normal subject under resting (A) and maximal Valsalva (B) with their relationship to the normalized arcus tendineus fascia pelvis (ATFP), shown here as the turquoise lines extending from the public symphysis (PS) to the ischial spines (yellow squares), or the P-IS line, for spatial reference. (C) and (D) are left side view of 3D models of one prolapse subject under resting (C) and maximal Valsalva (D). Pubic symphysis (PS) and sacrum (Sa) are shown in middle sagittal plane. **Ut**: uterus; **Cx**: cervix; **Vag**: vagina; **CL**: cardinal ligament; **USL**: uterosacral ligament.

Figure 6.4 reveals that the resting length of ligaments did not differ in women with and without prolapse (CL, $p = 0.051$; USL, $p = 0.797$). The straining length of cardinal and uterosacral ligaments differed significantly in women with and without prolapse (CL, $p = 0.003$; USL, $p = 0.037$). Cardinal ligament during straining was longer than that in resting in both healthy ($p = 0.005$) and prolapse ($p = 0.003$) groups. The cardinal ligament lengthened from resting to strain for women with (30 ± 16 mm) and without (15 ± 9 mm) prolapse ($p = 0.033$). Uterosacral ligament did not. In addition, at rest and during straining, the cardinal ligament was substantially longer than the uterosacral ligament in all comparisons ($p < 0.001$).

By looking at the ligaments between rest and strain in Figure 6.3, it appeared that the uterosacral ligament rotated around its origin from the sacrum. We therefore quantified ligament axis relative to body axis from rest to strain, and found that the angle change for the uterosacral ligament (normal $-23^{\circ} \pm 17$, prolapse $-32^{\circ} \pm 18$) were greater than that for the cardinal ligament (normal $-7^{\circ} \pm 10$,prolapse $-6^{\circ} \pm 5$) as shown in Figure 6.5. From resting to straining, both ligaments angles significantly differed in all comparisons (CL, $p = 0.037$ for normal and $p = 0.036$ for prolapse; USL, $p = 0.003$ for normal and $p < 0.001$ for prolapse). In addition at resting and straining, angle of cardinal ligament is smaller than uterosacral ligament in all comparisons ($p < 0.001$).

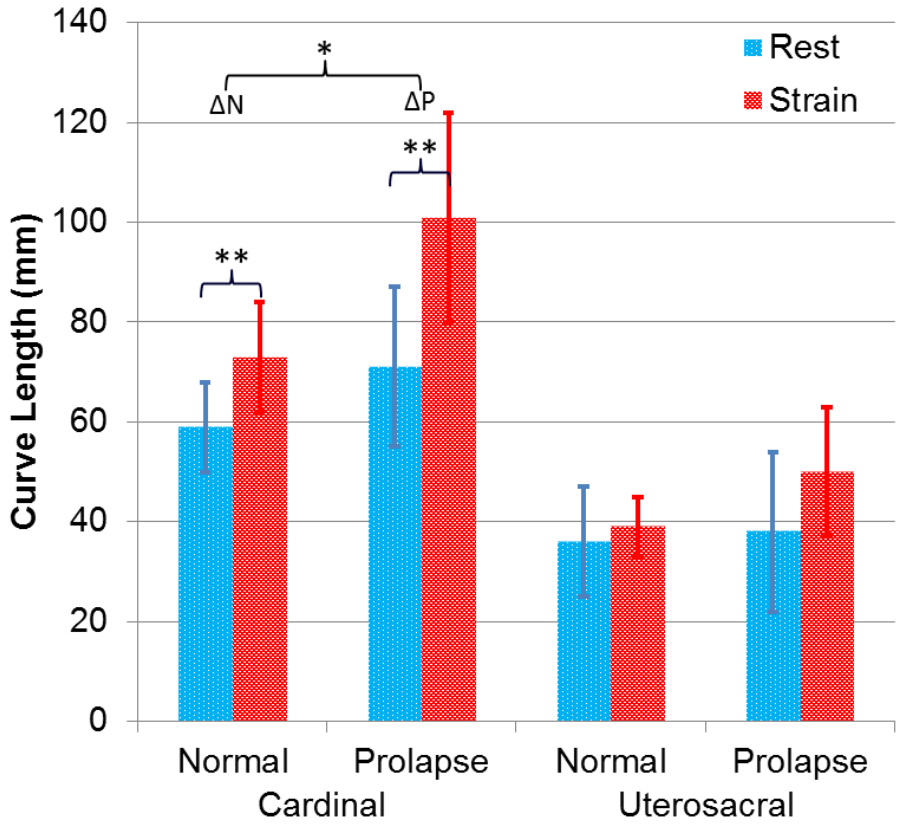

Figure 6.4 Ligament curve length comparison. Relationships between cardinal and uterosacral ligament curved lengths at rest and strain in women with normal support and prolapse. Statistical significant differences for rest versus strain comparisons, and ligament changes difference for normal versus prolapse comparisons are both marked (*, $p < 0.05$; **, $p < 0.01$). Other comparisons are discussed in the text.

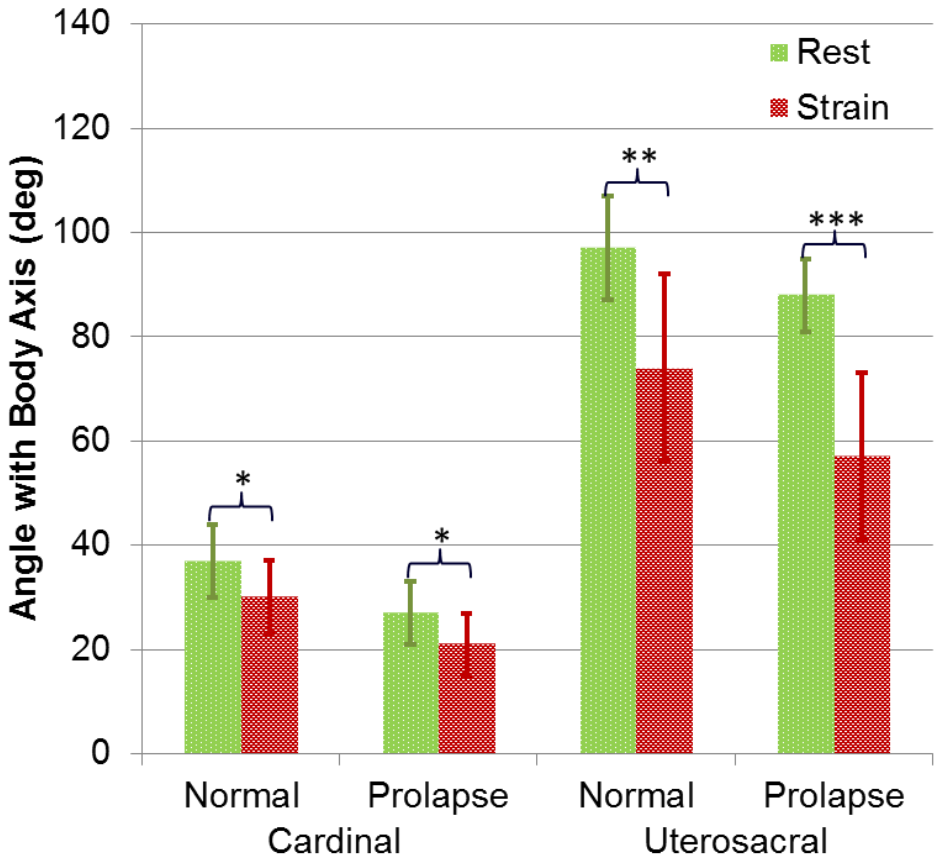

Figure 6.5 Angle with body axis comparison. Relationships between cardinal and uterosacral ligament angles with body axis at rest and strain in women with normal support and prolapse. Statistical significant differences for rest versus strain comparisons, and ligament changes difference for normal versus prolapse comparisons are both marked (*, $p < 0.05$; **, $p < 0.01$; ***, $p < 0.001$). Other comparisons are discussed in the text.

The measurement results were summarized in Table 6.2.

Table 6.2 Ligaments Measurement

		Cardinal Ligament				Uterosacral Ligament		
		Normal Mean ± SD (mm)	Prolapse Mean ± SD (mm)	p-value		Normal Mean ± SD (mm)	Prolapse Mean ± SD (mm)	p-value
Straight Length	CL_Lr	50 ± 8	65 ± 15	0.013	USL_Lr	33 ± 9	35 ± 14	0.754
	CL_Lv	59 ± 11	93 ± 24	0.001	USL_Lv	35 ± 5	45 ± 13	0.028
	CL_ΔL	10 ± 10	29 ± 17	0.008	USL_ΔL	6 ± 3	13 ± 11	0.118
Curve Length	CL_LCr	59 ± 9	71 ± 16	0.051	USL_LCr	36 ± 11	38 ± 16	0.797
	CL_LCv	73 ± 11	101 ± 21	0.003	USL_LCv	39 ± 6	50 ± 13	0.037
	CL_ΔLC	15 ± 9	30 ± 16	0.033	USL_ΔLC	7 ± 4	15 ± 12	0.094
Angle	CL_βr (deg)	37 ± 7	27 ± 6	0.003	USL_βr	97 ± 10	88 ± 7	0.039
	CL_βv (deg)	30 ± 7	21 ± 6	0.007	USL_βv	74 ± 18	57 ± 16	0.044
	CL_Δβ (deg)	-7 ± 10	-6 ± 5	0.849	USL_Δβ	-23 ± 17	-32 ± 18	0.298

Lr: line length under rest; Lv: line length under strain; ΔL: line length change;
LCr:curve length; LCv: curve length under strain; ΔLC: curve length change;
β is the angle from the ligament to body axis

Figure 6.6 and Figure 6.7 show comparisons between anterior and posterior vaginal prolapse groups. The difference of curve length and angle of cardinal and uterosacral ligaments between women with AVP and PVP was not all significantly different. Only a few comparisons were found significantly difference at the 0.05 level. Cardinal was longer from resting to straining for AVP ($p = 0.024$). Length change of uterosacral ligament differed between AVP and PVP ($p = 0.044$). Resting uterosacral was significantly longer for PVP than AVP ($p = 0.046$).

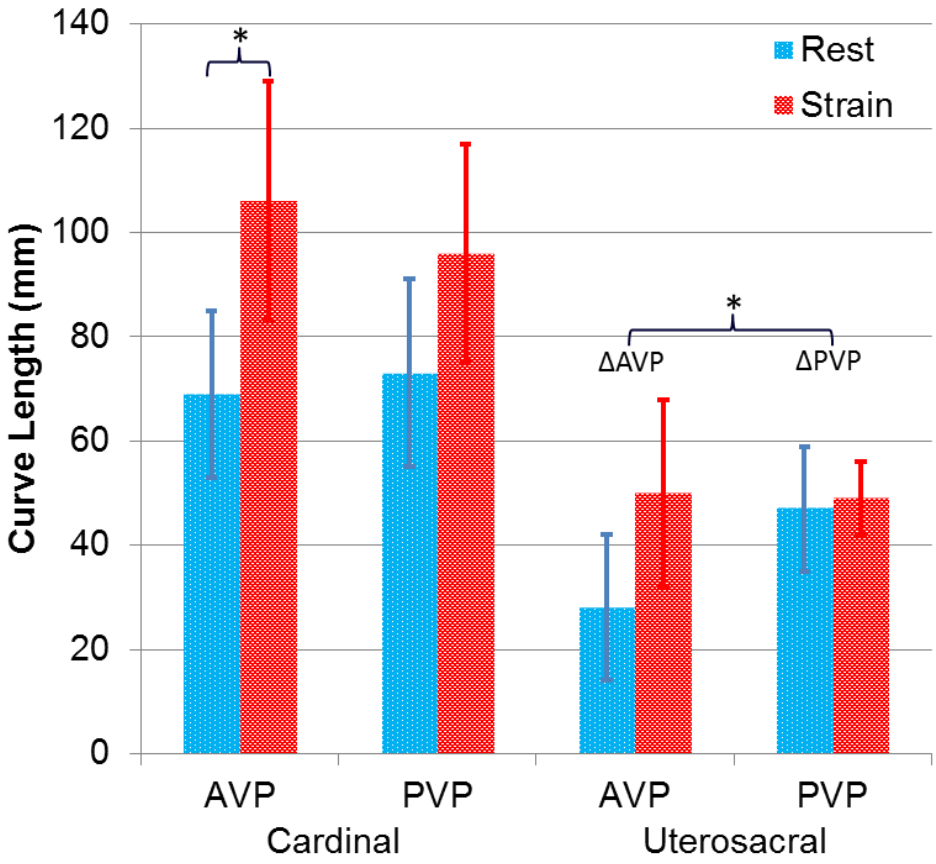

Figure 6.6 Ligament curve length comparison between AVP and PVP. Relationships between cardinal and uterosacral ligament curved lengths at rest and strain in women with AVP and PVP. Statistical significant differences for rest versus strain comparisons, and ligament changes difference for AVP versus PVP comparisons are both marked (*, $p < 0.05$). Other comparisons are discussed in the text.

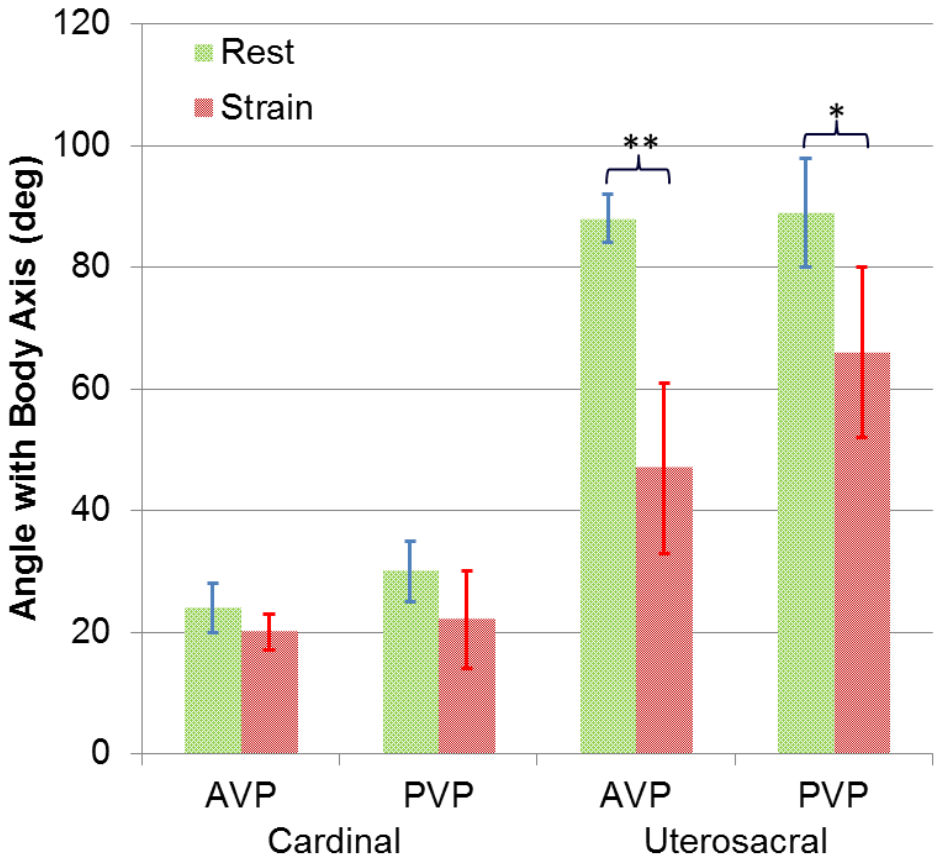

Figure 6.7 Angle with body axis comparison between AVP and PVP. Relationships between cardinal and uterosacral ligament angles with body axis at rest and strain in women with AVP and PVP prolapse. Statistical significant differences for rest versus strain comparisons, and ligament changes difference for normal versus prolapse comparisons are both marked (*, $p < 0.05$; **, $p < 0.01$). Other comparisons are discussed in the text.

6.4 Discussion

In these subject-specific 3-D Stress MR-based models studying CL and deep USL, we have detected that the length and angle of ligaments differed from resting to straining and changed between normal and prolapse subjects. We partially accept the hypotheses that a) the length of ligaments at rest is no different between prolapse and normal women at rest; b) CL ligament elongation (length change from rest to Valsalva) for each ligament is greater in prolapse than normal women, while this is not the case for USL; c) CL has greater changes in the ligament length, while USL has more changes in ligament angle.

Significant difference was detected at the change of best fit curve of cardinal ligament (p =0.003) and uterosacral ligament (p = 0.037) under maximal Valsalva between case and control groups. Previous research (Larson et al. 2010; Luo et al. 2012) showed the downward translation of the upper part of vagina is one of the main characteristics of both cystocele and rectocele. In addition, the cardinal ligament is relatively vertical in the standing position while the deep uterosacral ligament is more likely dorsally directed (Chen et al. 2012), as we presented in the result section. The direction of descent is influenced by the presence of the levator plate. These findings might help to explain that cardinal ligament has larger tension than uterosacral ligament when the apex is loaded with arbitrary force, and thus change of cardinal ligament with prolapse is greater than that of uterosacral ligament. But the angle change of uterosacral ligament with prolapse is larger than that of the cardinal ligament.

The CL and USL are not like skeletal ligaments that consist of homogenous tissues. They are visceral ligaments and are most like a mesentery, comprised of varying combinations of blood vessels, nerves, smooth muscle and areolar tissue (Campbell 1950; Range and Woodburne 1964; Cole et al. 2006; Ramanah et al. 2012). The CL and USL support both the cervix and have distinct differences in composition (Campbell 1950; Range and Woodburne 1964). In addition, they have different lines of action (Chen et al. 2012) with the cardinal being relatively vertical in the standing posture and the uterosacral more dorsally directed. It has been possible to study these in cadavers but understanding how they change in living women has only now become possible through their identification in MRI (Tunn et al. 2001; Umek et al. 2004). The degree to which each ligament lengthens can help determine the nature and direction of apical support

loss. Clinically it is known that different directions of apical support can result in different types of operative failure. In a study by Maher (Maher et al. 2004) sacrospinous colpopexy was associated with a higher rate of cystocele postoperatively (14%) than abdominal sacral colpopexy (7%) but the reverse was true for rectocele which was less frequent in the sacrospinous group (7%) than the abdominal group (17%). This is due to the more dorsal location of the sacrospinous suspension putting the anterior wall at risk and the more vertical sacral colpopexy putting the posterior wall at risk. Knowing how much each ligament changes under load in women with prolapse compared to normal support would help understanding the problems above.

Surgeons use the apical ligaments in repair, shortening the cardinal ligaments and using the uterosacral ligaments to re-suspension the vagina as strategies to elevate the vaginal apex (Lee and Hagen 1992; Shull et al. 2000). Our study developed data concerning how much each ligament has lengthened and the amount of elevation needed to return to normal. This could help developing scientific strategies for surgical improvement.

This study has several limitations. First, our study was based on a small sample of women with distal posterior and anterior predominant prolapse versus women with normal support. We specifically selected women with predominant rectoceles and cystoceles in order to have a more homogeneous sample. Some of the differences we found that did not reach statistical significance may do so with larger samples. This article provides estimates of these differences that form the basis for future power calculations. It would be worth studying women who have uterine prolapse in association with cystocele or rectocele to gain an understanding of more complicated prolapse.

Second, the MR images were obtained in the supine position and not during defecation. There might be small change of ligaments length and angles in the standing position. However, these studies are similar to supine pelvic examination with Valsalva that has been used by clinicians to examine the prolapse and perform a POP-Q examination (except for somewhat less thigh abduction).

This study is a first step to create a technique and analyze the cardinal and uterosacral ligaments changes from resting to max Valsalva, with and without pelvic organ prolapse. It can compare the ligament length and angle for CL and USL, under resting and straining, with normal support and prolapse. To enhance the level of precision, Future study should be based on a larger sample size and more complex prolapse.

References

Boyles, S. H., Weber, A. M., & Meyn, L. (2003). Procedures for pelvic organ prolapse in the United States, 1979-1997. *Am J Obstet Gynecol, 188*(1), 108-115.

Campbell, R. M. (1950). The anatomy and histology of the sacrouterine ligaments. *Am J Obstet Gynecol, 59*(1), 1-12, illust.

Chen, L., Ramanah, R., Hsu, Y., Ashton-Miller, J. A., & Delancey, J. O. (2012). Cardinal and deep uterosacral ligament lines of action: MRI based 3D technique development and preliminary findings in normal women. *Int Urogynecol J*.

Cole, E. E., Leu, P. B., Gomelsky, A., Revelo, P., Shappell, H., Scarpero, H. M., et al. (2006). Histopathological evaluation of the uterosacral ligament: is this a dependable structure for pelvic reconstruction? *BJU Int, 97*(2), 345-348.

Larson, K. A., Hsu, Y., Chen, L., Ashton-Miller, J. A., & DeLancey, J. O. (2010). Magnetic resonance imaging-based three-dimensional model of anterior vaginal wall position at rest and maximal strain in women with and without prolapse. *Int Urogynecol J, 21*(9), 1103-1109.

Larson, K. A., Luo, J., Guire, K. E., Chen, L., Ashton-Miller, J. A., & DeLancey, J. O. (2012). 3D analysis of cystoceles using magnetic resonance imaging assessing midline, paravaginal, and apical defects. *Int Urogynecol J, 23*(3), 285-293.

Lee, R. A., & Hagen, J. V. (1992). *Atlas of gynecologic surgery*: WB Saunders Co.

Luo, J., Larson, K. A., Fenner, D. E., Ashton-Miller, J. A., & Delancey, J. O. (2012). Posterior vaginal prolapse shape and position changes at maximal Valsalva seen in 3-D MRI-based models. *Int Urogynecol J, 23*(9), 1301-1306.

Maher, C. F., Qatawneh, A. M., Dwyer, P. L., Carey, M. P., Cornish, A., & Schluter, P. J. (2004). Abdominal sacral colpopexy or vaginal sacrospinous colpopexy for vaginal vault prolapse: a prospective randomized study. *Am J Obstet Gynecol, 190*(1), 20-26.

Olsen, A. L., Smith, V. J., Bergstrom, J. O., Colling, J. C., & Clark, A. L. (1997). Epidemiology of surgically managed pelvic organ prolapse and urinary incontinence. *Obstet Gynecol, 89*(4), 501-506.

Ramanah, R., Berger, M. B., Parratte, B. M., & Delancey, J. O. (2012). Anatomy and histology of apical support: a literature review concerning cardinal and uterosacral ligaments. *Int Urogynecol J*.

Range, R. L., & Woodburne, R. T. (1964). The Gross and Microscopic Anatomy of the Transverse Cervical Ligament. *Am J Obstet Gynecol, 90*, 460-467.

Shull, B. L., Bachofen, C., Coates, K. W., & Kuehl, T. J. (2000). A transvaginal approach to repair of apical and other associated sites of pelvic organ prolapse with uterosacral ligaments. *American Journal of Obstetrics and Gynecology, 183*(6), 1365-1374.

Subak, L. L., Waetjen, L. E., van den Eeden, S., Thom, D. H., Vittinghoff, E., & Brown, J. S. (2001). Cost of pelvic organ prolapse surgery in the United States. *Obstet Gynecol, 98*(4), 646-651.

Summers, A., Winkel, L. A., Hussain, H. K., & DeLancey, J. O. (2006). The relationship between anterior and apical compartment support. *Am J Obstet Gynecol, 194*(5), 1438-1443.

Tunn, R., DeLancey, J. O., & Quint, E. E. (2001). Visibility of pelvic organ support system structures in magnetic resonance images without an endovaginal coil. *Am J Obstet Gynecol, 184*(6), 1156-1163.

Umek, W. H., Morgan, D. M., Ashton-Miller, J. A., & DeLancey, J. O. (2004). Quantitative analysis of uterosacral ligament origin and insertion points by magnetic resonance imaging. *Obstet Gynecol, 103*(3), 447-451.

CHAPTER 7

MEASUREMENT OF THE 3D GEOMETRY OF THE FASCIAL ARCHES IN WOMEN WITH A UNILATERAL LEVATOR DEFECT AND "ARCHITECTURAL DISTORTION"

Abstract

Introduction and Hypothesis: The arcus tendineus fascia pelvis (ATFP) and arcus tendineus levator ani (ATLA) are elements of anterior vaginal support. This study describes their geometry in women with unilateral levator ani muscle defects and associated "architectural distortion."

Methods: Fourteen subjects with unilateral defects underwent MRI. 3D models of the arcus were generated. The locations of these relative to an ilial reference line were compared between the unaffected and affected sides.

Results: Pronounced changes occurred on the defect sides' ventral region. The furthest point of the ATLA lays up to a mean of 10 mm ($p = 0.01$) more inferior and 6.5 mm ($p = 0.02$) more medial than that on the intact side. Similarly, the ATFP lays 6 mm ($p = 0.01$) more inferior than on the unaffected side.

Conclusions: The ventral arcus anatomy is significantly altered in the presence of levator defects and architectural distortion. Alterations of these key fixation points will change

the supportive force direction along the lateral anterior vaginal wall, increasing the risk for anterior vaginal wall prolapse.

Key words: Pelvic organ prolapse, Cystocele, Paravaginal defect, Arcus tendineus fascia pelvis, Arcus tendineus levator ani, Levator ani muscle

7.1 Introduction

Some 11% of US women require surgical repair for their pelvic floor dysfunction, and this number will likely increase as the population ages (Olsen et al. 1997; He et al. 2005; Jelovsek et al. 2007). The anterior vaginal wall is both the most common site of pelvic organ prolapse (Olsen et al. 1997) and the most frequent site of operative failure (Benson et al. 1996; Shull et al. 2000; J. K. Nguyen 2001; C. F. Maher et al. 2001; C. Maher and Baessler 2006; J. N. Nguyen and Burchette 2008). An improved understanding of the pathomechanics of anterior vaginal wall support is needed to understand the causes of anterior wall prolapse and operative failure.

Magnetic resonance imaging (MRI) resolution has improved to the point that it is possible to examine the geometry of the individual structures and combinations of structures involved in anterior vaginal wall support. For example, a pattern of soft tissue abnormality termed “architectural distortion,” or AD, was recently described in which the lateral vaginal wall is seen to extend beyond its normal location, appearing to contact the obturator internus muscle (Huebner et al. 2008). Women with AD are more likely (78%) to have anterior wall prolapse than both women with levator defects but no AD (61%) as well as those with normal levators and no AD (31%) (Huebner et al. 2008). This distortion occurs in a structurally important region of anterior vaginal wall support at the

interconnection between three key support structures: (1) the arcus tendineus fascia pelvis or fascial arch, (2) the arcus tendineus levator ani or levator arch, and (3) the pubic portion of the levator ani muscle (Figure 7.1). We have observed the dislocation of these two arches in women with architectural distortion (Huebner et al. 2008).

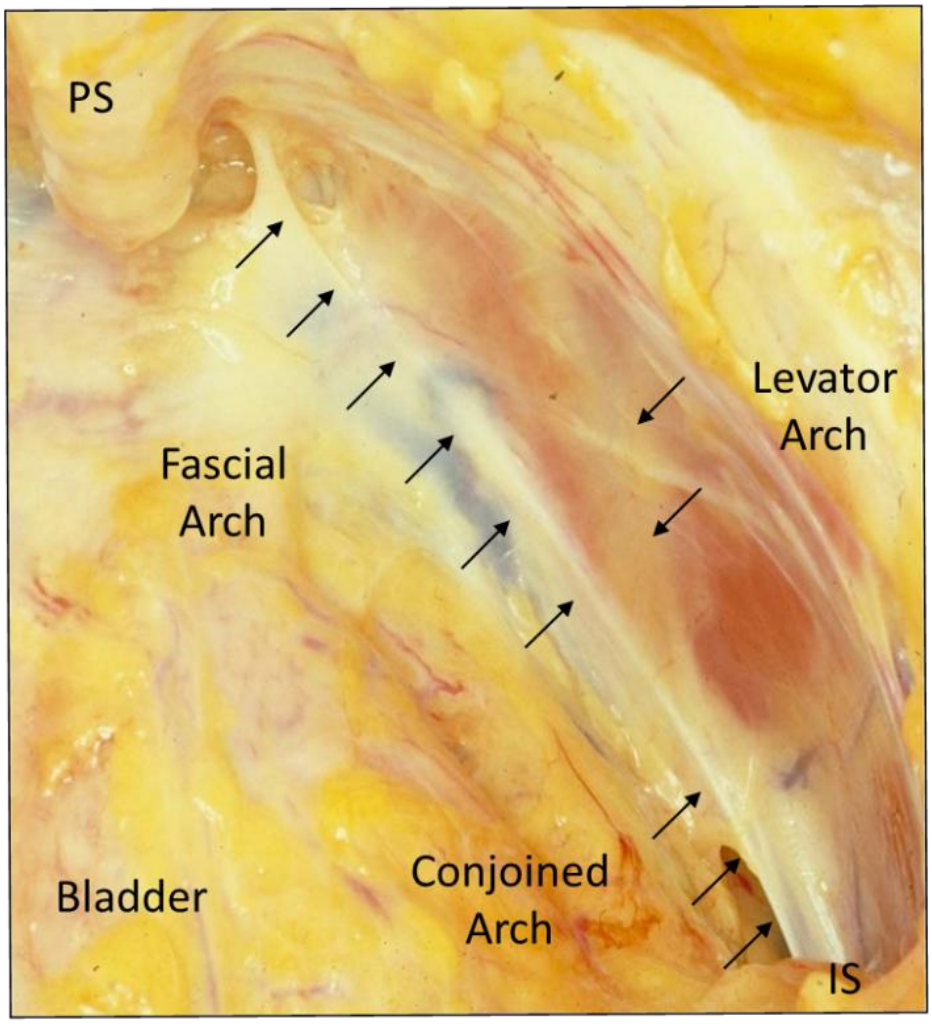

Figure 7.1 Right pelvic sidewall. View looking down into space of Retzius from above towards the right pelvic sidewall. *PS* pubic symphysis, *IS* ischial spine

The lack of a reliable method has hitherto precluded making measurements to test hypotheses concerning the status of these arches. This paper describes a technique using 3D models to establish fascial and levator arch locations and to compare each structure's location relative to a reference line in a unique group of women. Each of these women had a unilateral levator defect and architectural distortion on one side but with intact anatomy on the contralateral side. This offers a unique opportunity to compare normal and distorted pelvic sidewall anatomy in the same individual. The study goal was therefore to compare normal and distorted pelvic sidewall anatomy in women with unilateral defects in order to better understand why this population is more predisposed to anterior wall prolapse.

7.2 Materials and methods

MRI scans from 14 women with unilateral levator defects and architectural distortion were selected from the University of Michigan institutional review board-approved (#1999-0395, #2002-0636, #1995-0477) case–control studies of pelvic organ prolapse and urinary incontinence. All 14 subjects had unilateral levator defects that were classified as "major defects" on MR imaging, meaning that more than half of the levator ani muscle was involved (Kearney et al. 2006) (Figure 7.2a). Architectural distortion was deemed present using earlier published criteria by Huebner, "lateral or posterior spill of the vagina from its normal position and posterior extension of the space of Retzius beyond the superior lateral sulcus of the vagina until it comes in contact with the superior surface of the iliococcygeal portion of the levator ani muscle"(Huebner et al. 2008) (Figure 7.2b).

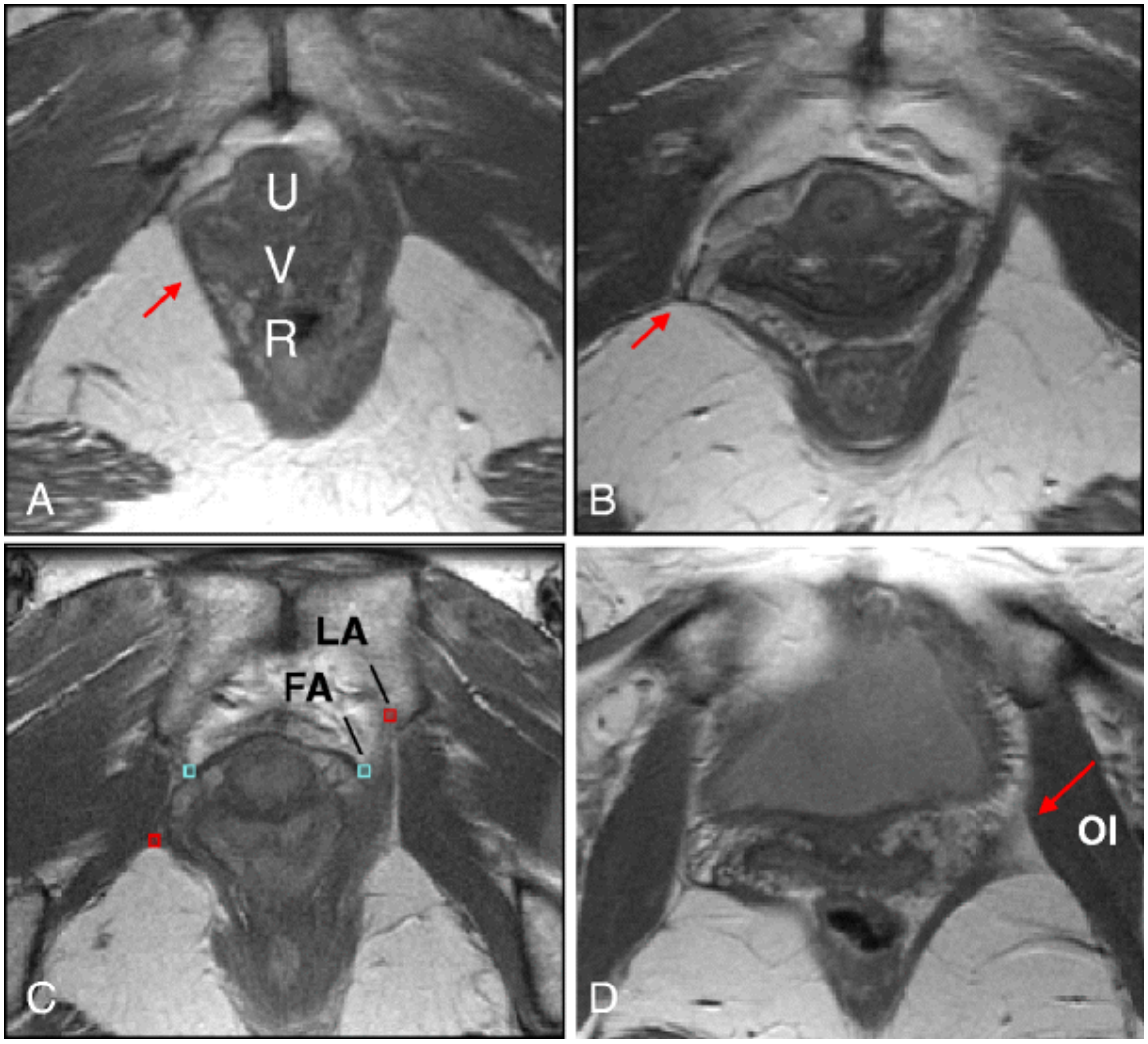

Figure 7.2 Axial MR image of pelvis. **a** Unilateral levator defect (*red arrow*). **b** Unilateral levator defect and architectural distortion (*red arrow*). **c** Levator arch (*LA*) at the ventral insertion of the levator muscle and fascial arch (*FA*) at the lateral end of pubovisceral muscle labeled on non-defect side. **d** *Red arrow* indicates the position of the placement of levator arch with bulkier portion of levator ani muscle converging with the obturator internus muscle.
U urethra, *V* vagina, *R* rectum, *OI* obturator internus

All 14 subjects underwent MR imaging of the pelvis in the supine position at rest. MR imaging was performed on either a 1.5-T superconducting magnet (Signa; General Electric Medical Systems, Milwaukee, WI, USA) or a 3-T Philips Achieva scanner (Philips Medical Systems, Best, The Netherlands) with a six-channel, phased-array coil being available after 2006. The visibility of the structures was not altered by this transition. Ultrasound gel was placed in the vagina in later scans to better outline its contour. For these standard anatomical scans made at rest, turbo spin echo techniques were used to image the sagittal, coronal, and axial planes. At rest, 30 images were obtained in each plane (repetition time range 2,300–3,000 ms, echo time 30 ms, 4 mm slice thickness, 1-mm gap, number of signal averages 2,256 × 255 voxels).

The original axial, sagittal, and coronal Digital Imaging and Communications in Medicine static images were imported into the 3D Slicer® software program (version 2.1b1, Brigham and Women's Hospital, Boston, MA, USA) and aligned, ensuring that structures co-localized in all three axes by a simultaneous review of 3D scan planes in the viewer. The 3D models were made of the pelvic bones, fascial, and levator arches on axial images by tracing their outlines (pelvic bones) or placing points on structure locations (arches) (Figure 7.3).

The actual fascial and levator arches are too small to be seen with standard MR techniques. However, their location can be determined by the anatomical fact that they occur at the intersections of visible structures, thereby allowing their position to be marked in individual images. Ventrally, near the pubic symphysis, the levator arch was identified either on the medial aspect of the convergence of the levator ani and obturator internus muscles or at the ventral insertion of the levator muscle when this was not

present (Figure 7.2c). At the dorsal location near the ischial spine, where the levator muscle is often "split," the levator arch was identified along with the bulkier portion (Figure 7.2d). The most dorsal aspect of the levator arch approached the ischial spine cranial to where the obturator internus wraps around the spine and in the plane where the sacrospinous ligament attachment is visible.

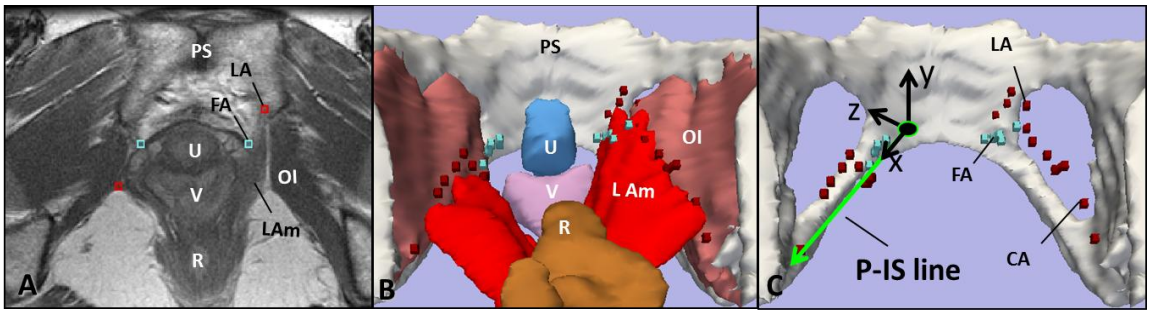

Figure 7.3 Building 3D model. **a** Axial image showing fascial arch (*FA*) and levator arch (*LA*). 3D models made from MRI showing arches with (**b**) and without (**c**) adjacent structures. P-IS reference line as *X*-axis in local pelvic sidewall coordinate system visible in **c** on defect side. *LAm* levator ani, *OI* obturator internus, *PS* pubic symphysis, *R* rectum, *U* urethra, *V* vagina

The fascial arch is identified ventrally at the lateral aspect of the pubovesical muscle based on previous anatomical and MRI observations (Delancey 1989; Chou and DeLancey 2001) (Figure 7.2c). In the more dorsal region, it is no longer identified as a separate structure but fuses to become one with the dorsal portion of the levator arch, also known as the conjoined arch. For the remainder of this paper, this conjoined arch will still be referred to as the levator arch. The 3D–MR coordinates of each point along the arches were recorded using fiducial markers within the Slicer® software program. Figure 7.3c illustrates the relationship of these models to the obturator internus, levator ani, bladder, vagina, and rectum.

To analyze the location of these structures both within a single subject comparing the normal and abnormal anatomic sides of the pelvis and between subjects, the

coordinates of our models were then translated or reassigned within local pelvic sidewall systems. In order to create this local system, 3D–MRI coordinates of the fascial arch insertion into the pubic symphysis and location of the ischial spine were identified to generate a reference line, the pubis to ischial spine or P-IS line (Figure 7.3c). This line became the X-axis of a new pelvic sidewall coordinate system. It was then divided into ten equal deciles in each subject to normalize the distance along the reference line. Using a best-fit curve technique, the fascial and levator arches were re-sampled at each decile along X-axis for comparison. The X, Y, and Z values for the levator and fascial arches were then recorded in this new system for comparison.

Blinded inter-rater reliability testing was performed on point placement with the senior and first author and found to have Pearson correlation coefficients ranging from 0.92 to 0.99 depending upon which arch and which axis were compared. In addition, the mean differences between raters indicated no systematic rater bias. Statistical analyses were performed using paired t tests to compare distances above and lateral to the reference line at each decile in normal (non-defect side) and abnormal (defect side) anatomy.

7.3 Results

The mean age of the 14 study participants was 47 ± 12 (SD) years, median parity two, and mean body mass index 25.6 ± 4.2 kg/m2. All subjects were Caucasian and only one had undergone hysterectomy. None had prior surgery for pelvic organ prolapse. Six (43%) subjects had prolapse defined as at least one Pelvic Organ Prolapse Quantification system point at least 1 cm beyond the hymenal ring on clinical examination. The predominant prolapse was located in the anterior compartment in four individuals, the

apical compartment in one individual, and equally in the anterior and posterior compartment in the final individual. All subjects had major, unilateral defects and architectural distortion as defined in the "Materials and methods" section. Right-sided defects predominated (79% vs. 21%; Table 7.1).

Table 7.1 Study participants' characteristics

Characteristics	Study population (n = 14)
Age (years)[a]	47 ± 12
BMI (kg/m^2)[a]	25.6 ± 4.2
Median parity	2
Race[a]	
Caucasian	14 (100%)
Hysterectomy[a]	1 (7%)
Levator defects[a]	
Right side	11 (79%)
Left side	3 (21%)

[a] Mean ± standard deviation or n (%)

The most pronounced differences in arch location when comparing normal with architectural distortion sidewalls occurred in the ventral region in the craniocaudal direction. Figure 7.4 depicts the craniocaudal relationships of the fascial and levator arches relative to the P-IS line, showing their locations at each decile. The X-axis is oriented along the P-IS line where "0" depicts the pubic insertion and "100" is the ischial spine.

Significant differences in location occurred at 10, 20, and 30 percentile for the fascial arch ($p = 0.03$, 0.001, and 0.012, respectively) and 30, 40, and 50 percentile for the levator arch ($p = 0.008$, 0.002, and 0.046, respectively). The most statistically significant differences for both arches occurred at the 30 percentile position. At this point, the fascial arch on the defect side was located 6 mm inferior to its position on the normal side (i.e., 4

mm below vs. 1.8 mm above, p = 0.01), while the levator arch was located more than 1 cm inferior to its normal position (i.e., 6.8 mm inferior to the P-IS line for the defect side and 3.4 mm superior to the P-IS line on the intact side).

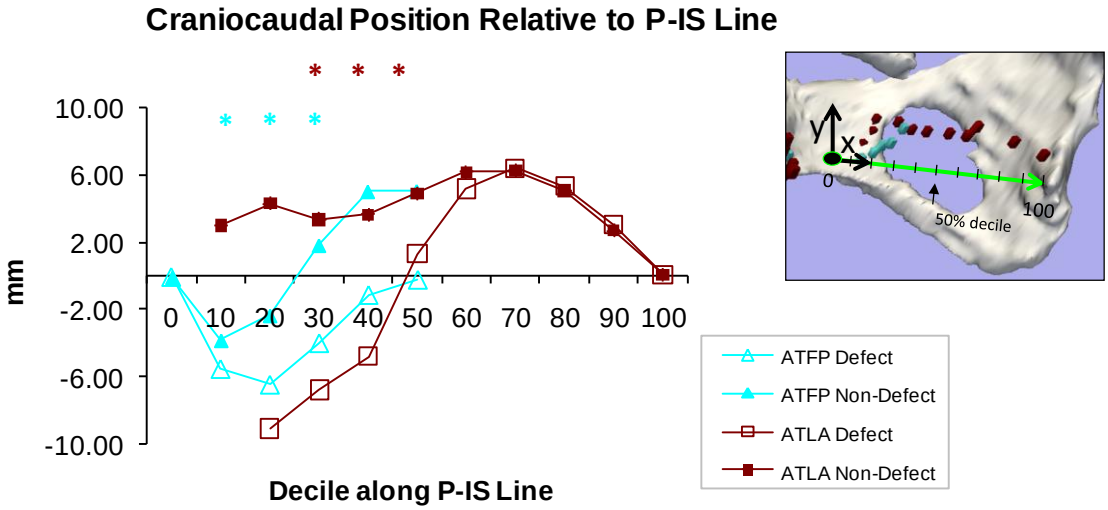

Figure 7.4 Craniocaudal position relative to P-IS line. View of *Y*-axis looking at pelvic sidewall. "0" is pubic end and "100" is at ischial spine. *Asterisks* reveal statistically significant differences between normal and abnormal sides.

Figure 7.5 depicts the mediolateral relationships of the arches relative to the P-IS line. Again, the most pronounced changes occurred in the ventral region. The ventral levator arch was more medially located on the defect side most significantly at the third decile (2 mm vs. 8.5 mm lateral to P-IS line at 30 percentile, p = 0.02). For the fascial arch, there was no difference in the mediolateral location when comparing intact and defect sides in both the fascial arch moved from medial to lateral as it fused with the levator arch.

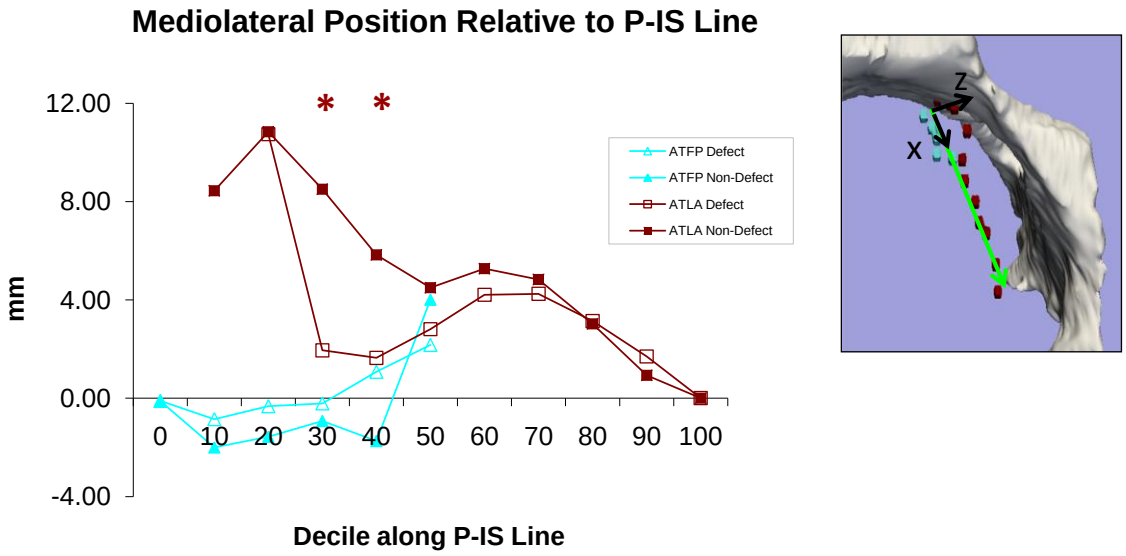

Figure 7.5 Mediolateral position relative to P-IS Line. View of *Z*-axis looking into pelvis from above. "0" is pubic end and "100" is at ischial spine. *Asterisks* reveal statistically significant differences between normal and abnormal sides.

7.4 Comment

This study describes the development of a novel 3D geometric approach for comparing of the anatomy of the fascial arches on the pelvic sidewall in the presence or absence of levator defects and architectural distortion. It also reports early observations using this technique. The method allows the location of the fascial and levator arches to be determined so that specific structural hypotheses can be tested in living women with known characteristics (i.e., architectural distortion). Using this measurement technique, we have found that fascial and levator arch anatomy is significantly altered in the presence of levator defects and architectural distortion. The levator arch lies 10.2 mm more caudally and 6.5 mm more medially and does not come as close to the pubis along pelvic sidewalls on the side where a levator defect is present. In the upright posture, it could be said to have "fallen" downward and medially from its usual location. Similarly,

the fascial arch extends more caudally as well on the defect side. These changes are most pronounced in the ventral region near the symphysis.

The fascial and levator arches form part of a larger structural complex involved in anterior vaginal wall support that we refer to as the "paravaginal complex." It consists of the two arches, the fascial connections between the vaginal wall and the arches, and the pubovisceral portion of the levator ani muscle. Together these structures provide support to the mid and distal anterior vaginal wall. Richardson was the first to call attention to the abnormalities between the lateral vaginal margin and the arcus tendineus in this region, noting the detachment of the anterior vaginal wall's pubocervical fascia from the arcus tendineus fascia pelvis in women with cystourethrocele (Richardson et al. 1976; Richardson et al. 1981). Later, muscle defects in this area were seen intraoperatively in approximately half of women with paravaginal defects, and these have later been objectively confirmed on MRI images (DeLancey 2002). The blinded comparison of normal and abnormal anatomy is not possible in the operating room; so, an assessment of these hypotheses has awaited the advent of modern imaging techniques.

Alterations in these key fixation points will change the supportive force vectors along the anterior vaginal wall. With levator defects, the levator arch and levator ani fall inferior to the fascial arch, thereby not being able to provide upward support in response to increased intra-abdominal pressure. In addition, this distal support loss changes the distribution of stress along the length of the vaginal wall and increases the load on intact proximal structures. This then begs the question as to why only 43% of the subjects in this particular study have prolapse even though they all have a unilateral levator defect and distortion. Perhaps the other 57% have compensated with other intact support

structures, suggesting that maybe Knudson's "two-hit hypothesis" applies in pelvic organ prolapse as well as cancer (Knudson 1971). Our prior studies included a high percentage of women with bilateral defects that may not have been able to compensate (Huebner et al. 2008).

Our findings support anatomical descriptions in the literature that note two arches which fuse to a single arch in the ventral region of the pelvis. Ocelli and Albright both visualized these features in cadaver dissections (Occelli et al. 2001; Albright et al. 2005). Albright divides the fascial arch into three regions with the levator arch joining the fascial arch in the proximal portion of the middle region, a little more dorsal than our findings; he also references an arcus tendineus rectovaginalis that is not included in our observations (Albright et al. 2005). Pit observed the levator and fascial arches merging in only four out of ten of their cadaver dissections; in the remaining six, it appeared to fuse with the ischial spine more laterally than the fascial arch (Pit et al. 2003). This discrepancy may be due to the distortion of these fine structures during the embalming process.

Findings from the present study extend the current observations of normal paravaginal anatomy in the literature by defining the normal locations and providing a more detailed picture of the interactions occurring between two important elements of the paravaginal complex and their distortion due to levator defects. It also introduces a quantitative system where the measurements of location can objectively be recorded to compare measurements in normal and abnormal anatomy. Most of the literature is based upon cadaver studies in which patient status is rarely known in regard to normal or abnormal levator muscles nor was there any emphasis on the locations of these structures

relative to an anatomic reference system. Huddleston did publish an MRI study examining what was labeled as paravaginal defects and describes three characteristic findings in 12 patients with cystourethroceles: upper defects causing the chevron sign, middle defects causing saddlebag sign, and a lower defect causing the mustache sign (Huddleston et al. 1995). A review of the images in this article, given more recent insights, indicates that these are patients with levator ani muscle defects.

Several factors must be considered when interpreting the results of this study. This study includes a modest number of unique subjects with unilateral defects, thus introducing the possibility that we are not capturing all the nuances of these unilateral defects. A strength of the study is that normal and abnormal anatomy can be compared within the same individual. In doing so, we make the assumption that the changes observed on the defect side do not influence arch geometry of the intact side. This seems reasonable because the anatomy on the unaffected side seems normal, and because if such changes were present, they would be expected to diminish the side-to-side differences, not exaggerate them. Although the normality of the side without architectural distortion was established by experienced examiners, it is possible that there may be subtle changes in this side when compared to individuals with no architectural distortion. This is under investigation at present. The modest sample size means that it is possible that some of the relationships that currently did not reach statistical significance in the ventral regions would do so in a larger sample. Another limitation is that a continuous structure was modeled using discrete points from serial MR images, then requiring a best fit curve to recreate this structure and possibly introducing error. We attempted to minimize this error by utilizing the best fit curve approach, incorporating our known 3D coordinates into our

final curve. In addition, we inspected the resulting lines and confirmed their fidelity using the original model. Finally, structures near the ischial spine are difficult to identify on the MR scans; however, our data appear reproducible given inter-rater reliability correlation coefficients between 0.92 and 0.99.

We also acknowledge that this is a somewhat uniform population (all Caucasian) and that this may limit the generalizability of our results. Further studies that compare the findings in these unilateral defects with those seen in women with bilateral defects are also needed, but our experience in looking at these defects suggests that these studies will be confirmatory. Finally, acquiring high-resolution MRI images with sufficient detail for the present analysis can currently only be carried out in the supine position. It would be ideal to have images in the upright posture or during straining, but images of sufficient quality for such an analysis are not at present available.

The present technique to create and quantify 3D models of the fascial and levator arches in the presence of unilateral levator defects and architectural distortion greatly enhances our ability to study anatomic alterations affecting mechanisms of pelvic floor prolapse. Our results suggest alterations in the anatomy within the paravaginal complex that may contribute to the increased rates of prolapse that we see among this population. Not only do our efforts bring us closer to understanding the normal locations of paravaginal structures, they also provide data to more accurately refine our biomechanical model of the pelvis to better understand the complex interactions between these structures and their roles in prolapse. In addition, now that we have a technique to establish the presence of architectural distortion and the geometric location of specific

structures, it will be possible in the future to conduct studies to compare the treatment outcomes of women with and without architectural distortion.

References

Albright, T. S., Gehrich, A. P., Davis, G. D., Sabi, F. L., & Buller, J. L. (2005). Arcus tendineus fascia pelvis: A further understanding. *American Journal of Obstetrics and Gynecology, 193*(3), 677-681.

Benson, J. T., Lucente, V., & McClellan, E. (1996). Vaginal versus abdominal reconstructive surgery for the treatment of pelvic support defects: A prospective randomized study with long-term outcome evaluation. *American Journal of Obstetrics and Gynecology, 175*(6), 1418-1421.

Chou, Q., & DeLancey, J. O. L. (2001). A structured system to evaluate urethral support anatomy in magnetic resonance images. *American Journal of Obstetrics and Gynecology, 185*(1), 44-50.

Delancey, J. O. L. (1989). PUBOVESICAL LIGAMENT - A SEPARATE STRUCTURE FROM THE URETHRAL SUPPORTS (PUBO-URETHRAL LIGAMENTS). *Neurourology and Urodynamics, 8*(1), 53-61.

DeLancey, J. O. L. (2002). Fascial and muscular abnormalities in women with urethral hypermobility and anterior vaginal wall prolapse. *American Journal of Obstetrics and Gynecology, 187*(1), 93-98.

He, W., Sengupta, M., Velkoff, V., & DeBarros, K. (2005). 65+ in the US: 2005, current population report, special studies. United States Government Printing Office, Washington DC. December 2005.

Huddleston, H. T., Dunnihoo, D. R., Huddleston, P. M., & Meyers, P. C. (1995). MAGNETIC-RESONANCE-IMAGING OF DEFECTS IN DELANCEYS VAGINAL SUPPORT LEVEL-I, LEVEL-II, AND LEVEL-III. *American Journal of Obstetrics and Gynecology, 172*(6), 1778-1784.

Huebner, M., Margulies, R. U., & DeLancey, J. O. L. (2008). Pelvic architectural distortion is associated with pelvic organ prolapse. *International Urogynecology Journal, 19*(6), 863-867.

Jelovsek, J. E., Maher, C., & Barber, M. D. (2007). Pelvic organ prolapse. *Lancet, 369*(9566), 1027-1038.

Kearney, R., Miller, J. M., Ashton-Miller, J. A., & DeLancey, J. O. L. (2006). Obstetric factors associated with levator ani muscle injury after vaginal birth. *Obstetrics and Gynecology, 107*(1), 144-149.

Knudson, A. G. (1971). MUTATION AND CANCER - STATISTICAL STUDY OF RETINOBLASTOMA. *Proceedings of the National Academy of Sciences of the United States of America, 68*(4), 820-&.

Maher, C., & Baessler, K. (2006). Surgical management of anterior vaginal wall prolapse: an evidencebased literature review. *International Urogynecology Journal, 17*(2), 195-201.

Maher, C. F., Murray, C. J., Carey, M. P., Dwyer, P. L., & Ugoni, A. M. (2001). Iliococcygeus or sacrospinous fixation for vaginal vault prolapse. *Obstetrics and Gynecology, 98*(1), 40-44.

Nguyen, J. K. (2001). Current concepts in the diagnosis and surgical repair of anterior vaginal prolapse due to paravaginal defects. *Obstetrical & Gynecological Survey, 56*(4), 239-246.

Nguyen, J. N., & Burchette, R. J. (2008). Outcome after anterior vaginal prolapse repair - A randomized controlled trial. *Obstetrics and Gynecology, 111*(4), 891-898.

Occelli, B., Narducci, F., Hautefeuille, J., Francke, J. P., Querleu, D., Crepin, G., et al. (2001). Anatomic study of arcus tendineus fasciae pelvis. *Eur J Obstet Gynecol Reprod Biol, 97*(2), 213-219.

Olsen, A. L., Smith, V. J., Bergstrom, J. O., Colling, J. C., & Clark, A. L. (1997). Epidemiology of surgically managed pelvic organ prolapse and urinary incontinence. *Obstetrics and Gynecology, 89*(4), 501-506.

Pit, M. J., De Ruiter, M. C., Nijeholt, A., Marani, E., & Zwartendijk, J. (2003). Anatomy of the arcus tendineus fasciae pelvis in females. *Clinical Anatomy, 16*(2), 131-137.

Richardson, A. C., Edmonds, P. B., & Williams, N. L. (1981). TREATMENT OF STRESS URINARY-INCONTINENCE DUE TO PARAVAGINAL FASCIAL DEFECT. *Obstetrics and Gynecology, 57*(3), 357-362.

Richardson, A. C., Lyon, J. B., & Williams, N. L. (1976). NEW LOOK AT PELVIC RELAXATION. *American Journal of Obstetrics and Gynecology, 126*(5), 568-573.

Shull, B. L., Bachofen, C., Coates, K. W., & Kuehl, T. J. (2000). A transvaginal approach to repair of apical and other associated sites of pelvic organ prolapse with uterosacral ligaments. *American Journal of Obstetrics and Gynecology, 183*(6), 1365-1373.

CHAPTER 8

EFFECT OF INTERACTIONS BETWEEN APICAL, ANTERIOR AND POSTERIOR SUPPORT IMPAIRMENTS ON THE RELATIVE SIZE OF CYSTOCELE AND RECTOCELE: A DYNAMIC ANATOMICALLY-BASED 2-D FINITE ELEMENT MODEL

Abstract

Introduction and Hypothesis: Describe a novel simplified anatomically-based finite element (FE) model with both anterior vaginal wall (AVW) and posterior vaginal wall (PVW) and their support system, and test the hypothesis that the size of anterior vaginal prolapse (AVP) and posterior vaginal prolapse (PVP) are only dependent on the anterior and posterior support with no interaction.

Methods: A simplified 2-dimensional FE model was created based on the mid-sagittal MR image of a 45 year-old multiparous healthy woman with average pelvic floor dimensions. The FE model included AVW, PVW, pubovisceral muscle (PVM), levator plate, cardinal and uterosacral ligaments (CL, USL), paravaginal anterior vaginal support (AVS), perineal membrane (PM), perineal body (PeB), and anal sphincter (AS). The changes of both AVW and PVW during a Valsalva were then simulated under different combinations of muscular and connective tissue impairments, and different intra-abdominal pressures (IAP).

Results: The development of rectocele and cystocele was sensitive to the levator and apical impairment, IAP, anterior and posterior support impairment. Type of prolapse was strongly related to the type of anterior or posterior support impairment. Increasing levator and apical impairment, and IAP resulted in a larger pelvic organ prolapse.

Conclusions: The size of AVP and PVP are not only dependent on anterior, posterior or apical support impairment, but also reliant on the interaction between different combinations of impairments, as well as organ competition.

Key words: pelvic organ prolapse, cystocele, rectocele, 2D, finite element model, dynamic

8.1 Introduction

Over 200,000 operations are performed each year for pelvic organ prolapse (Boyles et al. 2003) with repair of posterior vaginal prolapse (PVP) included in 87% (Silva et al. 2006). Studies of structural deformations seen in women with anterior vaginal prolapse (AVP, cystocele) have received considerable attention (Hsu et al. 2008a; Larson et al. 2010a; Larson et al. 2012a). To investigate the interaction between muscular and connective tissue support on AVP, computer models (Chen et al. 2006; Chen et al. 2009) were created to simulate the development of AVP under effect of combination of levator and apical supports. But a knowledge gap remains as to how and why a PVP (rectocele) forms. Although there are MR image-based PVP studies (Lewicky-Gaupp et al. 2010; Luo et al. 2012) that analyzed the structural deformation and characteristics, till today to our knowledge, there is no model for studying the interaction between muscular and connective tissue support on PVP.

There are nearly twice as many procedures required for prolapse compared to that required for correction of SUI (Boyles et al. 2003, 2004). Fortunately, surgical management of SUI is successful with objective failures under 10% (Meschia et al. 2006), while prolapse recurrence is much higher (Olsen et al. 1997; Blanchard et al. 2006). Meanwhile, for some patients only with AVP and without PVP before surgeries, PVP happens after the patients' AVP get repaired (Withagen et al. 2012; Milani et al. 2012). Same things can also be true for AVP happening after surgeries to patients with PVP and without AVP before surgeries (Withagen et al. 2012; Milani et al. 2012). As described above, there are computer models of cystocele (Chen et al. 2006; Chen et al. 2009) dealing with interaction with muscular and apical support, but we still lack of information on how AVP interacts with PVP. Interaction between AVP and PVP needs to be clarified to help with prevention and treatment improvement.

Therefore, in this study, we aim to describe a novel simplified anatomically-based finite element (FE) model with both anterior vaginal wall (AVW) and posterior vaginal wall (PVW) and their support system, and to test the hypotheses that 1) the size of AVP and PVP are only dependent on the anterior and posterior support impairment, and levator and apical support system, and 2) the anterior and posterior prolapses do not interact with each other.

8.2 Materials and Methods

8.2.1 Geographic Model and Finite Element Mesh

The simulation model was created based on a 45 year-old multiparous healthy woman, who was selected from an ongoing University of Michigan Institutional Review Board-approved (IRB # 1999–0395) case-control study of pelvic organ prolapse. In our

vaginal dimension analysis of 84 normal subjects in Chapter 2, this subject's vaginal dimension (AVW: 59 mm; PVW: 98 mm; Cervix: 38mm) represented an average dimension. In mid-sagittal plane, for the 84 subjects, the AVW curved length was 62 ±10 mm, and the PVW curved length was 97 ±18 mm, and the cervix curved length was 39 ± 10 mm.

As described in our previous work (Luo et al. 2012), the subject in this study underwent supine multiplanar, two-dimensional, fast spin, proton density MR imaging both at rest and during maximal Valsalva using a 3 T superconducting magnet (Philips Medical Systems Inc., Bothell, WA, USA) with version 2.5.1.0 software. At rest, each 30 images were serially obtained at the axial, sagittal, and coronal, with 20×20 cm fields of view, 4 mm slice thickness, and a 1 mm gap between slices.

A detailed 3-dimensional (3D) model of 23 pelvic structures was created, as previously described (Luo et al. 2011) using 3D Slicer software (version 3.4.1; Brigham and Women's Hospital, Boston, MA). The model included the muscles, ligaments, and fascia of the pelvic floor and the organs it supports. Bones, blood vessels, and the perineum were illustrated as well. Each structure was traced with the use of the most clearly visible axial and/or coronal plane images, and lofted into a 3D virtual model that was based on our previous anatomic work (Hsu et al. 2005; Margulies et al. 2006; Hsu et al. 2008b; Brandon et al. 2009; Larson et al. 2010b). A 2-D finite element (FE) model was then created by projecting the 3-D geometry of AVW, PVW and its support system onto the mid-sagittal plane as shown in Figure 8.1. Panels (A) and (B) show the mid-sagittal MR image without and with structures highlighted. Panels (C) and (D) show the FE models, one showing POP-Q (Bump et al. 1996) location, and the other showing

intra-abdominal pressure (IAP). Attachments of the pubovisceral muscle (PVM) and one portion of levator ani (LA) muscle to the pubic bone and the lines-of-action of the apical supports were located based on the 3D model.

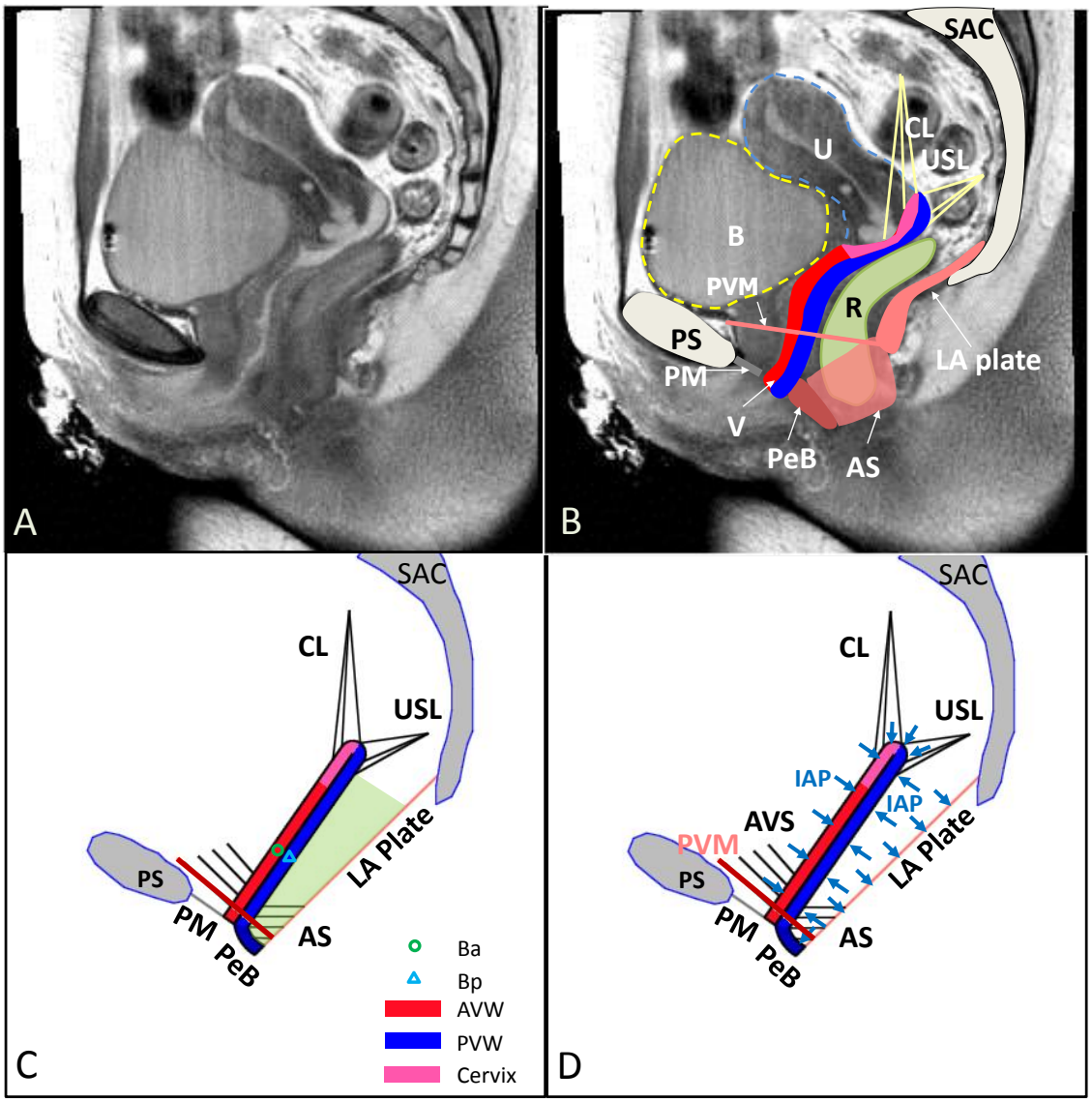

Figure 8.1 Model Development. (**A**)&(**B**) Mid-sagittal MR image without and with main structures highlighted; (**C**)&(**D**) Simplified 2-D finite element model (filled & free edges). In (**C**), POP-Q location Ba is shown as empty green circle and Bp is shown as empty turquoise triangle, both under resting condition by definition, 3 cm above the hymenal ring that is at the perineal membrane. Intra-Abdominal pressure is applied on both anterior and posterior compartment, showing as light blue arrows in (**D**). PS, pubic symphysis; SAC, sacrum; B, bladder; U, uterus; R, rectum; V, vagina; C, cervix; LA, levator ani; PVS, posterior vaginal support; AVS, anterior vaginal support; PVM, pubovisceral muscle; AS, anal sphincter; CL, cardinal ligament; USL,

uterosacral ligament; AVW, anterior vaginal wall; PVW, posterior vaginal wall; IAP, intra-abdominal pressure.

The 2-D FE model mesh was generated by Abaqus version 6.11 (Dassault Systèmes Simulia Corp., Providence, RI, USA) and the simulation was solved using Abaqus Explicit Solver.

The anterior and posterior vaginal wall, cervix, and perineal body were modeled as 2D deformable element using 6-node modified quadratic plane strain triangular element with 1 mm thickness. The pubovisceral muscle was modeled as 2D linear truss element attached at a point corresponding to the midline projection of its origin to the midsagittal plane and attached to a levator plate hinged at its attachment to the distal sacrum (Larson et al. 2009). The perineal membrane and levator plate were simulated as rigid body anchored laterally at the level of the ischiopubic rami (Stein and DeLancey 2008; Brandon et al. 2009). The pubic bone and sacrum were simulated as display bodies. The cardinal and uterosacral ligaments, anterior vaginal support, and posterior vaginal support (showing as anal sphincter, in reality, it includes other structures) were simulated as connector elements (Larson et al. 2012b).

8.2.2 Contact and Boundary Conditions

The anterior and posterior vaginal wall used frictionless finite sliding kinematic contact, which is a strictly enforced contact algorithm. Posterior vaginal wall and levator plate used frictionless finite sliding penalty contact algorithm. Top of perineal membrane was fixed for translation but allowed for rotation. Bottom of perineal membrane was kinematic coupling with bottom of anterior vaginal wall. Bottom of pubovisceral muscle was kinematic coupling with levator plate. Bottom of perineal body was kinematic coupling with bottom of levator plate. Top of levator plate was fixed at the sacrum for

translation but allowed for rotation. The origins of anterior vaginal support were on the arcus tendineus fascia pelvis (ATFP) in 3D, and were only projected on the mid-sagittal plane. All origins for anterior vaginal and apical supports were fixed for translation and allowed for rotation.

8.2.3 Material Properties

In this study, all the deformed structures including the connector elements were assumed to be hyperelastic. For simplicity, the hyperelastic deformed structures were assumed to be isotropic and quasi-incompressible while using Abaqus explicit solver. All the material properties values were extracted from existing literatures (Yamada 1970; Bartscht and DeLancey 1988). The properties of levator muscle were only considered as representing passive stretch, since in Valsalva, patients were instructed to relax their pelvic floor muscle.

8.2.4 Simulation Process

The purpose of the simulation was to predict how the structures would deform under IAP increasing. Sensitivity analysis was applied with combinations of different muscular and connective tissue impairments, and different maximum IAP. The IAP was applied perpendicular to the nodes on the surface of anterior vaginal wall, cervix, posterior vaginal wall, perineal body, and levator plate (Figure 8.1 D).To reduce time for simulating Valsalva process, the simulation time was scaled to 1 second.

8.2.5 Model Validation

The model was validated by comparing the deformation of anterior and posterior vaginal wall (with perineal body), against with published MR-based cystocele and

rectocele deformation study (Larson et al. 2010a; Luo et al. 2012) to check whether predicted prolapse deformation characteristics were reasonable.

8.3 Results

Figure 8.2 shows two examples of the simulation results from model validation for rectocele and cystocele, respectively. Both were with levator 90% impairment and under 160 cm H_2O IAP. The rectocele showed four main characteristics, including "kneeling", downward displacement, forward protruding, and perineal descent. Those characteristics were also observed in our published case-control study (Luo et al. 2012), which analyzed 10 rectoceles and 10 controls. The cystocele showed three main characteristics, including "cupping", downward displacement, and distal pivot. This was consistent with another case-control study (Larson et al. 2010a).

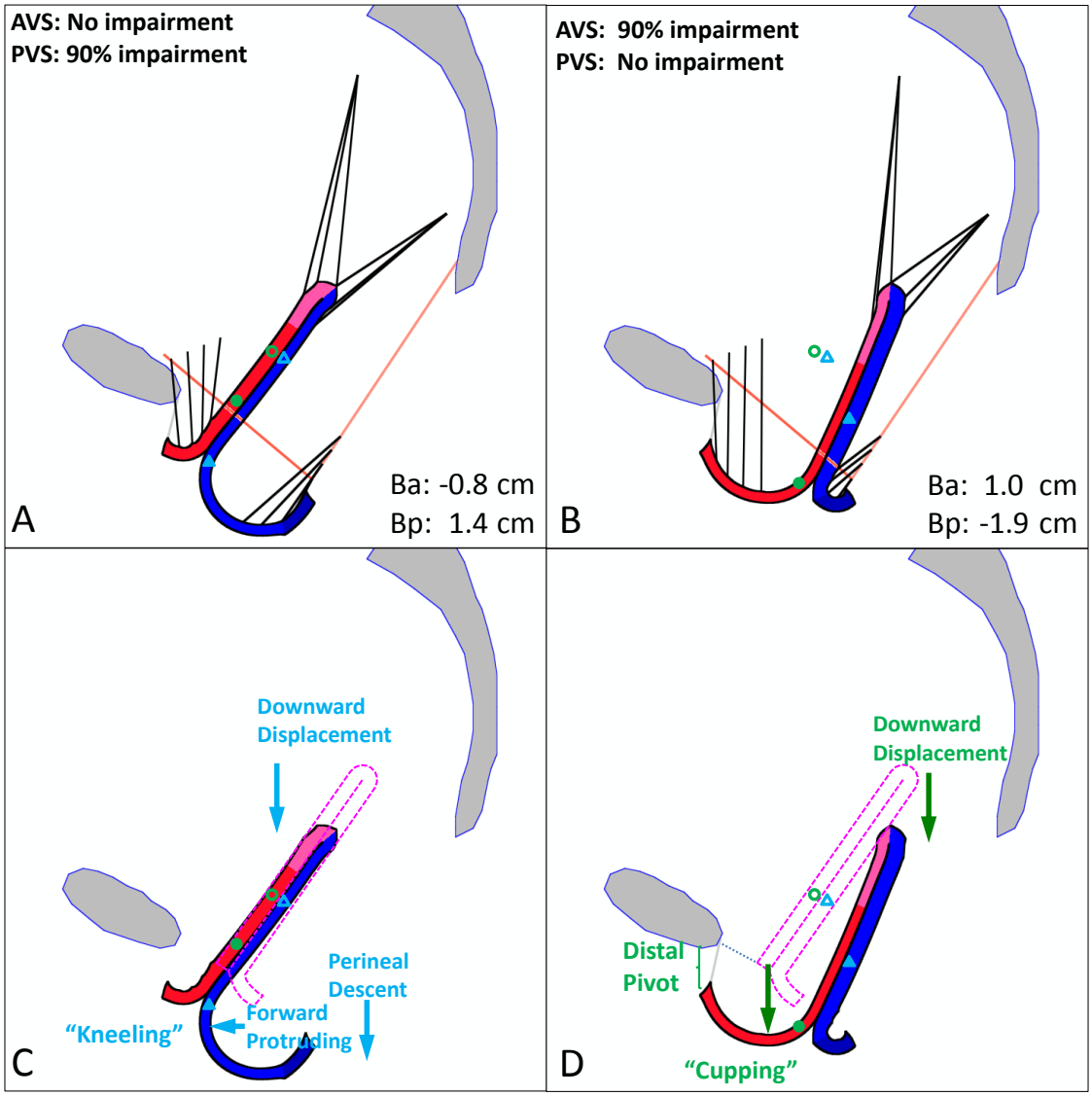

Figure 8.2 Posterior and anterior vaginal prolapses for model validation. (**A**) shows PVP with posterior 90% impairment and (**B**) shows AVP with anterior 90% impairment, both with levator function 90% impairment and 160 cm H_2O. In (**C**), "kneeling", downward displacement, forward protruding, and perineal descent are seen for PVP. In (**D**), "cupping", distal pivot, and downward displacement are seen for AVP. Vaginal wall in resting is shown as dashed pink outline. POP-Q location Ba is shown as empty green circle and Bp is shown as empty turquoise triangle under resting condition. Under strain condition, Ba is shown as full green circle and Bp is shown as full turquoise triangle. Values of Ba and Bp are also shown at the right lower corner of each panel.

Effect of interaction between anterior and posterior support impairment is shown in Figure 8.3, and change of prolapse size with the effect is shown in Figure 8.4. These simulations were all under 140 cm H_2O with PVM 80% impairment, and no apical

support impairment. Increasing anterior impairment could result in greater variation of Ba of AVP than Bp, when keeping posterior support impairment constant. Increasing anterior support impairment could lead to larger cystocele (comparing Figure 8.4 C and A, F and D) and less exposed posterior vaginal wall (exposed vagina means non-contact area of the vaginal wall), which indicated the development of cystocele could protect PVW. It is also true that the development of rectocele could protect AVW. Bp of PVP showed a greater change than Ba with the increase of posterior support impairment while keeping anterior support impairment constant. Increasing posterior support impairment could lead to greater rectocele (comparing Figure 8.4 D and A, E and B, F and C) and less exposed anterior vaginal wall.

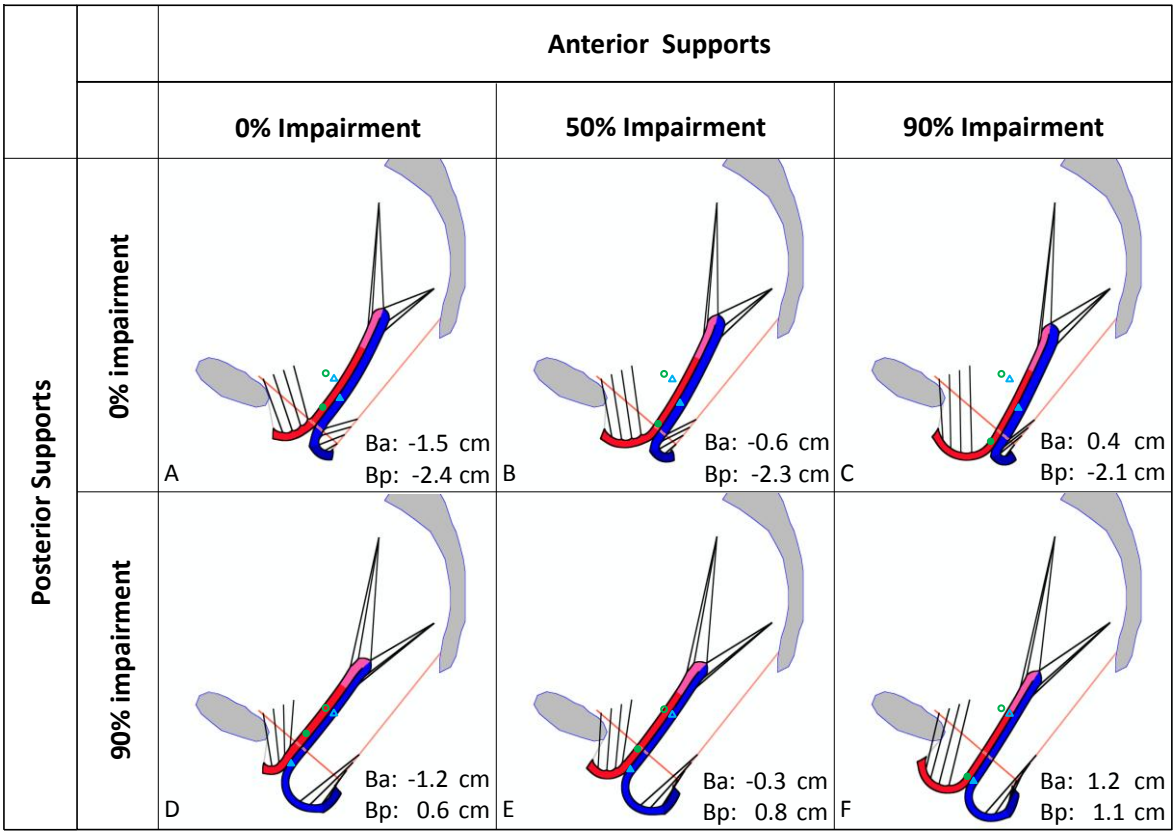

Figure 8.3 Effect of anterior and posterior support impairment under 140 cm H_2O with PVM 80% impairment. (**A**) to (**C**) show models without posterior support impairment, and with changes in anterior support 0%, 50% and 90% impairment. (**D**) to (**E**) show models with posterior support 90%

impairment, and with changes in anterior support 0%, 50% and 90% impairment. POP-Q location Ba is shown as empty green circle and Bp is shown as empty turquoise triangle under resting condition. Under strain condition, Ba is shown as full green circle and Bp is shown as full turquoise triangle. Values of Ba and Bp are also shown at the right lower corner of each panel.

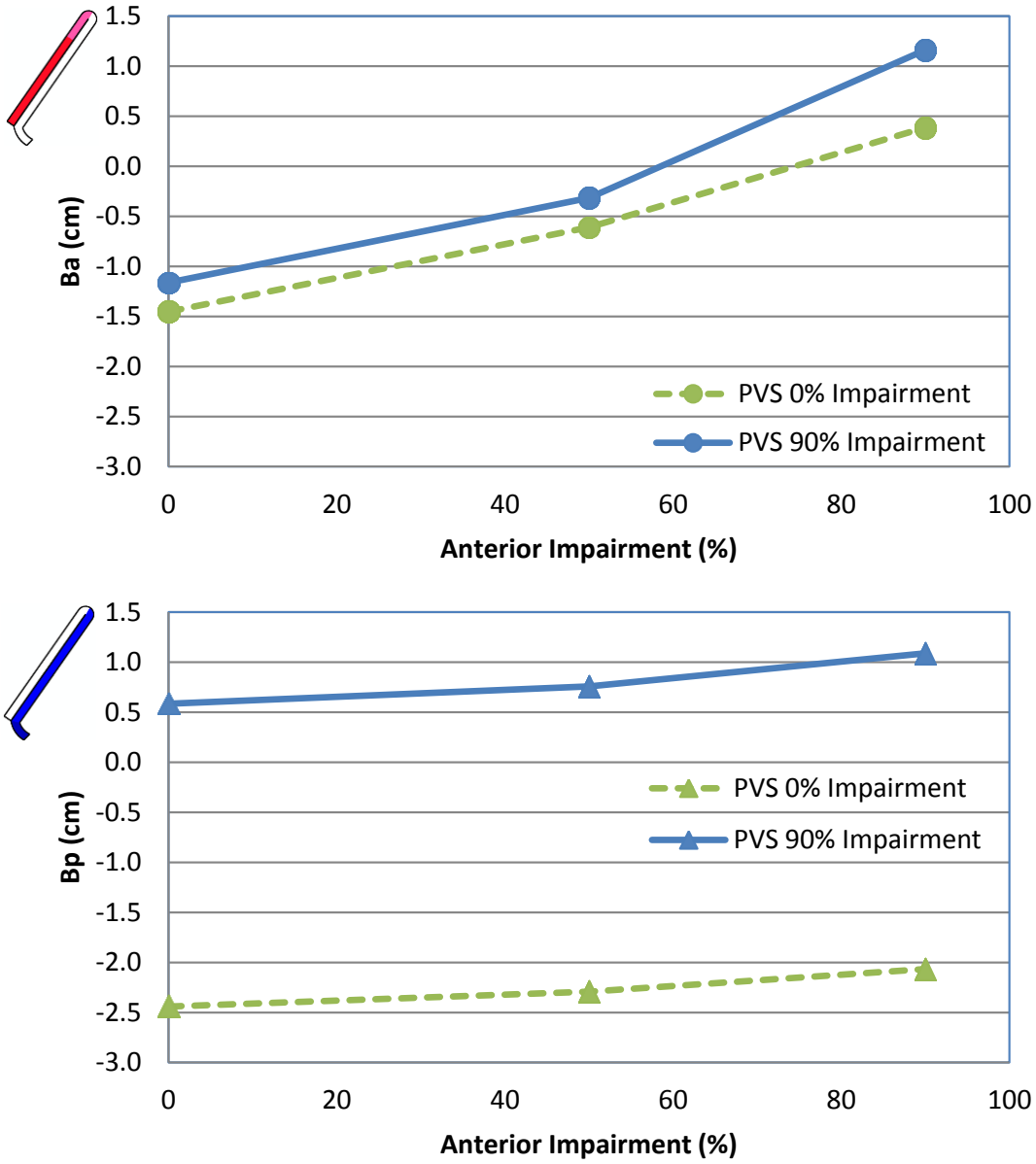

Figure 8.4 Prolapse size with effect of anterior and posterior impairment under 140 cm H_2O with PVM 80% impairment. Vaginal wall is shown for reference as Ba is for anterior vaginal wall and Bp is for posterior vaginal wall.

The effect of IAP, apical and levator impairment on the posterior vaginal prolapse is shown below.

Figure 8.5 shows the effect of IAP and apical impairment on posterior vaginal prolapse, with PVM 80% impairment, posterior support 90% impairment, and no anterior support impairment. Figure 8.6 shows the change of prolapse size based on this effect. With the increase of the IAP and apical impairment, the values of Ba and Bp both increased, but Bp increased faster than Ba with only posterior support impairment. The average compliance of posterior compartment was 0.33 mm/cm H_2O without apical impairment and 0.36 mm/cm H_2O with 60% apical impairment, while for anterior compartment was 0.16 mm/cm H_2O without apical impairment and 0.17 mm/cm H_2O with 60% apical impairment.

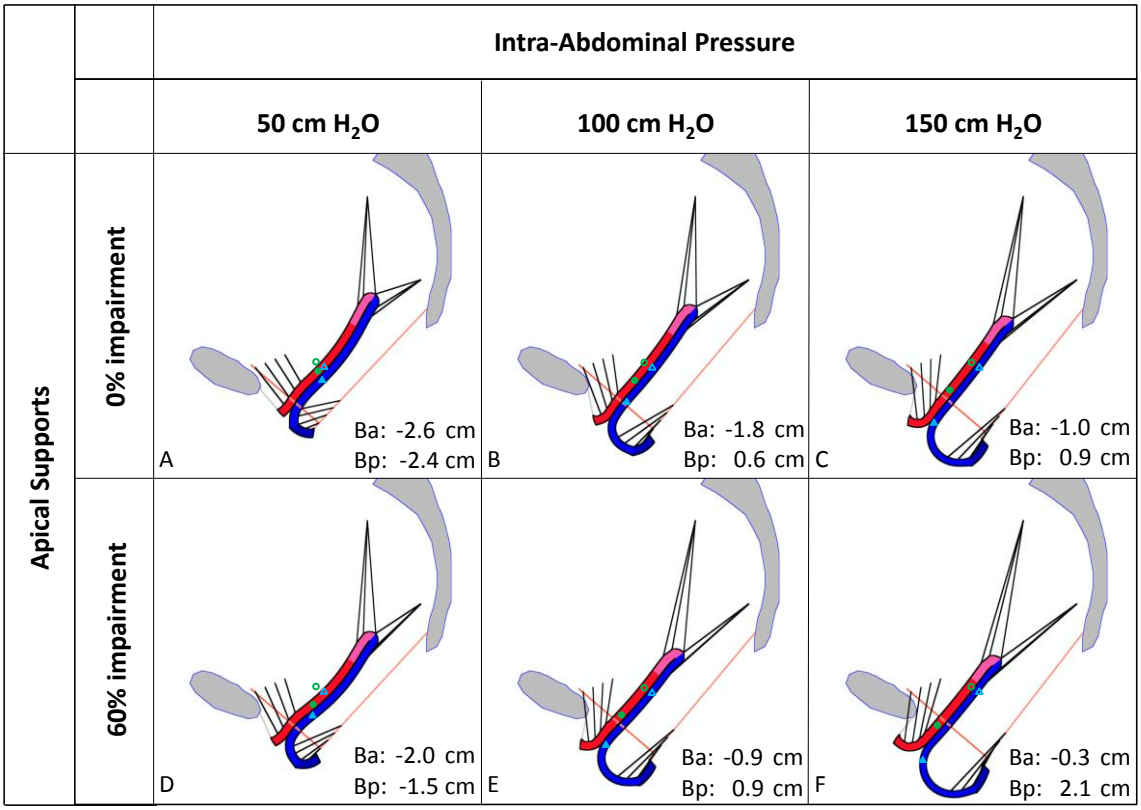

Figure 8.5 Effect of IAP and apical impairment on PVP with PVM 80% impairment, posterior 90% impairment, and no anterior impairment. POP-Q location Ba is shown as empty green circle and Bp is shown as empty turquoise triangle under resting condition. Under strain condition, Ba is shown as full green circle and Bp is shown as full turquoise triangle. Values of Ba and Bp are also shown at the right lower corner of each panel.

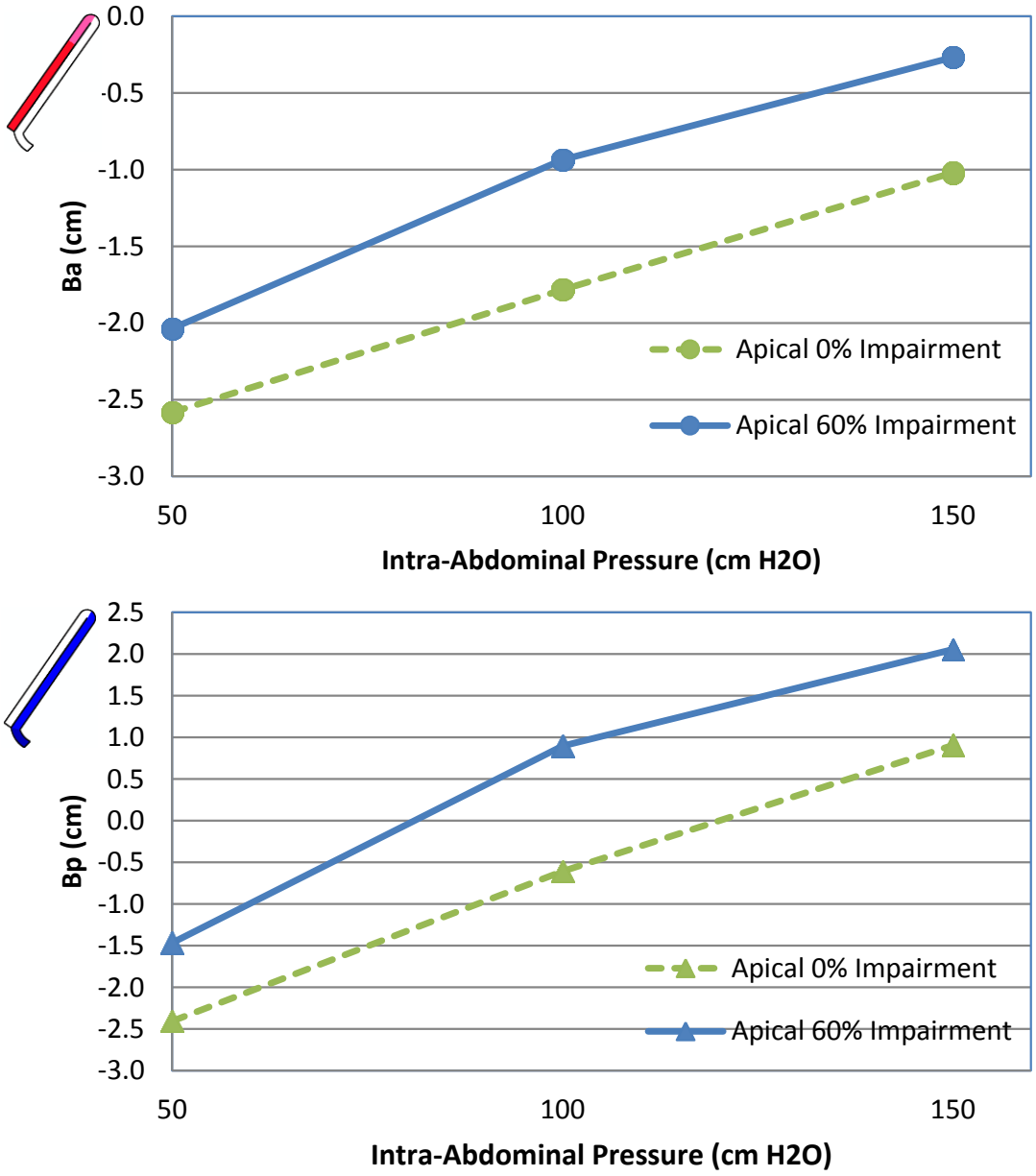

Figure 8.6 Prolapse size with effect of IAP and apical impairment with PVM 80% impairment, posterior support 90% impairment, and no anterior support impairment.

Figure 8.7 shows the change of prolapse size based on the effect of apical and levator impairment on posterior vaginal prolapse, under 140 cm H_2O with posterior support 90% impairment and no anterior support impairment. Without anterior support impairment, the change of the anterior vaginal wall dependent location Ba was less than

that of the posterior vaginal wall dependent location Bp. All the Ba values were negative (above the hymen) which indicated no anterior vaginal prolapse happened, while all the Bp values were positive (below the hymen) and 7 of 9 were above 1.0 which indicated bigger posterior vaginal prolapse. In addition, when LA had impairment from 50% to 90%, both Ba and Bp showed greater changes than those when LA had impairment from 10% to 50%. Ba's maximum change was 0.03 cm from LA's 10% to 50% impairment and 0.25 cm from LA's 50% to 90% impairment; Bp's maximum change was 0.14 cm from LA's 10% to 50% impairment and 0.72 cm from LA's 50% to 90% impairment;

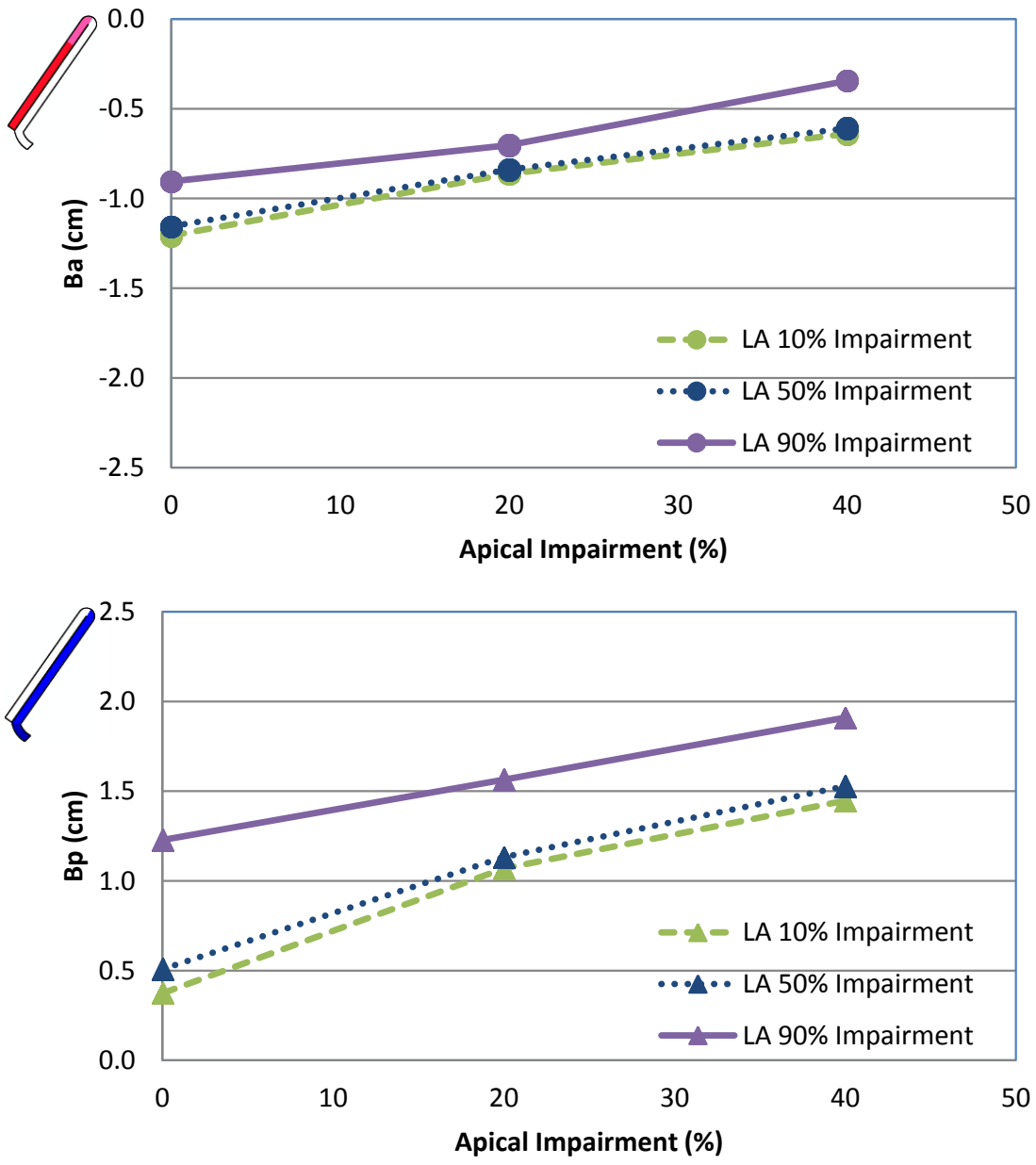

Figure 8.7 Prolapse size with effect of PVM impairment and apical impairment on posterior vaginal prolapse under 140 cm H_2O with posterior 90% impairment and no anterior impairment.

8.4 Discussion

This 2-D novel dynamic FE model included both anterior and posterior vaginal walls, muscular and connective tissue supports. It was used for simulating the formation of a cystocele and rectocele, or both, dependent on the conditions. Based on the simulation results, we rejected the hypothesis and concluded that the size of AVP and PVP are not only dependent on the anterior and posterior support impairment, as well as levator and apical support system, and the anterior and posterior prolapses do interact with each other. The levator and apical impairment, along with the anterior and posterior support impairment, could result in prolapse happening. Moreover, the development of either cystocele or rectocele could protect the posterior or anterior compartment.

Levator and apical impairment could result in cystocele, which has been demonstrated in previous simulation studies (Chen et al. 2006; Chen et al. 2009). This study not only confirmed previous result, but also proved that levator and apical impairment could also result in rectocele. Our findings are also consistent with clinical studies about apical and levator impairment (Summers et al. 2006; DeLancey et al. 2007; Dietz and Simpson 2008). Study also showed that levator muscle generates 40% less vaginal closure force during maximal voluntary muscle contraction (Ashton-Miller and DeLancey 2009), which confirmed that the levator impairment may lead to conditions fostering the cystocele or rectocele.

Characteristics of cystocele and rectocele from this study's simulation are consistent with published literatures (Larson et al. 2010a; Luo et al. 2012). It should be noted that in this 2-D FE model, we only showed the main characteristics which could be summarized from the mid-sagittal deformation, except for the vaginal widening. For the

vaginal widening characteristics, although there is no significant difference between women with and without pelvic organ prolapse (Larson et al. 2012a; Luo et al. 2012), it would be good to analyze why this happens and how important of this issue is in our future 3-D simulation study.

We found that the anterior support impairment was more related to AVP while posterior support impairment was more related to PVP. It could be easily explained by the pressure difference between IAP and atmosphere applied on each compartment and with the supporting force provided by the support system. With less anterior or posterior support, the support system could reduce the related anterior or posterior support force, which is the total force on each vaginal wall.

Furthermore, we did observe the interaction between AVW and PVW, which could be called as 'organ competition' (Kelvin and Maglinte 1997; Comiter et al. 1999; Safir et al. 1999; Stovall 2000; Kaufman et al. 2001; Kester et al. 2003; Lewicky-Gaupp et al. 2010). This main component behind organ competition is the total force (i.e.: Fa for anterior total force and Fb for posterior total force) applied on each compartment. If Fb > Fa, PVP can happen first. While the opening hiatus size is a quasi-static constant under some specific support system impairment, the more exposed PVW could take more space provided by the hiatus, and thus decreasing the exposed AVW and protecting the AVW from getting more pressure difference, and vice versa when Fa > Fb. The above phenomenon could explain some clinical findings (Withagen et al. 2012; Milani et al. 2012) that either cystocele or rectocele happened after a rectocele or cystocele repair only. An anterior support repair surgery will only correct the cystocele and reduce the

protection for PVW, and while there is posterior impairment, the rectocele will then happen after the surgery. This might be why the prolapse recurrence is so high.

We found that intra-abdominal pressure played an important role in the development of prolapse, which was consistent with other studies (O'Dell et al. 2007; Chen et al. 2009). While the anterior and posterior compartments are not in a balanced condition, larger IAP will definitely lead to increase prolapse size. As chronic coughing (Rinne and Kirkinen 1999), heavy physical activity (Woodman et al. 2006) , and obesity (Hendrix et al. 2002; Moalli et al. 2003), etc. are associated with chronic increased IAP, women with mild small prolapse are suggested to reduce the chronic increased IAP by reducing the above symptoms or activities.

To our knowledge, this is the first dynamic model to investigate the interaction between anterior and posterior vaginal walls, along with muscular and connective tissue supports. With this model, we can develop either rectocele or cystocele, or both of them under different conditions, which cannot happen on one single subject in reality. The interaction between AVP and PVP suggests that future surgeries for repairing the cystocele or rectocele should take this issue into consideration, and more reasonable repairing procedures are needed.

It should be noted that this study also has several limitations. First, this is a 2-D simplified model with most of the prolapse characteristics being investigated, except vaginal widening which is not significant between prolapse and normal patients (Larson et al. 2010a; Luo et al. 2012). Future 3-D model should analyze the vaginal widening along with paravaginal supports. Second, we did not consider the active contraction of levator ani muscle. This might not be a significant limitation, since we simulated the

vaginal wall deformation under Valsalva condition while patients were instructed to relax the levator ani muscle. Third, we only considered isotropic material properties. It would be better to consider the anisotropic material properties for levator ani muscle as it consists of different portions with different fiber direction.

In general, this study created a novel 2D dynamic model, including both anterior and posterior vaginal wall, and muscular and connective support, to investigate the mechanism of prolapse development. The result of this study could provide surgeons more insights to repair pelvic organ prolapse. Our future 3-D model study will provide more information on vaginal widening and paravaginal support information.

References

Ashton-Miller, J. A., & DeLancey, J. O. L. (2009). On the biomechanics of vaginal birth and common sequelae. *Annual Review of Biomedical Engineering* (Vol. 11, pp. 163-176).

Bartscht, K. D., & DeLancey, J. O. L. (1988). A technique to study the passive supports of the uterus. *Obstetrics and Gynecology, 72*(6), 940-943.

Blanchard, K. A., Vanlangendonck, R., & Winters, J. C. (2006). Recurrent pelvic floor defects after abdominal sacral colpopexy. *J Urol, 175*(3 Pt 1), 1010-1013; discussion 1013.

Boyles, S. H., Weber, A. M., & Meyn, L. (2003). Procedures for pelvic organ prolapse in the United States, 1979-1997. *Am J Obstet Gynecol, 188*(1), 108-115.

Boyles, S. H., Weber, A. M., & Meyn, L. (2004). Ambulatory procedures for urinary incontinence in the United States, 1994-1996. *Am J Obstet Gynecol, 190*(1), 33-36.

Brandon, C. J., Lewicky-Gaupp, C., Larson, K. A., & Delancey, J. O. (2009). Anatomy of the perineal membrane as seen in magnetic resonance images of nulliparous women. *Am J Obstet Gynecol, 200*(5), 583 e581-586.

Bump, R. C., Mattiasson, A., Bo, K., Brubaker, L. P., DeLancey, J. O., Klarskov, P., et al. (1996). The standardization of terminology of female pelvic organ prolapse and pelvic floor dysfunction. *Am J Obstet Gynecol, 175*(1), 10-17.

Chen, L., Ashton-Miller, J. A., & DeLancey, J. O. (2009). A 3D finite element model of anterior vaginal wall support to evaluate mechanisms underlying cystocele formation. *J Biomech, 42*(10), 1371-1377.

Chen, L., Ashton-Miller, J. A., Hsu, Y., & DeLancey, J. O. (2006). Interaction among apical support, levator ani impairment, and anterior vaginal wall prolapse. *Obstet Gynecol, 108*(2), 324-332.

Comiter, C. V., Vasavada, S. P., Barbaric, Z. L., Gousse, A. E., & Raz, S. (1999). Grading pelvic prolapse and pelvic floor relaxation using dynamic magnetic resonance imaging. *Urology, 54*(3), 454-457.

DeLancey, J. O. L., Morgan, D. M., Fenner, D. E., Kearney, R., Guire, K., Miller, J. M., et al. (2007). Comparison of levator ani muscle defects and function in women with and without pelvic organ prolapse. *Obstetrics and Gynecology, 109*(2), 295-302.

Dietz, H., & Simpson, J. (2008). Levator trauma is associated with pelvic organ prolapse. *BJOG: An International Journal of Obstetrics & Gynaecology, 115*(8), 979-984.

Hendrix, S. L., Clark, A., Nygaard, I., Aragaki, A., Barnabei, V., & McTiernan, A. (2002). Pelvic organ prolapse in the Women's Health Initiative: gravity and gravidity. *American Journal of Obstetrics and Gynecology, 186*(6), 1160-1166.

Hsu, Y., Chen, L. Y., Summers, A., Ashton-Miller, J. A., & DeLancey, J. O. L. (2008a). Anterior vaginal wall length and degree of anterior compartment prolapse seen on dynamic MRI. *Int Urogynecol J, 19*(1), 137-142.

Hsu, Y., Fenner, D. E., Weadock, W. J., & DeLancey, J. O. (2005). Magnetic resonance imaging and 3-dimensional analysis of external anal sphincter anatomy. *Obstet Gynecol, 106*(6), 1259-1265.

Hsu, Y., Lewicky-Gaupp, C., & DeLancey, J. O. (2008b). Posterior compartment anatomy as seen in magnetic resonance imaging and 3-dimensional reconstruction from asymptomatic nulliparas. *Am J Obstet Gynecol, 198*(6), 651 e651-657.

Kaufman, H. S., Buller, J. L., Thompson, J. R., Pannu, H. K., Demeester, S. L., Genadry, R. R., et al. (2001). Dynamic pelvic magnetic resonance imaging and cystocolpoproctography alter surgical management of pelvic floor disorders. *Diseases of the Colon and Rectum, 44*(11), 1575-1584.

Kelvin, F. M., & Maglinte, D. D. T. (1997). Dynamic cystoproctography of female pelvic floor defects and their interrelationships. *American Journal of Roentgenology, 169*(3), 769-774.

Kester, R. R., Leboeuf, L., Amendola, M. A., Kim, S. S., Benoit, A., & Gousse, A. E. (2003). Value of express T2-weighted pelvic MRI in the preoperative evaluation of severe pelvic floor prolapse: a prospective study. *Urology, 61*(6), 1135-1139.

Larson, K. A., Hsu, Y., Chen, L., Ashton-Miller, J. A., & DeLancey, J. O. (2010a). Magnetic resonance imaging-based three-dimensional model of anterior vaginal wall position at rest and maximal strain in women with and without prolapse. *Int Urogynecol J, 21*(9), 1103-1109.

Larson, K. A., Hsu, Y., & Delancey, J. O. (2009). The relationship between superior attachment points for anterior wall mesh operations and the upper vagina using a 3-dimensional magnetic resonance model in women with normal support. *Am J Obstet Gynecol*.

Larson, K. A., Luo, J., Guire, K. E., Chen, L., Ashton-Miller, J. A., & DeLancey, J. O. (2012a). 3D analysis of cystoceles using magnetic resonance imaging assessing midline, paravaginal, and apical defects. *Int Urogynecol J, 23*(3), 285-293.

Larson, K. A., Luo, J., Yousuf, A., Ashton-Miller, J. A., & Delancey, J. O. (2012b). Measurement of the 3D geometry of the fascial arches in women with a unilateral levator defect and "architectural distortion". *Int Urogynecol J, 23*(1), 57-63.

Larson, K. A., Yousuf, A., Lewicky-Gaupp, C., Fenner, D. E., & DeLancey, J. O. (2010b). Perineal body anatomy in living women: 3-dimensional analysis using thin-slice magnetic resonance imaging. *Am J Obstet Gynecol, 203*(5), 494 e415-421.

Lewicky-Gaupp, C., Yousuf, A., Larson, K. A., Fenner, D. E., & Delancey, J. O. (2010). Structural position of the posterior vagina and pelvic floor in women with and without posterior vaginal prolapse. *Am J Obstet Gynecol, 202*(5), 497 e491-496.

Luo, J., Ashton-Miller, J. A., & DeLancey, J. O. L. (2011). A model patient: Female pelvic anatomy can be viewed in diverse 3-dimensional images with a new interactive tool. *Am J Obstet Gynecol, 205*(4), 391.e391-391.e392.

Luo, J., Larson, K. A., Fenner, D. E., Ashton-Miller, J. A., & Delancey, J. O. (2012). Posterior vaginal prolapse shape and position changes at maximal Valsalva seen in 3-D MRI-based models. *Int Urogynecol J, 23*(9), 1301-1306.

Margulies, R. U., Hsu, Y., Kearney, R., Stein, T., Umek, W. H., & DeLancey, J. O. (2006). Appearance of the levator ani muscle subdivisions in magnetic resonance images. *Obstet Gynecol, 107*(5), 1064-1069.

Meschia, M., Pifarotti, P., Bernasconi, F., Magatti, F., Vigano, R., Bertozzi, R., et al. (2006). Tension-free vaginal tape (TVT) and intravaginal slingplasty (IVS) for

stress urinary incontinence: a multicenter randomized trial. *Am J Obstet Gynecol, 195*(5), 1338-1342.
Milani, A. L., Withagen, M. I. J., & Vierhout, M. E. (2012). Outcomes and predictors of failure of trocar-guided vaginal mesh surgery for pelvic organ prolapse. *American Journal of Obstetrics and Gynecology, 206*(5), 440.e441-440.e448.
Moalli, P. A., Ivy, S. J., Meyn, L. A., & Zyczynski, H. M. (2003). Risk factors associated with pelvic floor disorders in women undergoing surgical repair. *Obstetrics & Gynecology, 101*(5, Part 1), 869.
O'Dell, K. K., Morse, A. N., Crawford, S. L., & Howard, A. (2007). Vaginal pressure during lifting, floor exercises, jogging, and use of hydraulic exercise machines. *International Urogynecology Journal, 18*(12), 1481-1489.
Olsen, A. L., Smith, V. J., Bergstrom, J. O., Colling, J. C., & Clark, A. L. (1997). Epidemiology of surgically managed pelvic organ prolapse and urinary incontinence. *Obstet Gynecol, 89*(4), 501-506.
Rinne, K. M., & Kirkinen, P. P. (1999). What predisposes young women to genital prolapse? *European Journal of Obstetrics & Gynecology and Reproductive Biology, 84*(1), 23-25.
Safir, M. H., Gousse, A. E., Rovner, E. S., Ginsberg, D. A., & Raz, S. (1999). 4-Defect repair of grade 4 cystocele. *Journal of Urology, 161*(2), 587-594.
Silva, W. A., Pauls, R. N., Segal, J. L., Rooney, C. M., Kleeman, S. D., & Karram, M. M. (2006). Uterosacral ligament vault suspension: five-year outcomes. *Obstet Gynecol, 108*(2), 255-263.
Stein, T. A., & DeLancey, J. O. (2008). Structure of the perineal membrane in females: gross and microscopic anatomy. *Obstet Gynecol, 111*(3), 686-693.
Stovall, D. W. (2000). Transvaginal ultrasound findings in women with chronic pelvic pain. *Obstet Gynecol, 95*(SUPPL. 1).
Summers, A., Winkel, L. A., Hussain, H. K., & DeLancey, J. O. (2006). The relationship between anterior and apical compartment support. *Am J Obstet Gynecol, 194*(5), 1438-1443.
Withagen, M. I., Milani, A. L., De Leeuw, J. W., & Vierhout, M. E. (2012). Development of de novo prolapse in untreated vaginal compartments after prolapse repair with and without mesh: A secondary analysis of a randomised controlled trial. *BJOG: An International Journal of Obstetrics and Gynaecology, 119*(3), 354-360.
Woodman, P. J., Swift, S. E., O'Boyle, A. L., Valley, M. T., Bland, D. R., Kahn, M. A., et al. (2006). Prevalence of severe pelvic organ prolapse in relation to job description and socioeconomic status: a multicenter cross-sectional study. *International Urogynecology Journal, 17*(4), 340-345.
Yamada, H. (1970). Strength of biological materials. *Strength of Biological Materials*.

CHAPTER 9

A 3-D BIOMECHANICAL MODEL TO EVALUATE PUTATIVE MECHANISMS UNDERLYING PELVIC ORGAN PROLAPSE

Abstract

Objective: To develop a 3D anatomically-based 2 compartment finite element (FE) computer model with apical support elements to investigate putative mechanisms underlying pelvic organ prolapse under increases in intra-abdominal pressure (IAP) that allows the effect of alterations in specific support structures to be measured. The null hypothesis was tested that the size of an AVP or PVP depends only on the degree of the impairment in the structural supports of that compartment and is not influenced by changes in the other compartment.

Methods: A subject-specific FE model was created based on magnetic resonance image (MRI) 3D geometry of an average sized 45 year-old multiparous healthy woman. The model included AVW, PVW, levator ani muscle, cardinal and uterosacral ligaments, paravaginal anterior vaginal support, arcus tendineus levator ani, posterior arcus, paravaginal posterior vaginal support, perineal body (PeB), and anal sphincter. Tissue material properties were assigned from published literature. The FE model equations were solved using Abaqus v 6.11 Explicit Solver. The sensitivity of changes in AVW and PVW geometry under increasing Valsalva intra-abdominal pressures were then

calculated under different combinations of muscular and connective tissue impairments. Validation against observed 3D deformation in women with prolapse was assessed.

Results: The development of rectocele and cystocele was sensitive to levator and apical impairment, IAP, as well as anterior and posterior paravaginal support. The type of prolapse was strongly related to the type of anterior or posterior support impairment. Greater levator impairment, larger apical impairment, and larger IAP can all lead to increased AVP and PVP. Increased impairment of the opposite compartment reduced prolapse size demonstrating interactions between the two compartments.

Conclusions: The development and size of AVP and PVP are dependent on the presence of an anterior, posterior, levator or apical support impairment. But they also depend on the interaction between different impairment combinations as well as on organ competition.

Key words: pelvic organ prolapse, cystocele, rectocele, 3D, finite element model, biomechanical model

9.1 Introduction

Pelvic floor dysfunction, including stress urinary incontinence (SUI) and pelvic organ prolapse (POP), results in 11% of U.S. women undergoing surgery (Olsen et al. 1997). Over 200,000 operations are performed for POP (Boyles et al. 2003) with repair of posterior vaginal prolapse (PVP) occurring in 87% (Silva et al. 2006) of cases. The annual estimated cost for these operations exceeds US $1 billion (Subak et al. 2001).

The geometric changes (Hsu et al. 2008a; Chen et al. 2009; Larson et al. 2010a; Larson et al. 2012) and putative biomechanical changes (Chen et al. 2009) associated

with the development of an anterior vaginal prolapse (AVP, cystocele) have only recently begun to receive attention. But a knowledge gap remains as to how and why a PVP (rectocele) forms. In Chapter 8, we started to investigate this using a two-dimensional (2D) anatomically-based finite element (FE) model with both AVW and PVW and their structural support systems. The model was useful for analyzing how both AVP and PVP might develop under the effect of specific isolated and combined muscular and connective tissue impairments. But the 2D model has significant limitations when investigating the effect of changes in paravaginal supports and/or vaginal widening.

Therefore, the goal of this study was to create a subject-specific 3-D anatomically-based FE model with representations of both AVW and PVW and their respective structural support systems. We tested the hypotheses that 1) the size of AVP and PVP are only dependent on anterior and posterior support impairments, respectively, along with impairment of levator and apical support systems, and 2) AVP and PVP do not mechanically interact with one another so as to affect their relative sizes.

9.2 Materials and Methods

9.2.1 Subject-specific Model Anatomy and Finite Element Mesh

The simulation model was based upon geometric data from a 45 year-old multiparous healthy woman, who was selected from an ongoing University of Michigan Institutional Review Board-approved (IRB # 1999–0395) case-control study of pelvic organ prolapse. As described in Chapter 8, this subject's vaginal dimension (AVW: 59 mm; PVW: 98 mm; Cervix: 38 mm) is representative of average female dimensions.

As described in our previous work (Luo et al. 2012), each subject in this study underwent supine multiplanar, two-dimensional, fast spin, proton density MR imaging

both at rest and during maximal Valsalva using a 3T superconducting magnet (Philips Medical Systems Inc., Bothell, WA, USA) with version 2.5.1.0 software. At rest, 30 images were serially obtained in the axial, sagittal, and coronal planes using a 20×20 cm field of view, 4 mm slice thickness, and a 1 mm gap between slices. Similarly, at maximal Valsalva, 14 images were serially obtained at the same three serial planes, with 36×36 cm fields of view, 6 mm slice thickness, and 1 mm gap. In order for the images to be considered adequate, they had to allow visualization of vaginal margins.

A detailed 3-D pelvic floor model which included 23 structures was created, as previously described (Luo et al. 2011), using 3D Slicer software (version 3.4.1; Brigham and Women's Hospital, Boston, MA). Each structure was traced using the most clearly visible axial and/or coronal plane images and lofted into a 3D virtual model based on our previous anatomic work (Hsu et al. 2005; Margulies et al. 2006; Hsu et al. 2008b; Brandon et al. 2009; Larson et al. 2010b). The volumetric 3D model was imported into Imageware (version 13.0; Siemens Product Lifecycle Management Software Inc., 2008). Vaginal walls, levator ani, and other pelvic floor structures were lofted to form smooth surfaces. The simplified models were then imported into Abaqus (version 6.11, Dassault Systèmes Simulia Corp., Providence, RI, USA), to generate the structural mesh used to simulate the prolapse. The model development process is shown schematically in Figure 9.1.

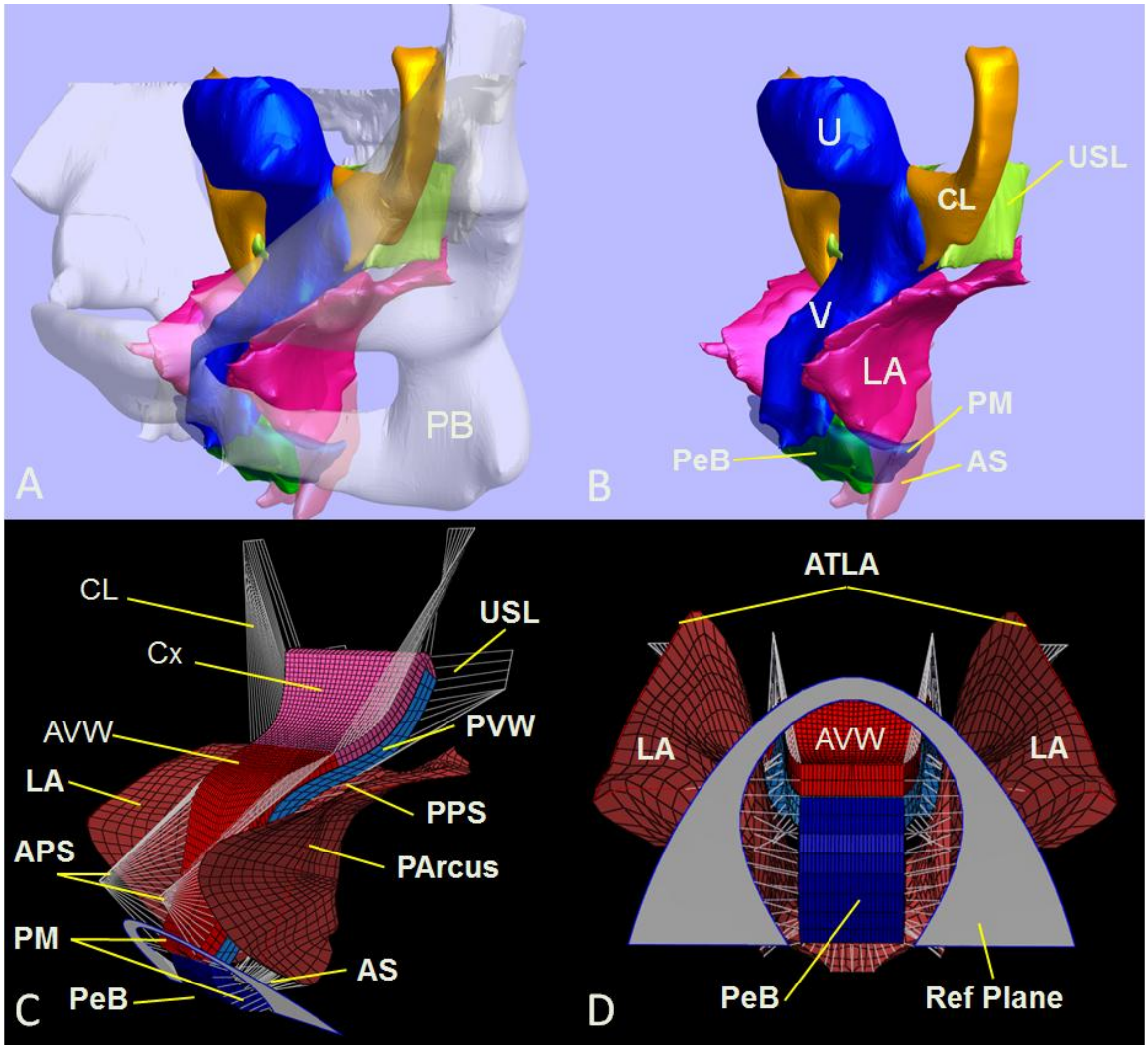

Figure 9.1 Model development. (**A**) and (**B**) MR-based 3D pelvic floor reconstruction model shown with and without pelvic bones; (**C**) and (**D**) 3-D finite element model in left three quarter view and bottom view. The region in the anterior vaginal wall occupied by the cervix was represented by a simplified region connecting both AVW and PVW. The bottom view is used to mimic what is seen during pelvic examination. The reference plane is located at the position of the hymen at rest, and is used to help visualize development of the prolapse. PB denotes pubic bone; U, uterus; V, vagina; CL, cardinal ligament; USL, uterosacral ligament; PeB, perineal body; PM, perineal membrane; LA, levator ani; Cx, cervix; AVW, anterior vaginal wall; PVW, posterior vaginal wall; APS, anterior paravaginal support; PArcus, posterior arcus; PPS, posterior paravaginal support; AS, anal sphincter; and ATLA, arcus tendineus levator ani.

The 3D FE model mesh was generated by Abaqus CAE mesh module and the simulation was solved using Abaqus Explicit Solver.

The finite element model consisted of total 7,182 elements and 10,151 nodes. The anterior vaginal wall, posterior vaginal wall, cervix, and perineal body were modeled using 3D deformable elements consisting of 5 mm-thick 8-node linear Hexagonal elements using reduced integration. The levator ani muscle was modeled as a deformable shell element using 4 mm-thick 4-node quadrilateral elements using reduced integration. The hymen reference plane was simulated as a display body. The cardinal and uterosacral ligaments, anterior vaginal support, and posterior vaginal support were simulated using connector elements. The arcus tendineus levator ani (ATLA) and posterior arcus were simulated using 2-node linear 3D truss elements. Each single simulation took about 4 hours to solve on a Linux-based (Red Hat Enterprise Linux version 5.8) High Performance Computing (HPC) cluster. The cluster, based on the Intel platform, consisted of four parallel 2.67 GHz cores (Intel Xeon X5650 processors) with 4 GB RAM per core interconnected with 40 Gbps InfiniBand networking.

9.2.2 Model Contact and Boundary Conditions

The anterior and posterior vaginal wall used a frictionless finite sliding penalty contact algorithm. The posterior vaginal wall and levator ani employed a frictionless finite sliding penalty contact algorithm. The origins of the perineal membrane from the pubic bone were fixed for translation but permitted rotation. The ends of the perineal body were connected with levator ani using connector elements. The top edges of levator ani (ICM) were tied to the ATLA. The origin and insertion of ATLA were both located on the pelvis and therefore set to be fixed for translation but allow rotation. The front edges of the levator ani (PCM) and posterior edges of the levator ani (ICM) were fixed for translation but also allowed rotation. The posterior arcus was tied to the levator ani,

and the origin and insertion of posterior arcus were fixed for translation but allowed rotation. The origins of anterior vaginal support were on the arcus tendineus fascia pelvis (ATFP) in 3-D space. All the origins for the anterior vaginal support and apical vaginal supports were fixed for translation and allowed rotation.

9.2.3 Model Material Properties

In this study all the deformable structures, including the connector elements, were assumed to be hyperelastic. For simplicity, the hyperelastic deformed structures was assumed to be isotropic and quasi-incompressible while using Abaqus Explicit Solver. All the material properties values were taken from the published literature (Yamada 1970; Bartscht and DeLancey 1988). The behavior of the levator muscle was only considered under passive stretch, since for the Valsalva maneuver patients were specifically coached to relax their pelvic floor muscles as much as possible.

9.2.4 Simulation Process

The purpose of the simulation was to predict how the structures would deform under increasing IAP. Sensitivity analyses were performed using different combinations of muscular and connective tissue impairments under different maximum IAP values. The impairment was simulated as decreased tensile stiffness. The prolapse size was quantified by POP-Q parameters Ba and Bp (Bump et al. 1996), which are 3 cm above the hymenal ring that is at the perineal membrane under resting condition by definition. The IAP was applied perpendicular to nodes on the surface of the anterior vaginal wall, cervix, posterior vaginal wall, perineal body, and levator ani. To reduce computation time, and to simulate the Valsalva process, the simulation time was scaled to 1 second.

9.2.5 Model Validation

Clinical images of a prolapse at rest and under maximal Valsalva pressure were used to validate a developing prolapse in the simulations. The model was further validated by comparing the deformations of the model anterior and posterior vaginal walls, against published 3-D models of cystocele and rectocele deformation 3-D Stress MR studies of women with these conditions (Larson et al. 2010a; Luo et al. 2012) to check whether predicted prolapse deformation characteristics were reasonable.

9.3 Results

Figure 9.2 shows one typical model-generated simulation example of AVP, which was developed under 140 cm H_2O IAP with 50% levator impairment, 90% anterior impairment, no posterior impairment and 20% apical support impairment. The model generated simulation result of AVP can be seen to be similar to that in a picture of a patient with AVP while performing a Valsalva supine for a clinical exam.

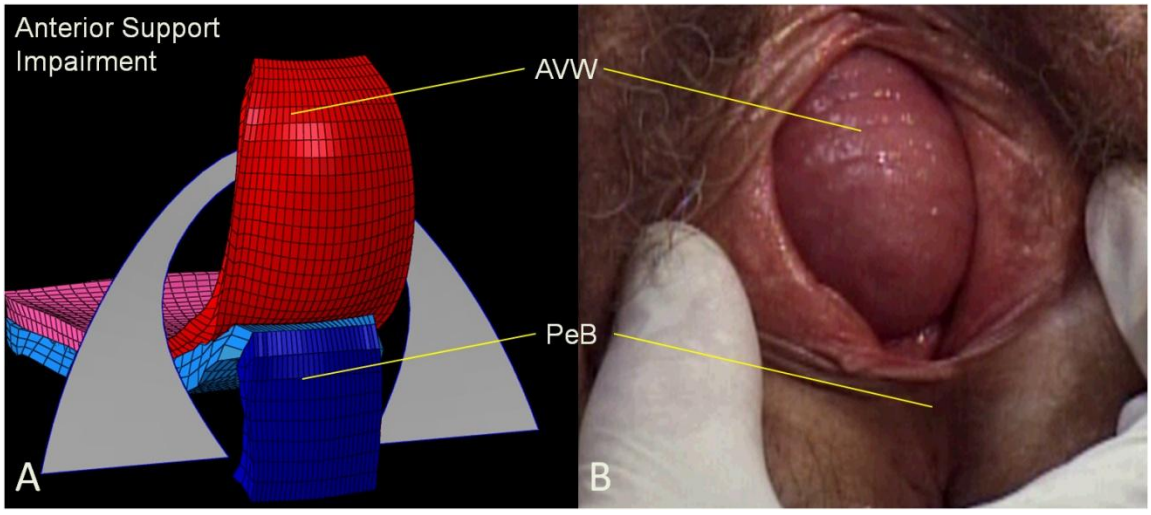

Figure 9.2 Comparison of model simulation and pelvic examination findings in anterior vaginal prolapse. **(A)** shows a model generated simulation result of AVP forming in a similar manner to that seen clinically in a picture of AVP in a patient performing a Valsalva in **(B)**.

The geometric characteristics of the model-generated AVP are shown in Figure 9.3 and Figure 9.4. Figure 9.3 first shows the characteristics of AVP in a mid-sagittal view, with evident sagittal "cupping", distal pivot, and downward displacement characteristic of AVP that are seen in 3-D stress MRI (Larson et al. 2010a). In addition to sagittal "cupping", coronal "cupping" is also seen for AVP (Figure 9.4 C and D) for the exposed portion of AVW.

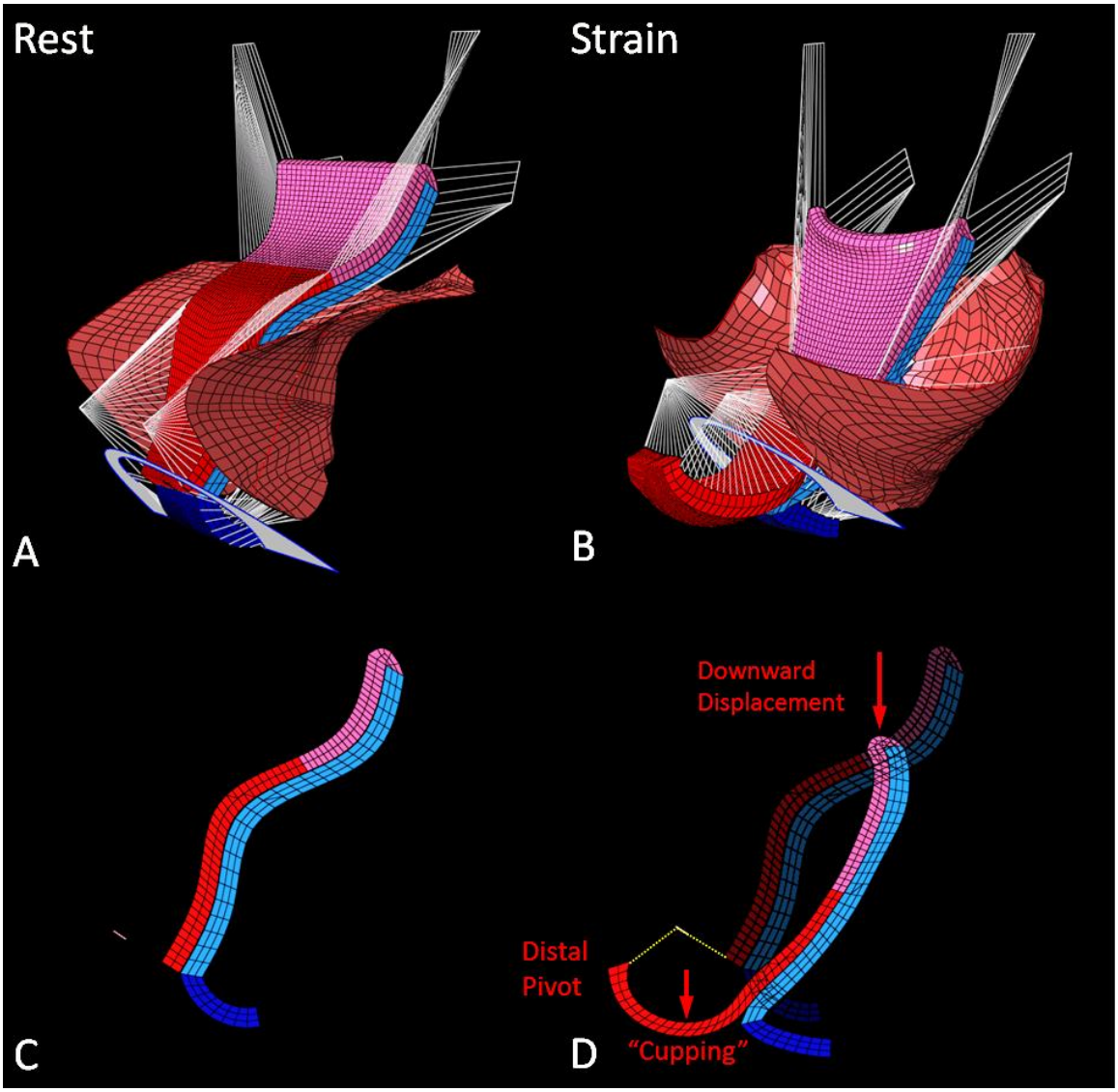

Figure 9.3 Anterior vaginal prolapse characteristics from rest to strain. **(A)** and **(B)** show left three quarter view of rest and AVP strain model. **(C)** shows middle sagittal view of model in rest. In **(D)**, sagittal "cupping", distal pivot, and downward displacement are seen for AVP.

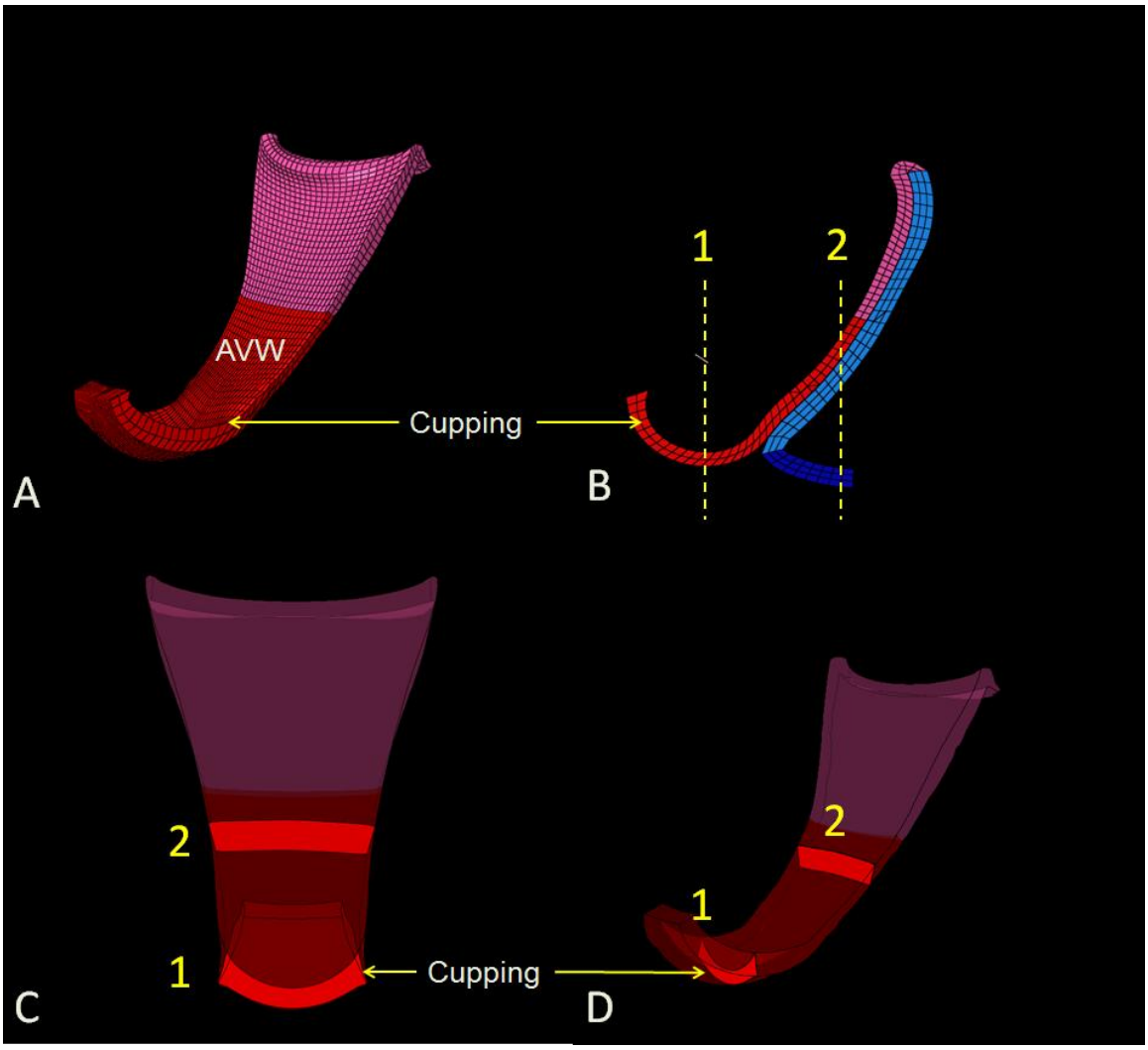

Figure 9.4 Anterior vaginal prolapse "cupping". **(A)** shows left three quarter view of anterior vaginal part. **(B)** shows the two cutting locations in middle sagittal plane. **(C)** and **(D)** show the resulting cutting cross section in front view and left three quarter view.

The model generated simulation result for a PVP is shown in Figure 9.5 and Figure 9.6. The shape of the PVP is similar to that seen in the clinical picture of a patient with PVP when performing a Valsalva (Figure 9.5 B). The characteristic "kneeling" profile of the PVP that is seen in 3-D stress MRI (Luo et al. 2012), along with downward displacement, forward protrusion, and perineal descent (Figure 9.6 B and D). Distal vaginal widening was not found for this PVP. One can also see that the length of the CL and USL increases more under strain than at rest. In addition, the angle subtended with

the body axis by those two ligaments changes from rest to strain, and the changed in angle for the USL is bigger than that for the CL (Figure 9.6 B).

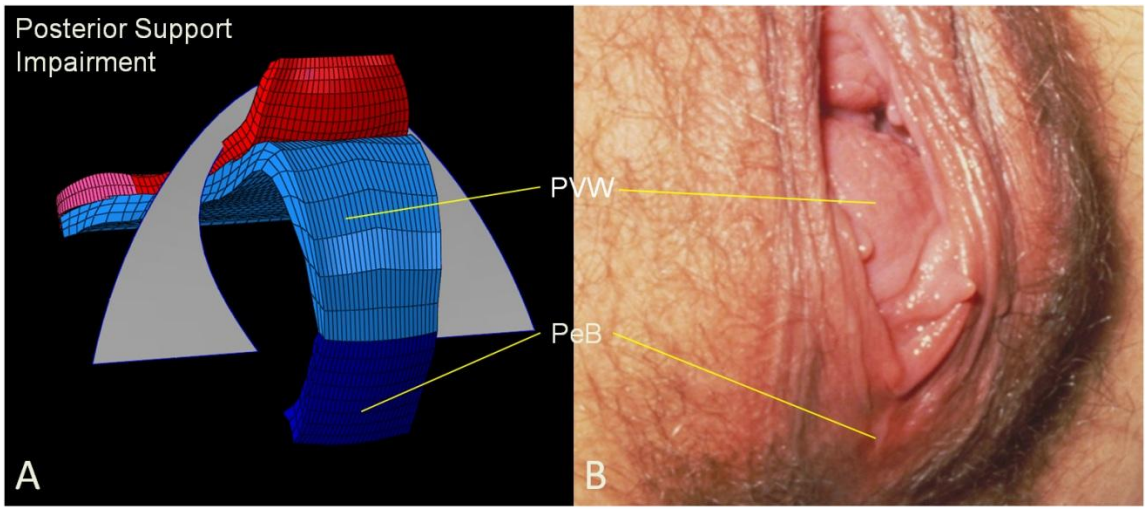

Figure 9.5 Posterior vaginal prolapse. **(A)** shows a model generated simulation result of PVP formed in the manner of one seen clinically in a picture from one patient performing a Valsalva in **(B)**.

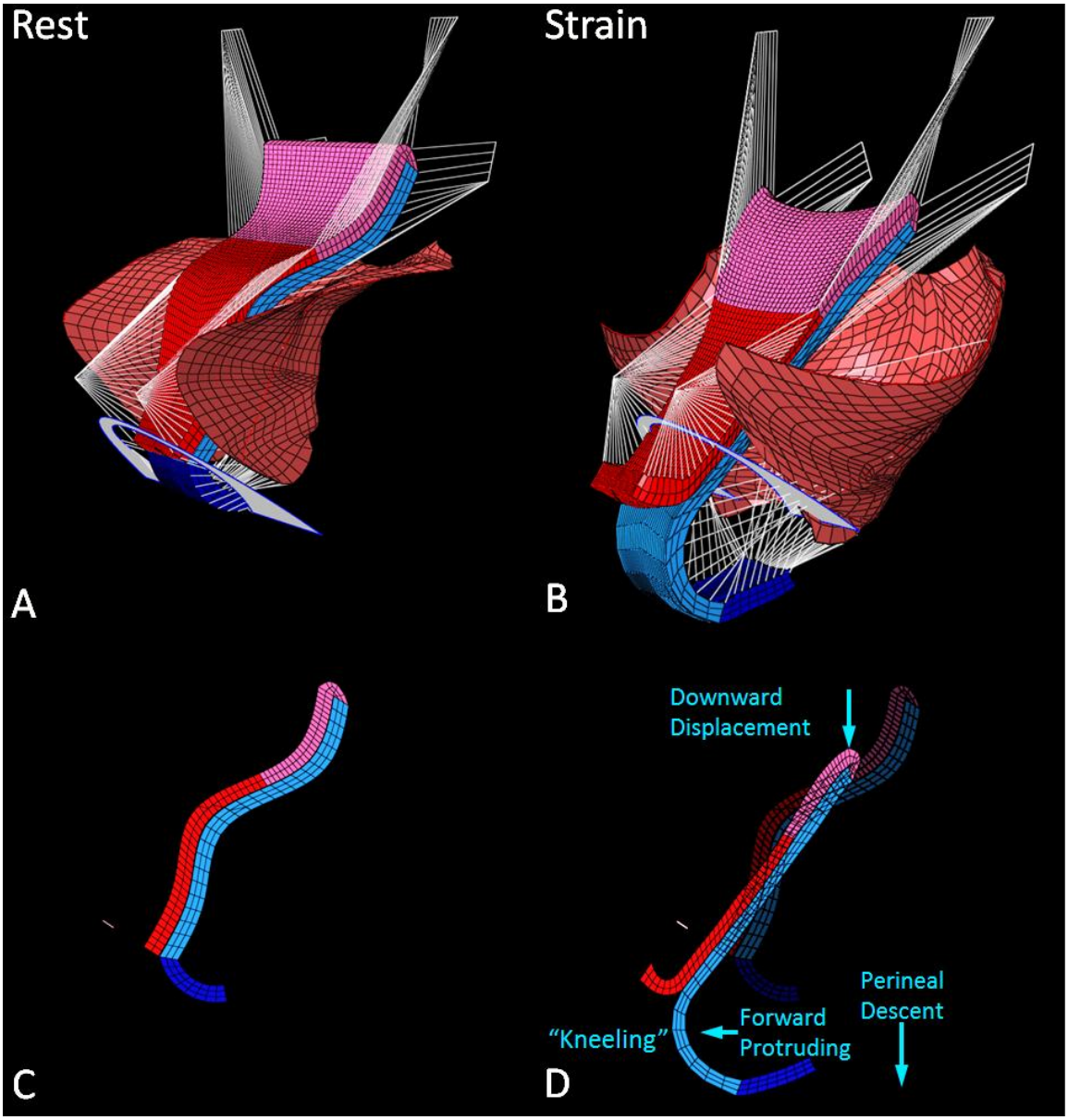

Figure 9.6 Posterior vaginal prolapse characteristics. **(A)** and **(B)** show left three quarter view of PVP model at rest and during a Valsalva . **(C)** shows a mid-sagittal view of the model at rest. In **(D)**, the "kneeling" profile, downward displacement, forward protrusion and perineal descent are all observed as being characteristic of PVP.

The mechanical interaction between AVW and PVW was first demonstrated in Chapter 8 using a 2D model. The 3D FE model shows a similar 'organ competition' phenomena (Figure 9.7). For example, under the same simulation conditions (140 cm H_2O, levator 50% impairment and apical 80% impairment) but with different anterior or

posterior support impairments, the presence of more impairment in the posterior compartment support reduces the cystocele size, and the presence of more impairment in the anterior compartment support reduces rectocele size.

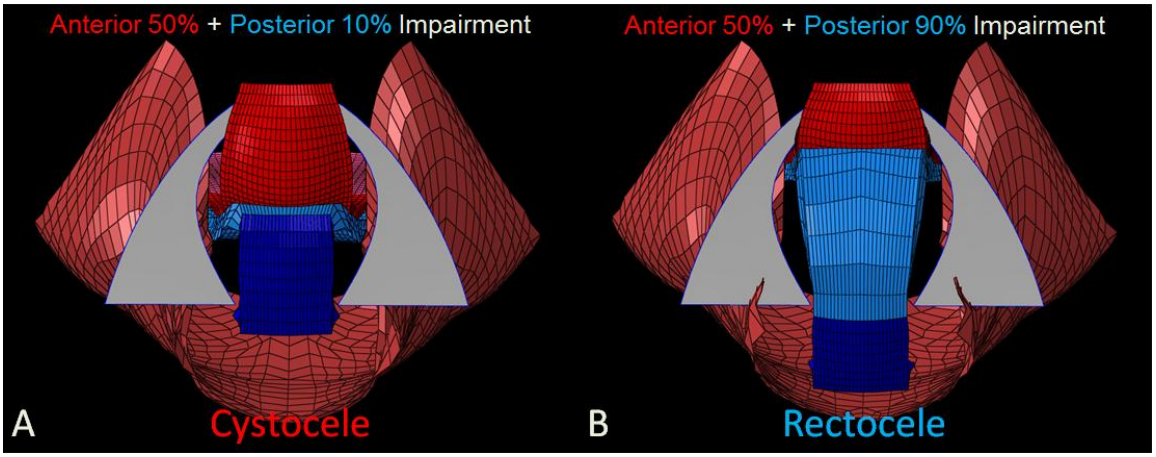

Figure 9.7 Examples of AVW and PVW 'organ competition'. Under 140 cm H_2O and with levator 50% impairment, **(A)** shows a model generated cystocele with anterior support 50% and posterior support 10% impairment; and **(B)** shows a rectocele with same anterior support impairment but posterior support 90% impairment. Presence of more impairment in posterior compartment support in **(B)** reduces the cystocele size, and vice versa in **(A)** for the rectocele.

To visualize the development of a typical PVP, Figure 9.8 shows the model simulation under systematically increasing values of IAP over time.

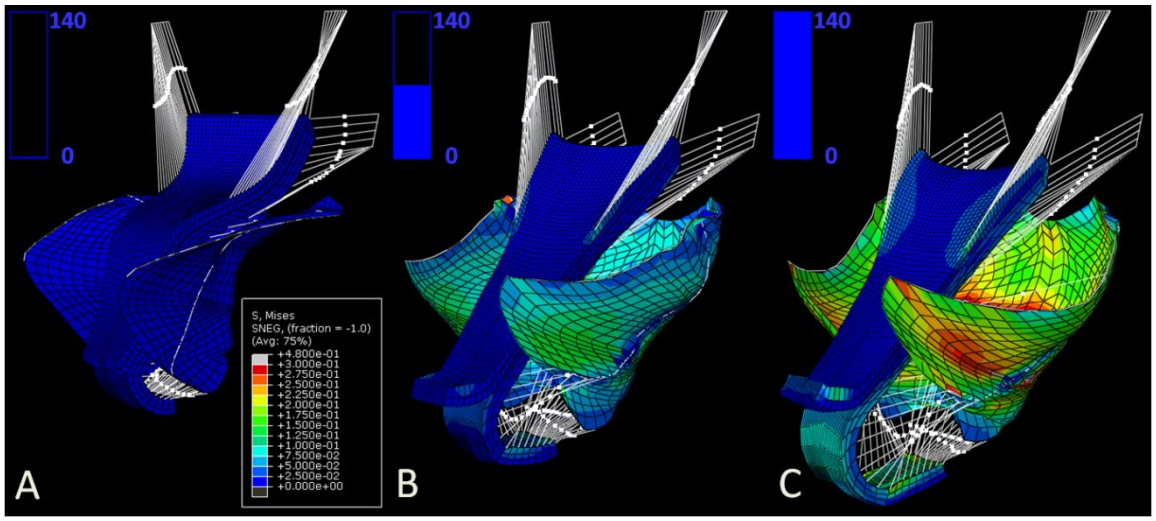

Figure 9.8 An example of the development of a typical PVP in a three-quarter, left and anterior view. The loading conditions for **(A)**, **(B)** and **(C)** were 0, 70, and 140 cm H_2O IAP, respectively,

all with levator 50% impairment, apical 80% impairment and posterior support 95% impairment, and without anterior support impairment. The color map shows stress distribution in different regions, with blue indicating low stress region, green indicating medium stress region, and red indicating high stress region. The box in the left upper corner shows the increase in the magnitude of IAP (from 0 cm to 140 cm H_2O) applied to the pelvic floor from **(A)** to **(C)**.

The biomechanical effect of changes in IAP and apical support on PVP size is shown in Figure 9.9. The simulations were run with levator 20% impairment, posterior support 95% impairment and no anterior support impairment. The simulation results show both Ba and Bp dimensions increasing as IAP was increased. We found that the greater the apical impairment was, the larger the PVP size. Note, however, that the Bp dimension changed more quickly than Ba when only posterior support impairment was present. The apical location moved caudally with both larger IAP and greater apical impairment. Without apical impairment, the compliance was 0.12 mm/cm H_2O for anterior compartment, 0.23 mm/cm H_2O for posterior compartment and 0.11 mm/cm H_2O for apex. But with 60% apical impairment, the compliance increased to 0.18 mm/cm H_2O for anterior compartment, 0.28 mm/cm H_2O for posterior compartment and 0.15 mm/cm H_2O for apex.

The effect of levator ani muscle and apical support on PVP size is shown in Figure 9.10. The conditions for these simulations were 140 cm H_2O IAP with 95% posterior support impairment and no anterior support impairment. When there was no anterior support impairment, all the Ba parameter values were less than zero (i.e., above the hymen) and the Bp values were greater than zero (i.e., below the hymen). The same effect of apical support impairment on PVP size is shown here also. PVP size increased when the apical impairment was increased. It should be noted that, when the levator

impairment was changed from 40% to 60%, the Bp parameter values were nearly twice as large as those when levator impairment was changed from 20% to 40%.

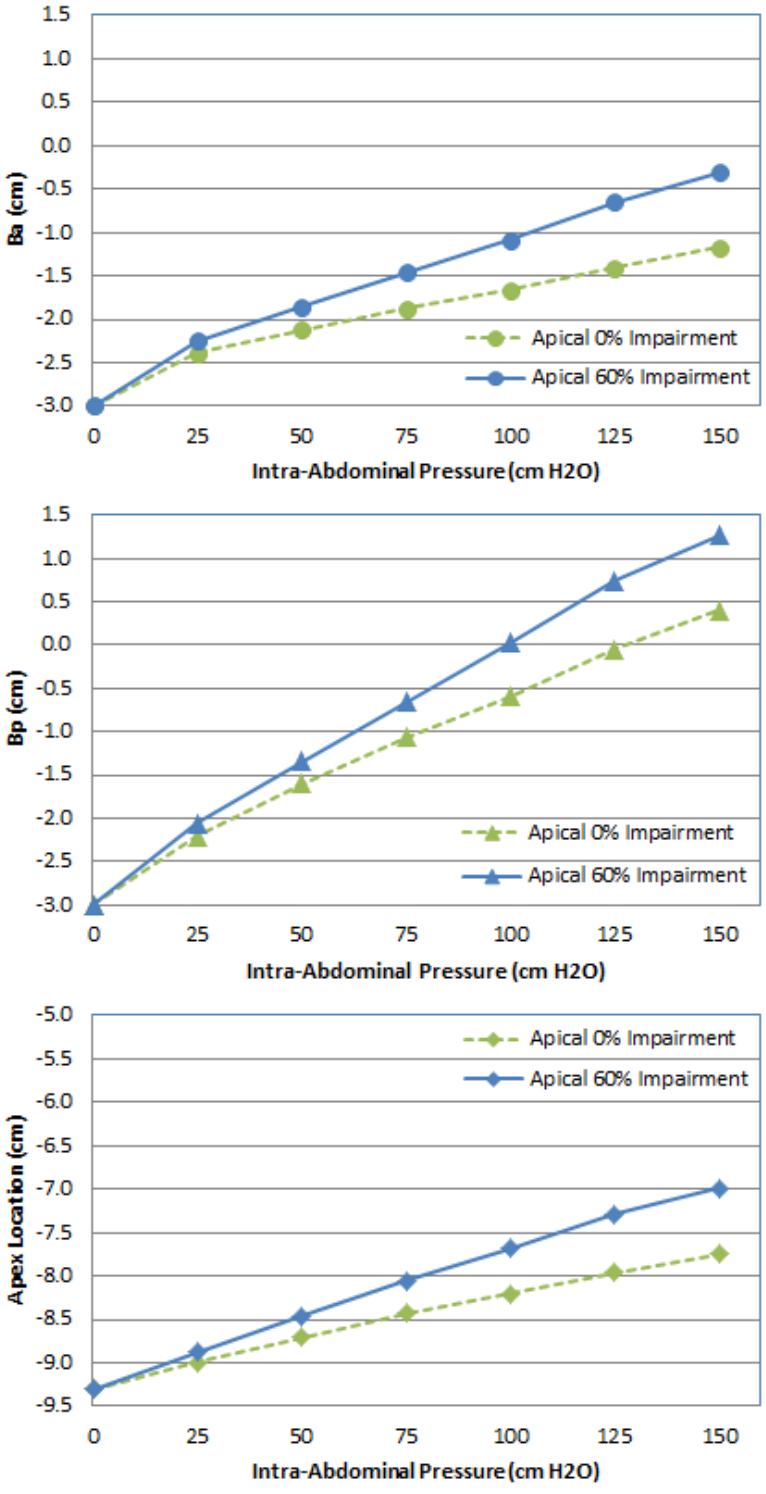

Figure 9.9 Predicted posterior vaginal prolapse size under increasing IAP and apical impairment. Simulations were run with 20% levator ani impairment, 95% posterior support impairment, and no anterior vaginal wall support impairment.

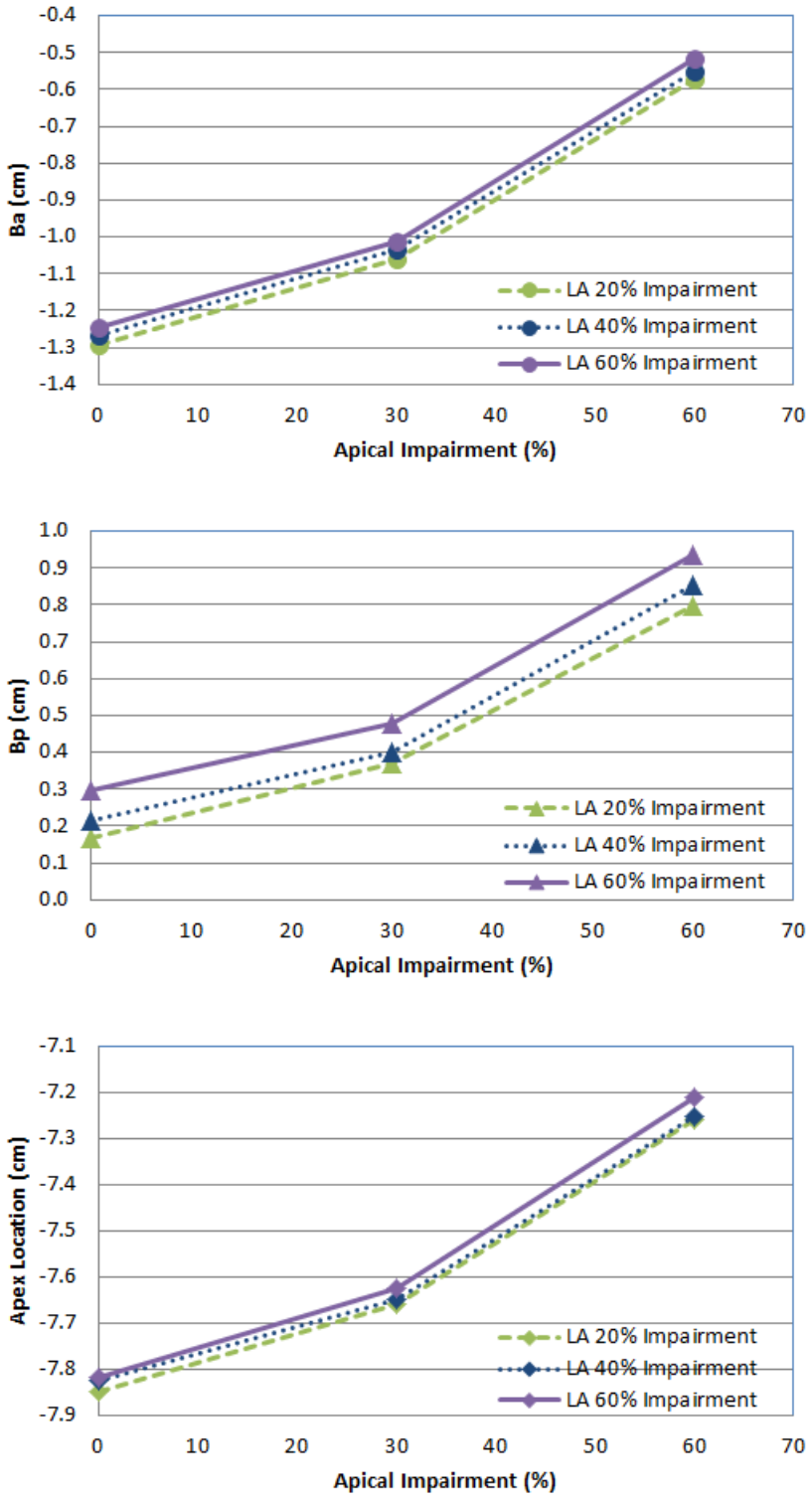

Figure 9.10 Predicted posterior vaginal prolapse size with increasing levator and apical impairment under 140 cm H_2O load. Simulations were run with 95% posterior support impairment and no anterior vaginal wall support impairment.

9.4 Discussion

This is the first subject-specific model for studying of the mechanisms underlying prolapse to include both the anterior and posterior vaginal walls as well as muscular and connective tissue supports in 3-D space. It is also the first model to simulate the formation of both a cystocele and rectocele, based on specific changes in the initial conditions. The model is based on normal has geometry based on that of a healthy living woman. It allows the consequences of specific alterations in individual components of the support system to be studied in a way that is not possible in human subjects where causing specific damage to an element of the support system to study its consequences is unethical. It is a strength that the simulation results show many similarities to the manner in which cystocele and rectocele may be seen to develop during clinical exams. Likewise, they also show similarities to the geometry of 3D models based on sequential images taken during "stress" MR examinations conducted during a Valsalva maneuver (Larson et al. 2010a; Luo et al. 2012).

Based on the simulation results shown in Figure 9.7 where the size of the cystocele was reduced by changing the supports of the posterior vaginal wall despite no change in the anterior supports, we therefore rejected the primary hypotheses stated in the Introduction. The size of AVP and PVP are not only dependent on the impairments of anterior and posterior support, but also impairments of the levator muscle and apical support system. In addition, the model clearly demonstrates that there is a mechanical interaction between the development of anterior and posterior prolapse via so-called 'organ competition' (Kelvin and Maglinte 1997; Comiter et al. 1999; Safir et al. 1999; Stovall 2000; Kaufman et al. 2001; Kester et al. 2003; Lewicky-Gaupp et al. 2010):

when one vaginal wall prolapses first, it can fill the genital hiatus thereby blocking prolapse of the other wall, and vice versa. When levator muscle and apical impairment are combined with anterior and posterior wall support impairment, this will result in a prolapse happening. But, it is a novel finding to show the mechanism by which the development of a cystocele tends to protect the posterior compartment from prolapsing under increasing IAP, and a rectocele tends to likewise protect the anterior compartment from prolapsing.

While this 3D FE model corroborates and extends the results found in the 2D FE model (Chapter 8), it provides much richer information about why prolapse can develop. For example, the predicted geometric characteristics of the simulated cystocele and rectocele are consistent with those in the published literature (Larson et al. 2010a; Luo et al. 2012). Although the 2D FE model showed several structural characteristics based on the deformations in the mid-sagittal plane, it was unable to demonstrate the cystocele "cupping" seen in the coronal section or the vaginal widening of the 3-D model based on comparing static MR scans at rest and under Valsalva. For the cystocele "cupping", we saw the same characteristic sagittal "cupping" and also the coronal "cupping" in this 3D FE model. Vaginal widening is not clearly visible in this model, which is consistent with previous studies (Larson et al. 2012; Luo et al. 2012) that vaginal widening is not significantly affected when prolapse patients are compared to women without prolapse.

That levator and apical impairment can result in cystocele has been demonstrated in earlier simulation studies (Chen et al. 2006; Chen et al. 2009). The present modeling study not only confirms those previous results, but also proved that levator and apical impairment can also contribute to rectocele. This is a finding that is consistent with

clinical studies about apical and levator impairment (Summers et al. 2006; DeLancey et al. 2007; Dietz and Simpson 2008). We noticed that when levator impairment increased to 60% from 40%, the PVP size was twice as large as when levator impairment increased from 20% to 40%. So, a larger levator impairment will decrease the vaginal closure force and allow a greater length of the vaginal wall to be exposed to the pressure differential (the difference between IAP and atmospheric pressure) acting across the exposed vaginal wall, thus fostering the development of cystocele or rectocele. This nonlinear behavior was similar to other hernia mechanics study (Engin and Akkas 1983). We also noticed that the movement direction of AVP is similar to the movement direction of the levator muscle, but the movement direction in PVP is in the opposite direction (c.f., Figure 9.3 and Figure 9.6). This could help explain why AVP occurs more commonly than PVP when there is only levator defect and no anterior support and posterior support impairment. It is also consistent with other studies which also show that the development of an AVP is more closely related to a levator impairment than is the case for a PVP (Berger et al. 2011). Put simply, we found that anterior support impairment often gave rise to AVW, while posterior support impairment more often gave rise to PVW (c.f., Figure 9.9 and Figure 9.10) in that Bp changes more than Ba while there is only posterior impairment. It could be easily explained by the pressure difference between big IAP and small atmospheric pressure applied on each compartment and with the supporting force provided by the support system structures. With less either anterior or posterior support, the support system will reduce the related either anterior or posterior support force, that is the total force on each vaginal wall, then the less supported compartment will deform more. This model also shows the importance the apical supports. We saw that 60%

impairment of the apical supports will lead to bigger prolapse size (1 cm bigger) and more apex descent, than those with normal apical supports under simulated condition (c.f., Figure 9.9).

The finding that degree of intra-abdominal pressure rise is correlated with increasing prolapse shows that the model reproduces clinical pelvic floor behavior. It is consistent with the widely held concept that prolapse and increased abdominal pressure are related (O'Dell et al. 2007; Chen et al. 2009). With levator 20% impairment, and apical 60% impairment, the posterior compartment compliance was 0.28 mm/cm H_2O. We can infer that with more levator and apical impairment, the compliance of the posterior compartment will increase. While the anterior and posterior compartments are not equilibrated, a larger IAP will definitely lead to bigger prolapse. As chronic coughing (Rinne and Kirkinen 1999), heavy physical activity (Woodman et al. 2006) , and obesity (Hendrix et al. 2002; Moalli et al. 2003), etc. are all associated to chronic increased IAP, women with mild small prolapse are suggested to reduce the chronic increased IAP by reducing the above symptoms or activities.

We also studied the interaction between AVW and PVW, which could explain how different types of prolapse develop. When there is only posterior support impairment and no anterior support impairment, or more posterior than anterior support impairment (c.f., Figure 9.7 and Figure 9.9), the change in PVP size was considerably larger than that of AVP size. For any given hiatal size, a more exposed PVW will take more of the available hiatal cross-sectional area, and as a result limit the area of AVW exposed to the IAP-atmospheric pressure differential thereby helping to protect the AVW from the pressure differential. The reverse is also true. Postoperative prolapse in a non-operated

compartment emphasizes the importance of understanding interactions between anterior and posterior supports (Withagen et al. 2012). An anterior support repair-only surgery will correct the cystocele and reduce the protection for PVW, and while there is posterior support impairment, there is an increased risk for rectocele after the surgery. This could also explain why the prolapse recurrence is high for these cases.

To our knowledge, this is the first 3-D FE computer model to investigate the interaction between anterior and posterior vaginal walls in the form of organ competition, along with muscular and connective tissue support impairments. A strength is that it includes accurate initial pelvic floor anatomy and geometry, and provides information on prolapse geometry that the 2D model lacks in the frontal and transverse planes. It also helps to visualize the prolapse formation better. This model shows rectocele and cystocele developing in 3D under different conditions, a phenomenon that cannot happen in one single subject in reality. Just as we saw the interaction between AVW and PVW, planning for improved future surgical approaches for repairing cystocele or rectocele might usefully consider this issue more carefully.

Our approach has several methodological limitations. Firstly, we had to simplify the geometry of the vaginal wall and levator muscle in order to keep the computational time tractable. Secondly, we did not consider the effect of an active contraction of the levator ani muscle. This might not actually be a significant limitation, since the goal was to simulate vaginal wall deformations under a Valsalva condition in which patients were specifically instructed to relax their levator ani muscle (in order to maximize the size of their prolapse). Thirdly, we only considered hyperelastic material properties in this study. It would have strengthened the analysis had we included the known viscous material

properties of the levator ani muscle and passive connective tissues. Our simulation results are therefore underestimates of the deformation, which would be expected to increase with time due to viscous effects (i.e. hysteresis effect). Forth, in order to evaluate the two support systems separately we have not yet evaluated the nature of connections between the anterior and posterior vaginal walls. Finally, this model only considers average size pelvic floor geometry and normal initial geometry; it would be useful to study how variations in initial geometry affect prolapse behavior.

References

Bartscht, K. D., & DeLancey, J. O. L. (1988). A technique to study the passive supports of the uterus. *Obstetrics and Gynecology, 72*(6), 940-943.

Berger, M. B., Fenner, D. E., Morgan, D. M., & DeLancey, J. O. (2011). Posterior-predominant vaginal prolapse: differences in anatomy and pelvic floor function compared to women with anterior-predominant vaginal prolapse or normal support. *Female Pelvic Med Reconstr Surg, 17*(5), S79.

Boyles, S. H., Weber, A. M., & Meyn, L. (2003). Procedures for pelvic organ prolapse in the United States, 1979-1997. *Am J Obstet Gynecol, 188*(1), 108-115.

Brandon, C. J., Lewicky-Gaupp, C., Larson, K. A., & Delancey, J. O. (2009). Anatomy of the perineal membrane as seen in magnetic resonance images of nulliparous women. *Am J Obstet Gynecol, 200*(5), 583 e581-586.

Bump, R. C., Mattiasson, A., Bo, K., Brubaker, L. P., DeLancey, J. O., Klarskov, P., et al. (1996). The standardization of terminology of female pelvic organ prolapse and pelvic floor dysfunction. *Am J Obstet Gynecol, 175*(1), 10-17.

Chen, L., Ashton-Miller, J. A., & DeLancey, J. O. (2009). A 3D finite element model of anterior vaginal wall support to evaluate mechanisms underlying cystocele formation. *J Biomech, 42*(10), 1371-1377.

Chen, L., Ashton-Miller, J. A., Hsu, Y., & DeLancey, J. O. (2006). Interaction among apical support, levator ani impairment, and anterior vaginal wall prolapse. *Obstet Gynecol, 108*(2), 324-332.

Comiter, C. V., Vasavada, S. P., Barbaric, Z. L., Gousse, A. E., & Raz, S. (1999). Grading pelvic prolapse and pelvic floor relaxation using dynamic magnetic resonance imaging. *Urology, 54*(3), 454-457.

DeLancey, J. O. L., Morgan, D. M., Fenner, D. E., Kearney, R., Guire, K., Miller, J. M., et al. (2007). Comparison of levator ani muscle defects and function in women with and without pelvic organ prolapse. *Obstetrics and Gynecology, 109*(2), 295-302.

Dietz, H., & Simpson, J. (2008). Levator trauma is associated with pelvic organ prolapse. *BJOG: An International Journal of Obstetrics & Gynaecology, 115*(8), 979-984.

Engin, A. E., & Akkas, N. (1983). Etiology and biomechanics of hernial sac formation. *J Biomed Eng, 5*(4), 329-335.

Hendrix, S. L., Clark, A., Nygaard, I., Aragaki, A., Barnabei, V., & McTiernan, A. (2002). Pelvic organ prolapse in the Women's Health Initiative: gravity and gravidity. *American Journal of Obstetrics and Gynecology, 186*(6), 1160-1166.

Hsu, Y., Chen, L. Y., Summers, A., Ashton-Miller, J. A., & DeLancey, J. O. L. (2008a). Anterior vaginal wall length and degree of anterior compartment prolapse seen on dynamic MRI. *Int Urogynecol J, 19*(1), 137-142.

Hsu, Y., Fenner, D. E., Weadock, W. J., & DeLancey, J. O. (2005). Magnetic resonance imaging and 3-dimensional analysis of external anal sphincter anatomy. *Obstet Gynecol, 106*(6), 1259-1265.

Hsu, Y., Lewicky-Gaupp, C., & DeLancey, J. O. (2008b). Posterior compartment anatomy as seen in magnetic resonance imaging and 3-dimensional reconstruction from asymptomatic nulliparas. *Am J Obstet Gynecol, 198*(6), 651 e651-657.

Kaufman, H. S., Buller, J. L., Thompson, J. R., Pannu, H. K., Demeester, S. L., Genadry, R. R., et al. (2001). Dynamic pelvic magnetic resonance imaging and cystocolpoproctography alter surgical management of pelvic floor disorders. *Diseases of the Colon and Rectum, 44*(11), 1575-1584.

Kelvin, F. M., & Maglinte, D. D. T. (1997). Dynamic cystoproctography of female pelvic floor defects and their interrelationships. *American Journal of Roentgenology, 169*(3), 769-774.

Kester, R. R., Leboeuf, L., Amendola, M. A., Kim, S. S., Benoit, A., & Gousse, A. E. (2003). Value of express T2-weighted pelvic MRI in the preoperative evaluation of severe pelvic floor prolapse: a prospective study. *Urology, 61*(6), 1135-1139.

Larson, K. A., Hsu, Y., Chen, L., Ashton-Miller, J. A., & DeLancey, J. O. (2010a). Magnetic resonance imaging-based three-dimensional model of anterior vaginal wall position at rest and maximal strain in women with and without prolapse. *Int Urogynecol J, 21*(9), 1103-1109.

Larson, K. A., Luo, J., Guire, K. E., Chen, L., Ashton-Miller, J. A., & DeLancey, J. O. (2012). 3D analysis of cystoceles using magnetic resonance imaging assessing midline, paravaginal, and apical defects. *Int Urogynecol J, 23*(3), 285-293.

Larson, K. A., Yousuf, A., Lewicky-Gaupp, C., Fenner, D. E., & DeLancey, J. O. (2010b). Perineal body anatomy in living women: 3-dimensional analysis using thin-slice magnetic resonance imaging. *Am J Obstet Gynecol, 203*(5), 494 e415-421.

Lewicky-Gaupp, C., Yousuf, A., Larson, K. A., Fenner, D. E., & Delancey, J. O. (2010). Structural position of the posterior vagina and pelvic floor in women with and without posterior vaginal prolapse. *Am J Obstet Gynecol, 202*(5), 497 e491-496.

Luo, J., Ashton-Miller, J. A., & DeLancey, J. O. L. (2011). A model patient: Female pelvic anatomy can be viewed in diverse 3-dimensional images with a new interactive tool. *Am J Obstet Gynecol, 205*(4), 391.e391-391.e392.

Luo, J., Larson, K. A., Fenner, D. E., Ashton-Miller, J. A., & Delancey, J. O. (2012). Posterior vaginal prolapse shape and position changes at maximal Valsalva seen in 3-D MRI-based models. *Int Urogynecol J, 23*(9), 1301-1306.

Margulies, R. U., Hsu, Y., Kearney, R., Stein, T., Umek, W. H., & DeLancey, J. O. (2006). Appearance of the levator ani muscle subdivisions in magnetic resonance images. *Obstet Gynecol, 107*(5), 1064-1069.

Moalli, P. A., Ivy, S. J., Meyn, L. A., & Zyczynski, H. M. (2003). Risk factors associated with pelvic floor disorders in women undergoing surgical repair. *Obstetrics & Gynecology, 101*(5, Part 1), 869.

O'Dell, K. K., Morse, A. N., Crawford, S. L., & Howard, A. (2007). Vaginal pressure during lifting, floor exercises, jogging, and use of hydraulic exercise machines. *International Urogynecology Journal, 18*(12), 1481-1489.

Olsen, A. L., Smith, V. J., Bergstrom, J. O., Colling, J. C., & Clark, A. L. (1997). Epidemiology of surgically managed pelvic organ prolapse and urinary incontinence. *Obstet Gynecol, 89*(4), 501-506.

Rinne, K. M., & Kirkinen, P. P. (1999). What predisposes young women to genital prolapse? *European Journal of Obstetrics & Gynecology and Reproductive Biology, 84*(1), 23-25.

Safir, M. H., Gousse, A. E., Rovner, E. S., Ginsberg, D. A., & Raz, S. (1999). 4-Defect repair of grade 4 cystocele. *Journal of Urology, 161*(2), 587-594.

Silva, W. A., Pauls, R. N., Segal, J. L., Rooney, C. M., Kleeman, S. D., & Karram, M. M. (2006). Uterosacral ligament vault suspension: five-year outcomes. *Obstet Gynecol, 108*(2), 255-263.

Stovall, D. W. (2000). Transvaginal ultrasound findings in women with chronic pelvic pain. *Obstet Gynecol, 95*(SUPPL. 1).

Subak, L. L., Waetjen, L. E., van den Eeden, S., Thom, D. H., Vittinghoff, E., & Brown, J. S. (2001). Cost of pelvic organ prolapse surgery in the United States. *Obstet Gynecol, 98*(4), 646-651.

Summers, A., Winkel, L. A., Hussain, H. K., & DeLancey, J. O. (2006). The relationship between anterior and apical compartment support. *Am J Obstet Gynecol, 194*(5), 1438-1443.

Withagen, M. I., Milani, A. L., De Leeuw, J. W., & Vierhout, M. E. (2012). Development of de novo prolapse in untreated vaginal compartments after prolapse repair with and without mesh: A secondary analysis of a randomised controlled trial. *BJOG: An International Journal of Obstetrics and Gynaecology, 119*(3), 354-360.

Woodman, P. J., Swift, S. E., O'Boyle, A. L., Valley, M. T., Bland, D. R., Kahn, M. A., et al. (2006). Prevalence of severe pelvic organ prolapse in relation to job description and socioeconomic status: a multicenter cross-sectional study. *International Urogynecology Journal, 17*(4), 340-345.

Yamada, H. (1970). Strength of biological materials. *Strength of Biological Materials*.

CHAPTER 10

GENERAL DISCUSSION

Pelvic organ prolapse is an abnormal downward displacement and deformation of the female pelvic organs. A current knowledge gap concerns the biomechanical mechanisms underlying the development of prolapse, and in particular posterior vaginal prolapse. We hypothesized that the occurrence, size and type of posterior vaginal prolapse is not explained by failure of any single structure; rather it involves failure of connective tissue supports at two, and possibly up to 20, anatomical sites, along with impairment of the levator ani muscle.

To test the above hypotheses, we needed to know following information: 1) What is the normal of pelvic floor anatomy and how can we get accurate 3D geometry of the pelvic floor supportive structures? (Chapters 2 & 3); 2) What are the phenomena of pelvic organ prolapse and how do we best measure them? (Chapters 4 & 5); 3) What biomechanical factors are related to pelvic organ prolapse? (Chapters 6 & 7); and finally, 4) How do we create one quantitative unified biomechanical model to test the above hypotheses? (Chapters 8 & 9).

Using *in vivo* magnetic resonance imaging we first visualized the detailed 3-D pelvic floor anatomy of 84 healthy women (Chapter 2). We found a large variation in vaginal dimension and shape in the 84 healthy women, and there was no single demographic characteristic can explain the vaginal dimension variation: there was more variation in

vaginal dimension and shape proximally than distally. Less variation proximally than distally could be explained by the spatial constraint imposed bilaterally by the levator ani muscle. The lower portion of the vagina corresponds to a high pressure zone due to contraction of the levator ani muscle that help close the hiatus and support the pelvic floor organs (Ashton-Miller and DeLancey 2009).

Based on the findings of Chapter 2, a detailed geometric 3-D MR-based interactive model of pelvic floor of an average dimensioned pelvic floor was then created (Chapter 3). This included 23 potential structures that may be involved in pelvic organ prolapse. Those structures include the muscles, ligaments, and fascia of the pelvic floor and the organs it supports. Bones, blood vessels, and the perineum are illustrated as well. This anatomically accuracy of this model helps the viewer avoid errors in comprehension that can arise from conceptual representations that are not based on living anatomy. This model clearly shows the anatomy of the levator ani muscle, while anatomy textbooks often erroneously show the female pelvic floor as a deep bowl-shaped structure with distorted relationships caused by loss of postmortem muscle tone along with the effect of high pressure embalming fluid. The model also clearly shows the three levels of supports (DeLancey 1992) for the pelvic floor. The 3-D model helps to visualize the contact information between the vagina and its supportive system, which can provide this information for potential biomechanical models. The techniques we created to reconstruct the 3-D MR-based normal pelvic floor model were then used to create 3-D MR-based prolapse models (Chapter 4 & 5).

Following the studies of normal anatomy in Chapters 2 & 3, we then studied the phenomena of the pelvic organ prolapse. We created 10 normal and 10 PVP 3-D MR-

based models to study the characteristics of PVP (Chapter 4). In those women we studied, increased folding ("Kneeling") of the vagina and an overall downward displacement were consistently present in rectocele. Forward protrusion, perineal descent and distal widening are sometimes seen as well. Those results provide the geometric basis for an accurate anatomically-based biomechanical computer model in Chapter 9.

Although the main purpose of the dissertation was to understand the mechanism underlying the development of PVP, in reality the main two types of prolapse, namely AVP and PVP, can occur at the same time but in differing degrees. A previous study from our group (Larson et al. 2010) shows downward translation, cupping, and distal rotation are three novel characteristics of AVP. The downward displacement is a characteristic of both AVP and PVP. The above information suggests AVP and PVP may result from similar failures but different mechanisms. In addition, the anterior vaginal wall (AVW) and posterior vaginal wall (PVW) always interact with each other. In Chapter 5 we then studied the AVP in 3-D using MR images from 10 normal and 10 AVP women, to assess relative contributions of "midline defects" (widening of the vagina) and "paravaginal defects" (separation of the lateral vagina from the pelvic sidewall). The results show that changes in lateral AVW location were considerably greater than changes in vaginal width in cases vs controls, both in number of sites affected and effect sizes. These "paravaginal defects" are highly correlated with apical descent. This study provides more knowledge about the AVP, and will function as a complementary research to help understand more of the mechanism underlying PVP. The results of Chapter 5 also provide insights for the biomechanical computer model to help understand how PVP can develop without AVP.

Since the apical descent or downward displacement as a characteristic of prolapse shows that the apical supports (or “Level 1” supports) play an important role in prolapse, and the “paravaginal defects” are related to the paravaginal fascia supports (or “Level 2” supports), Chapters 6 and 7 then investigate the failure of the two factors and their contribution to prolapse.

Based on a case - control study (10 cases and 10 controls), the apical support system was analyzed based on 3-D MRI-based prolapse and non-prolapse models (Chapter 6). The length of the ligaments at rest was no different between prolapse and healthy women at rest; CL ligament elongation (length change from rest to Valsalva) for each ligament was greater in prolapse than healthy women, while USL was not (at the same sample size); CL exhibited more changes in the ligament length, while USL had more changes in ligament angle with normal support and prolapse. Knowing how much each ligament changes under load in women with prolapse compared to normal support helps one understand how prolapse can occur with downward displacement.

The paravaginal fascia supports include the arcus tendineus fascia pelvis (ATFP) and arcus tendineus levator ani (ATLA). In Chapter 7 we analyzed the 3-D MRI-based arcus models of subjects with unilateral defects and show the ventral arcus anatomy is significantly altered in the presence of levator defects and architectural distortion. Alterations of these key fixation points will change the supportive force direction along the lateral AVW, and indirectly change the interaction between PVW. The results of Chapters 6 and 7 also provide the basis for the biomechanical model in Chapter 9.

Finally, two biomechanical computer models were used to test the dissertation hypotheses. The models include a 2-D finite element (FE) dynamic model (Chapter 8)

and an anatomically more accurate, 3-D, subject specific FE model (Chapter 9). Those unified models help to test a series of "what-if" problems, including situations in which tests are not ethically possible in living women.

The model-generated simulation results show that the development and size of AVP and PVP are not only dependent on a single anterior, posterior or apical support impairment: they also depend on the interaction between different combinations of impairments, as well as with organ competition.

The levator and apical impairment, along with the posterior support impairment, will result in the occurrence of a PVP. Increased IAP will lead to a larger PVP. These results help fill a gap in understanding the mechanism of PVP.

In addition, one interesting result shows that under 140 cm H_2O and with levator 50% impairment, a model with anterior 50% and posterior 10% support impairment will generate a cystocele; and a model with same anterior support impairment but posterior support 90% impairment will generate a rectocele. Thus, presence of more impairment in posterior compartment support reduces the cystocele size, and vice versa. This addresses another knowledge gap in which we sought to understand the interaction between AVP and PVP. This finding could help explain common clinical findings. For example, postoperative prolapse in a non-operated compartment emphasizes the importance of understanding such interactions between anterior and posterior supports(Withagen et al. 2012). An anterior support repair-only surgery will correct the cystocele but simultaneously reduce the protection for PVW, and if there is posterior support impairment, the probability for rectocele increases after the anterior support surgery.

When this dissertation work started in the year 2009, there only existed one 2-D and one 3-D biomechanical computer model to study AVP. No model of PVP was available. This dissertation therefore extends the literature about the mechanism of pelvic organ prolapse: not only the mechanism of posterior vaginal prolapse, but also the interaction between AVP and PVP. The availability of an anatomically accurate 3-D biomechanical computer model now also makes it possible to help design and test surgical implants (i.e., vaginal mesh) before they are applied to living women. But it is also sometimes helpful to have a conceptual model to explain a phenomenon. Just such a model is presented in Figure 10.1 to explore the pathomechanics of pelvic organ prolapse.

In this conceptual model, inputs to the support system include the intensity (α) of the pubovisceral ("PV") muscle contraction (yielding tension,T), intra-abdominal pressure (p_a) and atmospheric pressure (p_o). "Pa" acts on the surface of the levator ani muscle (1) so as to increase T and help determine total hiatal area (2). It can also drive the uterus partially into the hiatus (dashed line), leaving the remaining hiatal aperture (3), which will be spanned by the distal anterior vaginal wall (AVW) along with distal posterior vaginal wall (PVW). With a competition between the AVW and PVW (4), the winner will be exposed to more pressure differential (ΔP_{AVW} or ΔP_{PVW}). The resulting tension (T_{AVW}) (5) in the AVW (7) then applies tension to its Apical (6) and Paravaginal Supports (8) (ATLA & ATFP) helping to determine the size (9) of the resulting cystocele (Ba). The resulting tension (T_{PVW}) (10) in the PVW (12) then applies tension to its Apical (11), Paravaginal (13) (Posterior Arcus), and distal supports (PeB and Sphincter) (14 and 15) helping to determine the size (16) of the resulting rectocele (Bp). Birth damage, aging, collagen/elastin disorder, and

hormonal effects (17) are postulated to affect the properties of the levator ani muscle (18) and all the other given structures.

There are several limitations to the approaches used in this dissertation. First, the MR images used for 3-D models were obtained in the supine position and not during defecation. However, the studies we used are similar to a supine pelvic examination with associated Valsalva that clinicians use to examine the prolapse and perform a POP-Q examination (except for somewhat less thigh abduction). Second, it is a limitation that we used gel in the vagina of some women (23 of 84) recruited for the vaginal dimensions study to help with visualization. But in some instances in healthy women it fills the upper vagina thereby changes the contour and the internal surface geometry of the vagina. However, by using gel, it also helps identify the AVW and PVW separately, and also helps identify the anterior and posterior fornix. And one good Valsalva can expel much of the surplus gel. Third, we did not consider the active contraction of levator ani muscle. This might not be a significant limitation, since we specifically asked the woman to perform a Valsalva with relaxed levator ani muscles. Fourth, we only consider isotropic hyperelastic material properties in this study; it would have been better to consider anisotropic, visco-hyperelastic material properties for levator ani muscle and connective tissue, and to have considered hysteresis. Although some studies have shown the fiber direction of levator ani (Shobeiri et al. 2008) and applied it into computer models (Jing et al. 2012), the fiber direction information was from cadaver tissue not living women. It would be useful and possible to study the fiber direction of levator ani based on 1 mm high quality MR image and then implement it into the current model. Prolapse usually

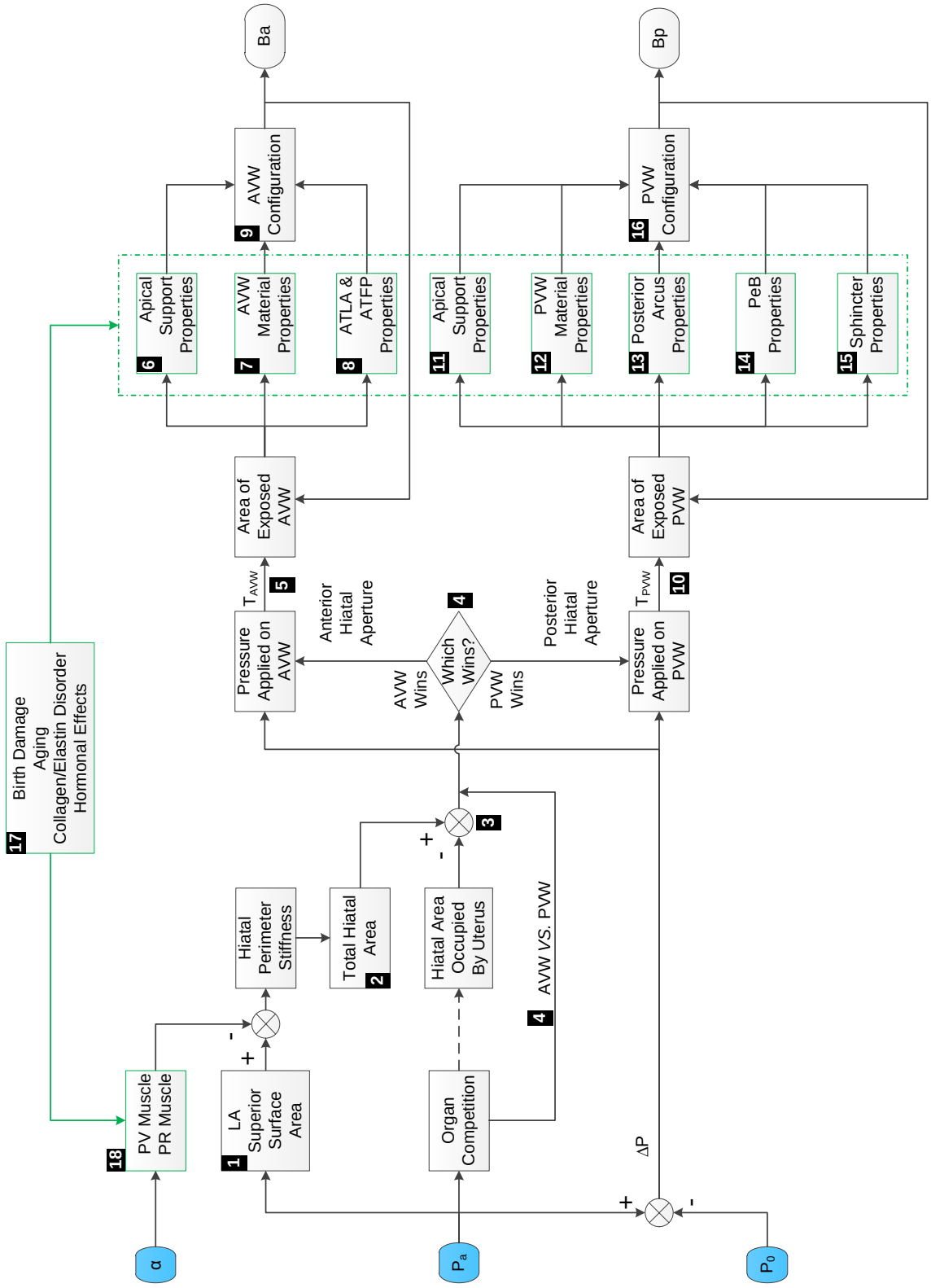

Figure 10.1 A conceptual model of the pathomechanics of pelvic organ prolapse.

happens over about 30 years after the first childbirth. So it would have been better to consider the time-dependent effects of viscous material properties, and to have considered loading rates and numbers and severity of loading cycles. The repeated loading might change the tissue's material properties such as stiffness by changing its structure or density (tissue adaption issue). Fifth, impairment of supportive structures was simulated by a simply decrease in its stiffness, not considering other issues such as initial geometry change. Sixth, the anatomy of the posterior paravaginal support and its attachment needs to be refined in detail in the future and then incorporated into this model. Seventh, the current validation was based on using clinical exam results and MR-based prolapse models. Even though the character of the prolapse is similar, ideally, it would be better to use data from living prolapse patients with detailed known impairments to compare with the model generated simulation results. However, based on current technique and knowledge, and ethical and legal restrictions, it is difficult to measure the detailed tissue condition for paravaginal supports and other connective tissues in living women. Eighth, we have seen that the vagina has a large variation in size and shape, but we only created one subject-specific model to study prolapse due to time limitations. It would be useful to study the mechanism of prolapse in subjects having a variety of vaginal dimensions. In addition, it might be interesting to also create biomechanical computer models from abnormal geometry, and to examine the effect of changing the initial geometry.

In summary, this dissertation fills several gaps in the existing literature: (1) the mechanism of posterior vaginal prolapse; and (2) the interaction between anterior vaginal prolapse and posterior vaginal prolapse. The dissertation also extends and improves

existing studies by providing: (1) in portable document format (PDF), a detailed 3-D interactive anatomic pelvic floor model; and (2) a more accurate anatomically realistic finite element model of the pelvic organ prolapse.

Despite its limitations, we believe this dissertation captures many of the important features of the mechanism of posterior vaginal prolapse, and the results support the working hypothesis proposed in Chapter 1.

References

Ashton-Miller, J. A., & DeLancey, J. O. L. (2009). On the biomechanics of vaginal birth and common sequelae. *Annual Review of Biomedical Engineering* (Vol. 11, pp. 163-176).

DeLancey, J. O. (1992). Anatomic aspects of vaginal eversion after hysterectomy. *Am J Obstet Gynecol, 166*(6 Pt 1), 1717-1724.

Jing, D., Ashton-Miller, J. A., & Delancey, J. O. (2012). A subject-specific anisotropic visco-hyperelastic finite element model of female pelvic floor stress and strain during the second stage of labor. *J Biomech, 45*(3), 455-460.

Larson, K. A., Hsu, Y., Chen, L., Ashton-Miller, J. A., & DeLancey, J. O. (2010). Magnetic resonance imaging-based three-dimensional model of anterior vaginal wall position at rest and maximal strain in women with and without prolapse. *Int Urogynecol J, 21*(9), 1103-1109.

Shobeiri, S. A., Chesson, R. R., & Gasser, R. F. (2008). The internal innervation and morphology of the human female levator ani muscle. *American Journal of Obstetrics and Gynecology, 199*(6), 686.e681-686.e686.

Withagen, M. I., Milani, A. L., De Leeuw, J. W., & Vierhout, M. E. (2012). Development of de novo prolapse in untreated vaginal compartments after prolapse repair with and without mesh: A secondary analysis of a randomised controlled trial. *BJOG: An International Journal of Obstetrics and Gynaecology, 119*(3), 354-360.

CHAPTER 11

CONCLUSIONS

The major findings of this dissertation are as follows:

(1) Among the 84 subjects studied, we found a large variation in vaginal dimension and shape. No single demographic characteristic explained the variation in vaginal dimensions. The average location of the cervical os was to the left side of pelvic mid-sagittal plane, the left side of the vagina was wider than the right side, on average, and there was more in variation in vaginal dimension and shape proximally than distally. (Chapter 2)

(2) The pelvic floor support system involves about 23 structures that include the muscles, ligaments, and fascia of the pelvic floor, bones, blood vessels, and the perineum, and the organs it supports. A 3-D interactive portable document file (PDF) of pelvic floor model is now possible and actually created, to help visualize the detailed structures without any specialized software. (Chapter 3)

(3) Increased folding ("Kneeling") of the vagina and an overall downward displacement are consistently present in rectocele. Forward protrusion, perineal descent and distal widening are sometimes seen as well. (Chapter 4)

(4) Changes in lateral AVW location were considerably greater than changes in vaginal width in the case-control study, both in number of sites affected and the

effect sizes. These "paravaginal defects" were highly correlated with apical descent. (Chapter 5)

(5) The length of both pairs of apical support ligaments at rest are no different between prolapse and normal women at rest; CL ligament elongation (length change from rest to Valsalva) was greater in prolapse than normal women, while USL was not (at this same sample size); CL exhibits greater differences in the ligament length, while USL exhibits larger differences in ligament inclination angle when comparing women with normal support and prolapse. (Chapter 6)

(6) The ventral arcus anatomy is significantly altered in the presence of levator defects and architectural distortion. Alterations of these key fixation points will change the supportive force direction along the lateral anterior vaginal wall, thereby increasing the risk for anterior vaginal wall prolapse. (Chapter 7)

(7) The combination of levator and apical impairment, along with the posterior support impairment, will result in PVP. Increasing IAP will lead to a larger prolapse. (Chapters 8 and 9)

(8) Under 140 cm H_2O and with levator 50% impairment, a model with anterior support 50% and posterior support 10% impairment will generate a cystocele; and a model with same anterior support impairment but posterior support 90% impairment will generate a rectocele. Presence of more impairment in posterior compartment support reduces the cystocele size, and vice versa. (Chapter 9)

(9) The development and size of AVP and PVP are not only dependent on a single anterior, posterior or apical support impairment: they also depend on the

interaction between different combinations of impairments, as well as with organ competition. (Chapters 8 and 9)

CHAPTER 12

SUGGESTIONS FOR FUTURE RESEARCH

This dissertation provides insights into the biomechanical mechanisms underlying the PVP as well as organ competition. It focused on the interaction among the following structures: 1) anterior vaginal wall; 2) posterior vaginal wall; 3) cervix; 4) levator ani muscle; 5) apical supports; 6) anterior paravaginal supports; 7) posterior paravaginal supports; 8) perineal membrane and perineal body. We also investigated the biomechanical factors from the change of the above the supporting systems that are involved in the development of prolapse and organ competition. However, several limitations of current study and some other related factors remaining to be investigated warrant further research work.

First, some regions of the present model need refinement, such as perineal membrane, the attachment of the perineal body, and the posterior arcus. The functional anatomy of those regions needs to be clarified and implemented in the 3-D FE model.

Second, more accurate material properties need to be implemented in the model. It would be better to measure visco-hyperelastic properties from the living women for the apical supports and other tissues, although it may be impossible for the smaller connective tissue. We have designed a computer controlled servo-motor driven testing apparatus to test *in vivo* apical supports materials properties. We hope to collect enough sample data to analyze the material properties in the next year.

Third, we need to investigate the effect of repeatitive loading. With the visco-hyperelastic material properties provided in the future, it will be possible to simulate the effect of repeated loading based on current model by changing the material properties and adding loading and unloading cycles.

Fourth, since we have seen that the vagina has large variations in size and shape, and the support system can be abnormal, we need to consider creating models with different vaginal dimensions and abnormal geometry, and then simulate the prolapse.

Other factors that could be considered in future research include the effects of childbirth, the effect of aging, the effect of chronic increased intra-abdominal pressure caused by chronic coughing, heavy physical activity and obesity, the effects of collagen and elastin disorders, the effect of neural muscular dysfunction, as well as the hormonal effects, and the effect of tissue adaption over time.

APPENDIX A

Below is a video embedded in PDF for instructing how to manipulate the interactive 3-D pelvic floor model. The video can be activated by clicking on the image.

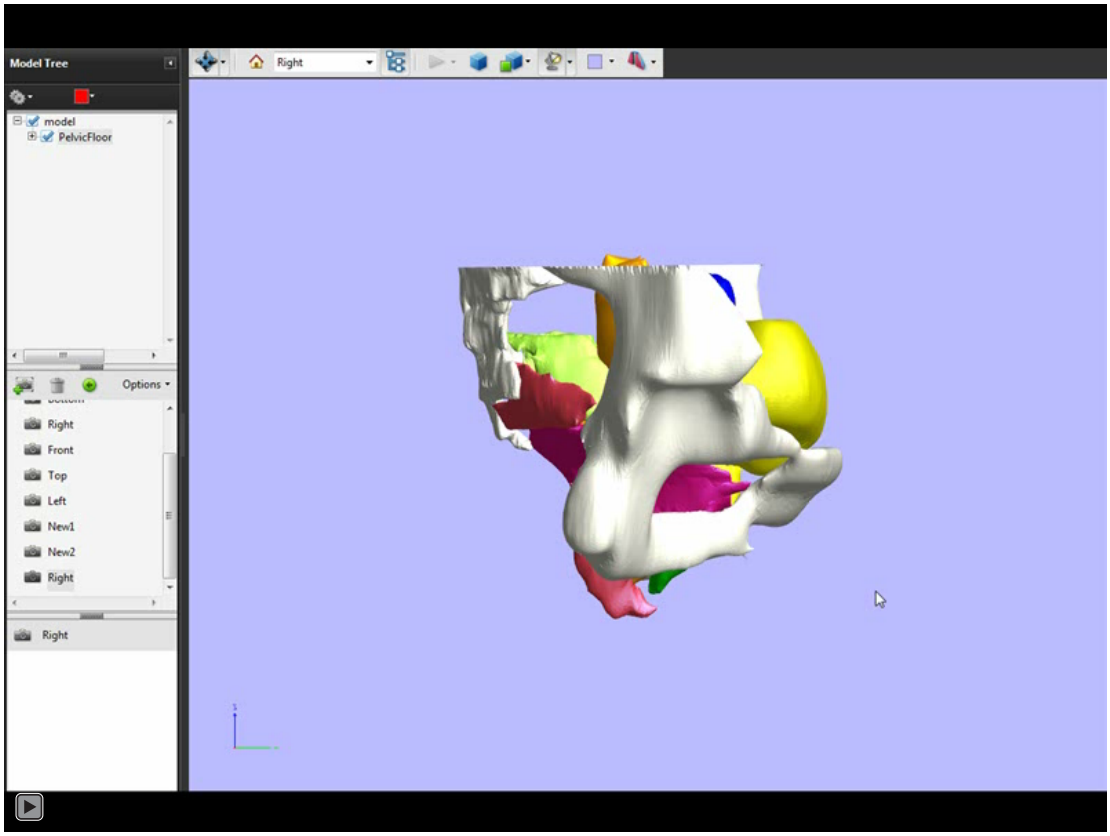

APPENDIX B

The interactive 3-D pelvic floor model was shown in the next page. The manipulation can be activated by clicking on the figure.